



저작자표시-비영리-변경금지 2.0 대한민국

이용자는 아래의 조건을 따르는 경우에 한하여 자유롭게

- 이 저작물을 복제, 배포, 전송, 전시, 공연 및 방송할 수 있습니다.

다음과 같은 조건을 따라야 합니다:



저작자표시. 귀하는 원저작자를 표시하여야 합니다.



비영리. 귀하는 이 저작물을 영리 목적으로 이용할 수 없습니다.



변경금지. 귀하는 이 저작물을 개작, 변형 또는 가공할 수 없습니다.

- 귀하는, 이 저작물의 재이용이나 배포의 경우, 이 저작물에 적용된 이용허락조건을 명확하게 나타내어야 합니다.
- 저작권자로부터 별도의 허가를 받으면 이러한 조건들은 적용되지 않습니다.

저작권법에 따른 이용자의 권리는 위의 내용에 의하여 영향을 받지 않습니다.

이것은 [이용허락규약\(Legal Code\)](#)을 이해하기 쉽게 요약한 것입니다.

[Disclaimer](#)

Ph.D Thesis

**Process Intensification of Gasification and
Reforming Technology for Enhanced Power
Generation with Carbon Capture and Storage**

Advisor: Professor Chonghun Han

BY

Usama Ahmed

August 2017

SCHOOL OF CHEMICAL AND BIOLOGICAL
ENGINEERING

COLLEGE OF ENGINEERING

SEOUL NATIONAL UNIVERSITY

**Process Intensification of Gasification and Reforming
Technology for Enhanced Power Generation with Carbon
Capture and Storage**

Advisor: Professor Chonghun Han

Ph.D Thesis Dissertation by:

Usama Ahmed

August 2017

School of Chemical and Biological Engineering
Seoul National University

Submitted to Seoul National University in partial fulfillment of the
requirements for the degree of Doctor of Philosophy in
Chemical & Biological Engineering

Approved by:

Chairman:	<u>Prof. Dr. Lee, Wonbo</u>
Vice Chairman:	<u>Prof. Dr. Han, Chonghun</u>
Member:	<u>Prof. Dr. Yoon, En Sup</u>
Member:	<u>Prof. Dr. Lim, Youngsub</u>
Member:	<u>Prof. Dr. Lee, Chuljin</u>

Abstract

Process Intensification of Gasification and Reforming Technology for Enhanced Power Generation with Carbon Capture and Storage

Usama Ahmed

School of Chemical & Biological Engineering

Seoul National University

IGCC is a pre-combustion technique which represents higher thermal efficiency with large scale implementation of CO₂ capture. On the other hand, NGCC power plants offers higher process performance compared to IGCC process with CCS technologies but the fluctuating and comparatively higher costs of natural gas limits its extensive implementation over coal based power generation systems. Therefore, process integration of coal gasification and natural gas reforming has been proposed to enhance the process performance while limiting the natural gas consumption. In this study, two IGCC based process models

have been developed and evaluated in terms of both the process performance and economics with CO₂ capture. Case 1 is taken as the conventional IGCC process, whereas, case 2 presents an idea of integrating methane reforming process with an IGCC technology. The high enthalpy steam generated during coal slurry gasification process in case 2 is used to assist the reforming process for H₂ generation. The integration of IGCC with methane reforming process not only supplies the heat required for the endothermic reforming process but also increases the heating value of the resulting syngas. This concept also provides an opportunity for process intensification since shared water gas shift reactors and CO₂ capture units will suffice the process needs. The net electricity generation capacity and efficiency for case 1 and case 2 is calculated as (375.08 MW_e, 472.92 MW_e) and (35.93%, 40.70%), respectively. While comparing the results, it has been seen that case 2 design offers nearly 4.7% higher efficiency compared case 1 design with CO₂ capture. The process economics analysis showed that the case 2 design requires a higher CAPEX and O&M throughout the project life compared to the case 1 design. However, due to the higher power generation capacity of case 2 design, it has a potential to reduce the LCOE by 5.81% compared to the case 1 design. Moreover, case 2 design

not only requires the less CO₂ capture and avoidance costs compared to the case 1 but also exhibits higher rate of return on the investment with the less payback time. With the higher efficiency and least SE_{CO₂}, case 2 has been considered as the most feasible option for electricity production at an economical price compared to the case 1 design.

To complete the chain of power generation systems with the CO₂ capture and storage, the CO₂ injection system has been also studied in detail. The transport of CO₂ for geological storage is economically feasible by ship when the storage site location is off-shore and installment of an off-shore pipeline requires a huge capital cost. Ship transportation requires the captured CO₂ to be in liquid phase under pressurized thermodynamic conditions. The injection of liquid CO₂ into the geological reservoir involves pressurization and heating in order to maintain the safe well head operating conditions. This study presents an improved design mechanism for CO₂ injection that can utilize the cold energy available from the liquid CO₂ to operate the two-stage NH₃ rankine cycle. The results showed that the 2-stage rankine cycle design consume approximately 56% less power compared to that of the base case design. Moreover, the economic analysis also showed that the specific cost of CO₂ injection can be reduced up to 6.2% using the improved design.

Finally, a sensitivity analysis has been also performed in order to investigate the effect of some important variables on the process performance and economics.

Keywords: IGCC, SMR, Process integration and intensification, Power generation, CCS, COE, Process economics, 2-stage rankine cycle, CO₂ transport & storage

Student Number: 2015-31025

Contents

Chapter 1 : Introduction.....	1
1.1 Climate change and CO ₂ emissions.....	1
1.2 Research Motivation.....	5
1.3 Research Objectives	6
1.4 Organization of Thesis.....	7
Chapter 2 : Overview of IGCC and Reforming Technologies	9
2.1 Background of IGCC power plants for abating CO ₂ emissions	9
2.2. Process description of IGCC technology.....	18
2.2.1 Solid Handling Equipment.....	18
2.2.2 Gasification Technology overview	19
2.2.3 Air Separation Unit (ASU).....	29
2.2.4 Syngas cooling	32
2.2.5 Water Gas Shift Reactor (WGSR)	33
2.2.5 Syngas clean up	36
2.2.6 Combined Cycle Power Generation	40
2.3 Overview of Methane Reforming Process.....	44
2.3.1 Steam Methane Reforming	45
2.3.2 Partial Oxidation.....	47
2.3.3 Dry Reforming (DMR)	48
2.3.4 Auto-thermal Reforming.....	48
2.3.5 Mixed Reforming	49
2.3.6 Tri-Reforming (TRM).....	50
2.4 Summary.....	51

Chapter 3 : Simulation Methodology and Performance Analysis ..53

3.1	Overview & Concept Development	53
3.2	Development of Process Models	57
3.2.1	IGCC Process Model with CO ₂ Capture (Case 1).....	57
3.2.2	Integration of IGCC and Methane Reforming Process with CO ₂ Capture (Case 2)	63
3.2.3	Design basis for model development.....	68
3.3	Performance Analysis	73
3.3.1	Evaluation of the process performance	73
3.3.2	Assessment of CO ₂ specific emissions	84
3.3.3	Performance comparison with Literature.....	85
3.3.4	Sensitivity Analysis	87
3.4	Summary	97

Chapter 4 : Economic Analysis..... 100

4.1	Capital Expenditure Calculation (CAPEX)	100
4.2	Operational Expenditure Calculation (OPEX).....	104
4.3	Project life and payback time	107
4.3	Estimation of cost of electricity (COE)	108
4.4	Cost of CO ₂ capture.....	113
4.5	Summary	114

Chapter 5 : CO₂ Topside Injection Process 116

5.1	Introduction.....	116
5.2	Process Design	122
5.2.1	Base Case	122
5.2.2	2-Stage Rankine Cycle.....	127
5.3	Results and Discussion	131

5.3.1	Energy Analysis.....	131
5.3.2	Economic Analysis	133
5.3.4	Process Comparison.....	136
5.4	Sensitivity Analysis	140
5.4.1	Well Head Temperature.....	140
5.4.2	Sea Water Temperature	142
5.4.3	CO ₂ Stream Composition.....	143
5.4.4	Project Life.....	145
5.5	Summary.....	147
Chapter 6 : Concluding Remarks.....		149
6.1	Conclusions	149
6.2	Future Works	151
APPENDIX		153
References		163
Abstract in Korean (국문초록).....		170
Acknowledgement.....		173

List of Figures

Figure 1-1: Greenhouse gas emissions by sector [1]	2
Figure 1-2: Global greenhouse gas emissions by gas [1].....	4
Figure 2-1: Cumulative worldwide capacity and growth.....	10
Figure 2-2: Number of gasifiers by primary feedstock.....	11
Figure 2-3: IGCC based energy conversion system concept	12
Figure 2-4: Coal handling facility [29]	19
Figure 2-5: Moving bed gasifier	24
Figure 2-6: Fluidized bed gasifier.....	25
Figure 2-7: Entrained flow gasifier.....	27
Figure 2-8: Characteristics of different gasification technologies.....	28
Figure 2-9: Simplified air separation unit (ASU) flow scheme[12]	32
Figure 2-10: Comparison of Sour and Sweet shift catalytic process	35
Figure 2-11: Simplified selexol process flow diagram for AGR	39
Figure 2-12: Combined Cycle flow diagram.....	41
Figure 2-13: Tubular SMR unit [45].....	46
Figure 2-14: H ₂ /CO ratio of syngas for various reforming techniques.	51
Figure 3-1: Case 1 – Conventional IGCC design for power generation with CO ₂ capture.....	59
Figure 3-2: Syngas composition at the gasifier for base case (case 1) and its comparison with the NETL report.....	61
Figure 3-3 : Syngas composition at the WGSR section for base case (case 1) and its comparison with the NETL report.....	62
Figure 3-4: Case 2 – Integration of IGCC and methane reforming process for power generation with CO ₂ capture	65
Figure 3-5: Validation of reforming model and its integration with the coal gasification process.....	66

Figure 3-6: Syngas composition at the outlet of reforming unit.....	67
Figure 3-7: Composition and heating value (MWth) of syngas at WGS inlet for case 1 and case 2.....	74
Figure 3-8: Power consumption break down for case 1 and case 2.....	79
Figure 3-9: Electricity generation from steam and gas turbine sections.....	80
Figure 3-10: Comparison of net power generation (MWe) capacity and efficiency of all cases.	83
Figure 3-11: The effect of coal water slurry ratio on syngas composition and heating values (Inlet of WGSR).....	88
Figure 3-12: Effect of O ₂ purity on the process performance	91
Figure 3-13: Effect of coal rank on syngas heating values for case 1 and case 2.....	93
Figure 3-14: Estimation of process performance for case 1 and case 2 for different coal ranks	94
Figure 3-15: Effect of CO ₂ capture rate on the process performance... ..	96
Figure 4-1: Investment payback time and cumulative cash flow estimation for case 1 and case 2.	107
Figure 4-2: Investment required and LCOE estimation for case 1 and case 2.	109
Figure 4-3: Sensitivity analysis of some un-certainty factors influencing LCOE.	110
Figure 4-4: Effect of fuel prices on the process economics of case 1.	111
Figure 4-5: Effect of coal and natural gas prices on O&M cost of case 2	112
Figure 5-1: Base Case Design for CO ₂ Injection.....	122
Figure 5-2: Relation between wellhead pressure and depth.....	125
Figure 5-3: CO ₂ hydrate curve assuming free water content	126
Figure 5-4: 2-Stage NH ₃ Rankine cycle.....	129

Figure 5-5: Ph diagram of 2-Stage Ammonia Rankine Cycle.....	130
Figure 5-6: Comparison of base case and the improved case	137
Figure 5-7: Energy Consumption of the Processes.....	138
Figure 5-8: Cost Estimation and Economic Analysis	139
Figure 5-9: Relation between well head temperature & specific energy	141
Figure 5-10: Effect of sea water temperature on the specific energy requirements	143
Figure 5-11: Effect of water content in CO ₂ stream on specific power requirements	144
Figure 5-12: Project life and its effect on the specific cost of CO ₂ injection.....	146

List of Tables

Table 2-1: Comparison of some power generation process.	14
Table 2-2: Comparison different power plants with and without CCS[15]	16
Table 2-3: Operating parameters of elevated and low pressure ASU ...	31
Table 2-4: Catalyst used for Sweet shift and Sour shift reaction.....	36
Table 2-5: Chemical Reagents used in AGR process.....	37
Table 2-6: Physical Solvents used in AGR process	38
Table 2-7: Fuel gas classification and calorific values[41, 42]	42
Table 3-1: Coal composition [37]	69
Table 3-2: Natural gas composition and NGCC process performance [37]	70
Table 3-3: Design Assumptions	71
Table 3-4: Stream flow rates during each section of the process	75
Table 3-5: Performance comparison with literature.....	86
Table 3-6: Overview of coal water slurry ratio on process performance	89
Table 4-1: Capital cost estimation	102
Table 4-2: Economic Assumptions	105
Table 4-3: Operational and maintenance cost estimation.....	106
Table 4-4: CO ₂ capture and avoided cost	114
Table 5-1: Base case specification	123
Table 5-2: Energy analysis of the top side injection system	132
Table 5-3: Capital cost estimation for the base case and 2-stage rankine cycle design	135

Chapter 1 : Introduction

1.1 Climate change and CO₂ emissions

Among various fossil fuels (coal, natural gas, crude oil, biomass, renewables, etc.), coal has been extensively used during the last many centuries for the purpose of power and electricity generation. As an important fuel that propelled the industrial revolution, coal has been widely used since the 1700s to drive steam engines, in the operation of blast furnaces for metal production, in the production of cement and in the generation of town gas for lighting and cooking. Since the late 19th century, coal has been used to power utility boilers for electricity generation. Although its dominance as an energy source was replaced by crude oil in the 1950s, coal is still the single most important fuel for electricity generation today.

Climate change and global warming are the widely discussed topics in the today's world. Both of these phenomenon pose a potential threat to not only the natural ecosystems but also to the human life. For years, the commercial efforts on clean coal processes have been centered on coal combustion for power generation to reduce the greenhouse gas (GHG) emissions. Various studies highlight the adverse consequences of GHG

emissions that includes the global temperature rise, increase of sea levels, flood, droughts and so on. The global GHG emissions can also be categorized on the basis of their sources. Approximately 25% of global emissions took place as a result of electricity and heat production, whereas, 21% emissions are directly associated with the industries. On the other hand, gasoline and diesel burning in the transportation section accounts for almost 14% emissions. It can be seen from analysis that ~60% of total emissions are directly connected with the power and electricity generation. *Figure 1-1* presents the brief overview of various sectors that are majorly involved in the GHG emissions.

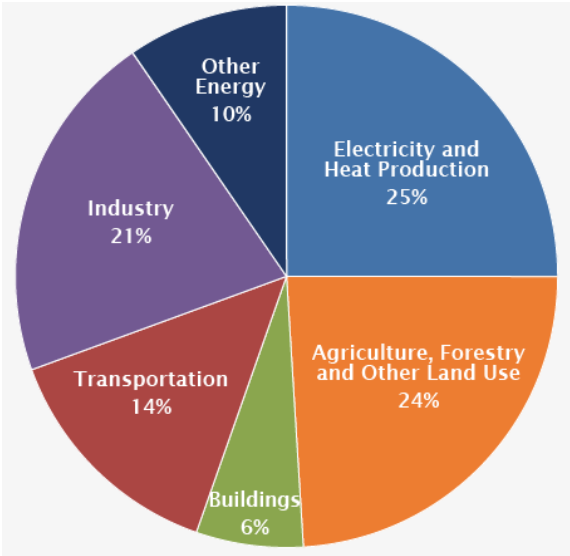


Figure 1-1: Greenhouse gas emissions by sector [1]

Moreover, the rapid growth of industry and population during the last few decades has also increased both the energy demand and pollution in the world. The conventional electricity and heat generation technologies relies on fossil fuels and accounts for nearly 42% of global CO₂ emissions [2]. *Figure 1-2* shows that carbon dioxide (CO₂), methane (CH₄), nitrous oxide (N₂O) and fluorinated gases (F-gases) are the major greenhouse gases responsible for global warming. Coal alone accounted for 46% of CO₂ emissions in 2013 and its consumption is expected to increase in the coming years to meet the world energy demand. However, coal fired power plants are also considered as one of the prime source of CO₂ emissions which is a primary cause of global warming. Therefore, power generation systems should be designed in a way to meet the world energy demand while addressing the environmental issues.

Greenhouse gas reduction can be achieved by increasing the power plants efficiencies, by decreasing power demand or by introducing the renewable energy sources with CCS (carbon capture and sequestration) technologies [4].

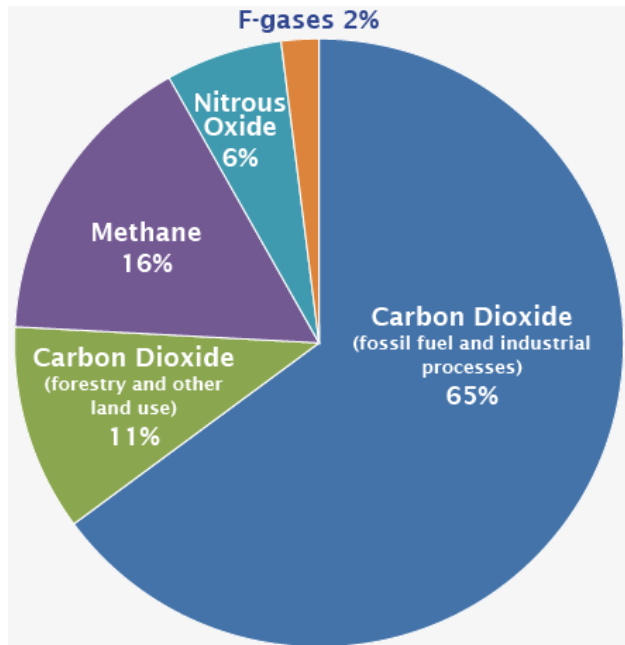


Figure 1-2: Global greenhouse gas emissions by gas [1]

CCS has been identified as a promising set of technologies to decrease the carbon emissions in the atmosphere. However, CCS implementation not only increases the financial and installation cost but also put energy penalties in terms of electricity production cost. CCS process consists of capturing carbon dioxide from the stationary point sources and transporting it to storage site for long term storage. CO₂ capture can be carried out in different ways depending on the type of solvent and mechanism used [5].

1.2 Research Motivation

The studies and reports published by International Energy Agency (IEA) and Intergovernmental Panel on Climate Change (IPCC) shows that GHG emissions are increasing at an alarming rate since the last few decades due to continuous increase in the electricity demand and will continue to increase if the emissions are not controlled. Most of the energy supply sector relies on fossil fuels for electricity and heat generation that accounts for almost 35% of total GHG emissions [3]. IPCC 2014 report on climate change also concluded that more than 75% of total GHG emissions contains CO₂. Coal is considered as one of the largest CO₂ emission sources in the energy sector that accounts for 40.58% of electricity generation in 2010. According to another report, the share of coal towards world energy output will increase by 33% in 2035 as compared to 2009 because of its abundant nature, affordability and an already existing infrastructure for power generation [4, 5]. Therefore, the power generation processes needs an improvement to enhance both the process efficiency while addressing the global warming issues. Currently operating post combustion carbon capture processes from coal would nearly double the cost of electricity (COE) while decreasing the net output by 7-10% [6]. Whereas pre-combustion processes have higher

capital investments but they are more energy efficient if CCS is implemented on large scale. IGCC power plants which is a commercial example of pre-combustion process provides an option to capture CO₂ with relatively low cost and less energy losses. Moreover, the integration of IGCC with the already developed processes has a potential to enhance the design robustness and process sustainability [7-9]. In this study, the conceptual design for integrating IGCC with the methane reforming process is proposed to enhance both the system reliability and sustainability while reducing GHG emissions.

1.3 Research Objectives

Integrated gasification and combined cycle (IGCC) technology has been developing since the last many decades, yet its commercialization for power generation still remains a major challenge. Numbers of previous studies reviewed the performance and economic analysis of IGCC technology for electricity generation with CCS techniques. However, the CAPEX, OPEX and the cost of electricity (COE) associated with the IGCC systems is still higher than the conventional coal fired power plants. Recently, the process integration and intensification methodologies have explored the new domain of enhancing the process

reliability while decreasing the overall investments. Therefore, this thesis is aimed to have following objectives:

- Development of all the essential unit processes associated with the IGCC technology to generate electricity.
- Integration of IGCC and methane reforming processes to enhance the process efficiency.
- To evaluate the key parameters that can affect the process performance and economics.
- To determine the pros and cons of process integration and its environmental impacts.
- Development of CO₂ transport and injection systems.
- Comparison of the developed model with the already existing systems.

1.4 Organization of Thesis

This thesis has been developed on the basis of two recently published articles by Ahmed et al. [8, 10] regarding IGCC process intensification and integration with the reforming technology, respectively. Moreover, some of the unpublished work included the CO₂ transport and injection systems for utilizing the CO₂ cryogenic energy. The thesis is organized

into six major sections. Chapter 1 represents the motivation and objective of this research as introduction. The brief overview of different coal based power generation systems and the associated GHG emissions is highlighted in this section. Chapter 2 contains the detailed literature review for the IGCC technology and the methane reforming processes for generating syngas. Chapter 3 represents the idea of integrating IGCC with the methane reforming process and its conceptual design. The IGCC process model is first developed and validated with the literature data. Then the conceptual design of integrating IGCC and reforming process is developed while highlighting their specific modelling techniques. This section also compares the process performance of both cases using some plant performance and environmental quality control indicators. Moreover, the sensitivity analysis has been performed on various process parameters to evaluate the reliability of the proposed design. Chapter 4 represents the detailed economic analysis to estimate the investment requirements, cost of electricity and cost of CO₂ capture for both cases. Chapter 5 discusses the CO₂ transport and injection systems and how the cryogenic energy in liquid CO₂ can be utilized to reduce the power consumptions of the process. Lastly, Chapter 6 represents the findings and conclusion of the thesis.

Chapter 2 : Overview of IGCC and Reforming Technologies

2.1 Background of IGCC power plants for abating CO₂ emissions

Gasification process which is also a key section of IGCC power plants have been developed over centuries for the production of syngas. Several refineries, fertilizer industries and chemical process industries have been using this technology for decades for specific purposes. Currently, more than 272 gasification plants are operating around the world that contain over hundreds of gasifiers. Gasification technologies find their applications in producing various chemicals, gaseous and liquid fuels and power production. *Figure 2-1* represents the current and future prospects of gasification technology [11].

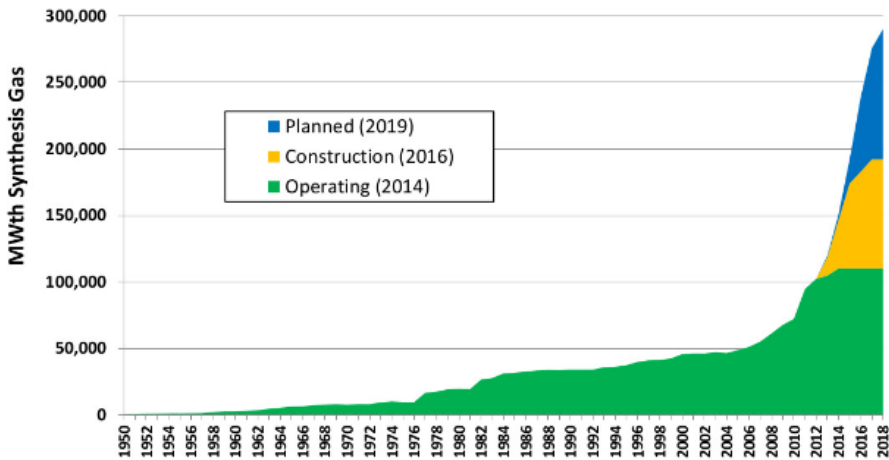


Figure 2-1: Cumulative worldwide capacity and growth

Integrated gasification combined cycle (IGCC) is a technology that itself is a combination of various process units which are combined together in order to generate electricity at higher efficiencies. The first coal fired IGCC power plant was demonstrated in 1972-1977 in Germany. This was followed by two more IGCC power plants in Cool Water (1984-1989) and Plaquemine (1987-1995) in USA. These projects were demonstrated to provide the operational and technical experience. This led to the construction of various large scale demonstration IGCC power plants in all over Europe and USA for the purpose of IGCC technology commercialization [12]. All these projects achieved or are expected to achieve the lowest levels of pollutant and air emissions.

IGCC technology can be used to produce both electricity and other fuels using multiple feedstocks while limiting the GHG emissions. As compared to the conventional pulverized coal (PC) power plant, gasification process provides great opportunity towards power plant efficiency and efficient removal of pollutants [13]. With the ability to produce gaseous product and the minimal environmental impacts, it has been widely used in the refineries and petro-chemical industries. *Figure 2-2* represents some of the feedstocks used in the gasification process where the share of coal remains at the top due to its large worldwide reserves [11].

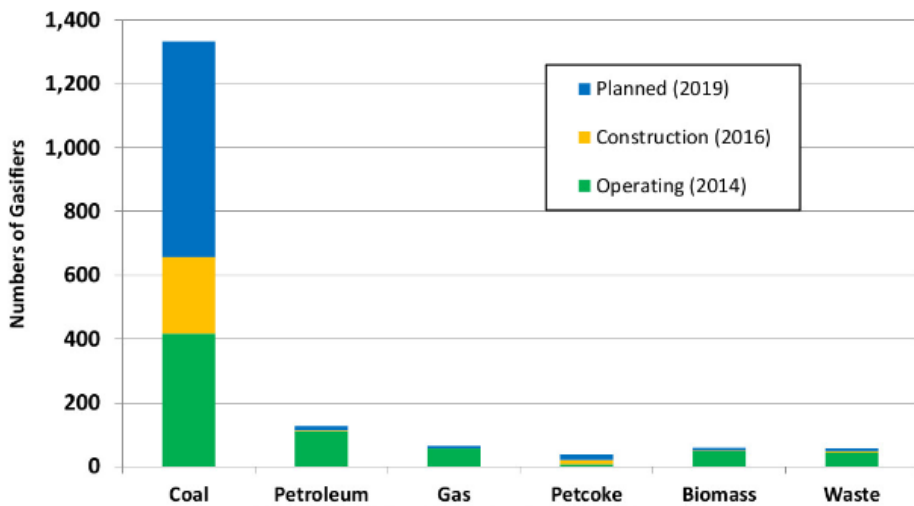


Figure 2-2: Number of gasifiers by primary feedstock

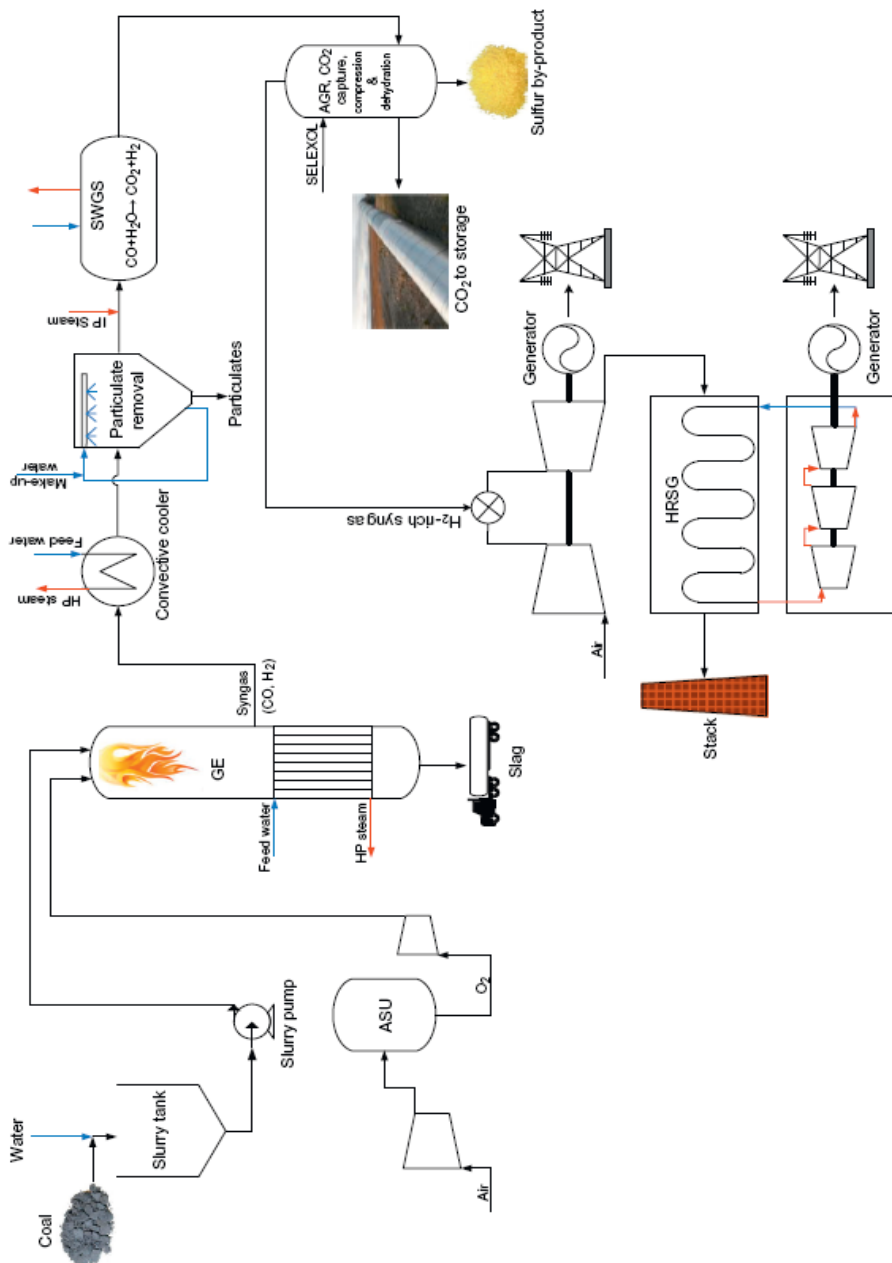


Figure 2-3: IGCC based energy conversion system concept

IGCC not only offers the less expensive CO₂ control mechanism but also offers to produce H₂ gas that can be utilized in various poly-generation processes [14, 15]. The general process flow diagram of IGCC process is represented in *Figure 2-3*. Gasification reactor converts the fuel into the gaseous state which can be purified from the impurities and burnt in the gas turbine to generate electricity. One of the key reaction in the IGCC power plants is the conversion of carbon mono-oxide into carbon di-oxide which can be captured in the CO₂ removal unit prior to its dilution with the air. Therefore, IGCC power generation processes have a potential to capture CO₂ at elevated pressures and at less cost compared to the other coal fired power plants.

It is also important to compare the performance and emissions of IGCC power plants with the other existing pulverized coal (PC) and oxy-fuel power plants. The PC power plants are equipped with a large scale heat exchanger network that uses steam as a working fluid. In PC power plants, coal is burned with air at ambient conditions and the heat generated during combustion is used to generate steam in the boiler. However combustion with air leads to decrease in partial pressure of CO₂ in the flue gas. Therefore huge volumes of flue gas has to be processed

to separate CO₂ that leads to higher operational costs. Typically 10-15% of the flue gas contains CO₂ while rest contains majorly N₂. On the other hand, oxy-fuel combustion processes offers higher partial pressure of CO₂ in the flue gas however main challenges with this technology is high energy costs associated with oxygen production and CO₂ separation from NO_x and H₂O in flue gas. *Table 2-1* shows the advantages and disadvantages between all the three processes.

Table 2-1: Comparison of some power generation process.

	Advantages	Disadvantages
Post combustion	<ul style="list-style-type: none"> • Applicable to the majority of existing power plants. • Retrofit technology option. 	Flue gas is: <ul style="list-style-type: none"> • Dilute in CO₂ • At ambient pressure Resulting in: <ul style="list-style-type: none"> • Low CO₂ partial pressure • Significantly higher performance or circulation volume required for high capture levels • CO₂ produced at low pressure compared to sequestration pressure.

<p>Pre combustion</p>	<p>Synthesis gas is:</p> <ul style="list-style-type: none"> • Concentrated in CO₂ • High pressure <p>Resulting in:</p> <ul style="list-style-type: none"> • High CO₂ partial pressure • Increased driving force for separation • Potential for reduction in compression cost and load. 	<ul style="list-style-type: none"> • Applicable to new plants <p>Commercial barriers:</p> <ul style="list-style-type: none"> • Availability • Cost of Equipment • Extensive supporting system requirement
<p>Oxy-fuel</p>	<ul style="list-style-type: none"> • High concentration of CO₂ in flue gas. • Retrofit and repowering technology option 	<ul style="list-style-type: none"> • Oxygen production cost and energy is still very high. • Higher SO_x, H₂O and O₂ content should be removed.

IGCC power plant's efficiency is generally higher than conventional subcritical PC plant if CCS is employed on large scale. *Table 2-2* shows the differences between IGCC power plant with PC and oxy-fuel power plants in terms of performance and energy penalties associated with and without CCS technology. The efficiency of PC power plants are estimated between 33% to 40% without CCS implementation however the efficiency drop of approximately 10% can be observed with CCS scheme. In case of IGCC process net plant efficiency is about 40% without CCS scheme however it decreases to 34% if CCS is implemented. It can be seen that energy penalties associated with IGCC process is only

19% whereas energy penalties associated with subcritical PC plants are as high as 40%[16]. Moreover IGCC power plants consumes roughly 30% less water as compared to PC power plants[17].

Table 2-2: Comparison different power plants with and without CCS[16]

Power plant type and capture system	Net plant efficiency (%) without CCS	Net plant efficiency (%) with CCS	Energy Penalty: Added fuel input(%) per net kWh output
Existing subcritical PC, post combustion capture	33	23	40%
New supercritical PC, post-combustion capture	40	31	30%
New supercritical PC, oxy-combustion capture	40	32	25%
New IGCC(bituminous coal), pre-combustion capture	40	34	19%
New natural gas combined cycle, post combustion capture	50	43	16%

Recently, a lot of research has been carried out in order to investigate the feasible designs for improvement in IGCC power plant efficiencies. As IGCC power plants are based on various sub sections so variation in any process can lead to increase or decrease in net power plant output and efficiency. For an instance, co-gasification techniques that employs the use of multiple fuels can be used to not only decrease ash fusion temperature but also oxygen consumption [18]. Coal gasification with

other feed stocks i.e. coke, sawdust, sewage sludge etc offers low SO_x and NO_x emissions while increasing hydrogen gas generation [19]. Cormos et al. [15] proposed a model of IGCC based on coal and biomass co-gasification technique for simultaneous production of electricity, H₂, synthetic natural gas (SNG) and fisher-tropsch (FT) fuel. Moreover low grade coals can be blended with the high grade coals in order to achieve the required syngas composition and the optimum slag viscosity [18]. While investigating the efficiency of IGCC power plant various CO₂ capturing mechanisms and solvents have been developed and analyzed. Urech et al. [20] comparative studies showed that there is a slight variation in the efficiencies of IGCC power plant while using different solvents. On the other hand, Padurean et al. [21] reported that the selexol process has least specific power and heating consumption as compared to other physical solvents. Kawabata et al. [22] proposed a model for IGCC with exergy recuperation that gives an efficiency of 33.2 % with 90 % CO₂ capture and 43 % without capture. Water gas shift reactions are used in conventional IGCC processes for increasing the production of the hydrogen gas however poor heat integration and catalytic poisoning may results in decreasing overall efficiency. Ferguson et al. [23] modified the water gas shift design in IGCC process and showed an

improved efficiency of 37.62%. Most of the previous researches were mainly focused on the optimization of the IGCC sub-processes [24, 25], while some studies attempted to optimize the whole IGCC plant [26, 27].

2.2. Process description of IGCC technology

IGCC technology is the complex integration of six major unit processes namely coal handling facility, gasification unit (GU) to generate syngas, air separation unit (ASU) to provide high purity oxygen, water gas shift reactor (WGSR), acid gas removal (AGR) unit to remove CO₂ and H₂S from the syngas and the combined cycle (CC) to generate power. The brief explanation of these sections are provided as follows:

2.2.1 Solid Handling Equipment

The coal handling facility contains the coal delivery systems mainly loading, conveying and storage equipment. For the IGCC power plants, coal is processed in various sub-sections i.e. coal crushing and grinding, screening, pulverizing and slurry making units. Depending upon the process need, coal can either be dried or coal-water slurry can be obtained. In the dry mode, coal should be dried enough to permit pneumatic transport without any risk of agglomeration or clogging. In some sub-bituminous and lignites, there is too much water that needs a

separate drying stage [6]. On the other hand, in case of slurry mode, coal is first crushed (usually in a cage mill) and then grinded in the presence of water in a ball or rod mill to obtain coal water slurry [28-30]. The generalized process flow diagram for coal handling facility is represented in *Figure 2-4*.

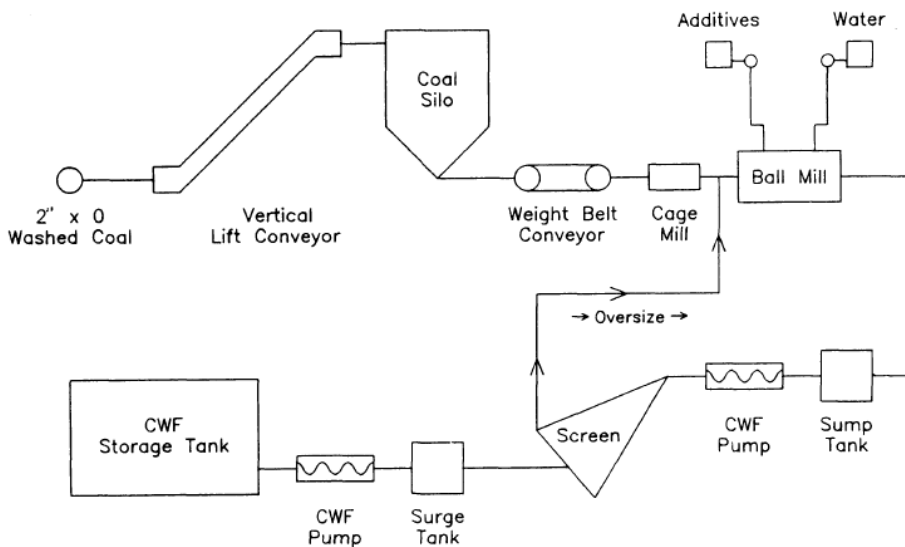


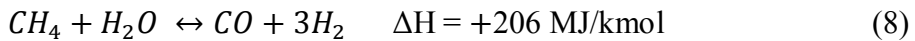
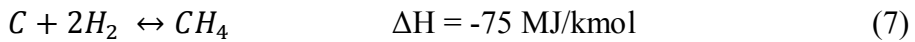
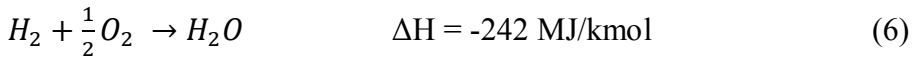
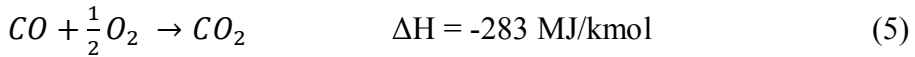
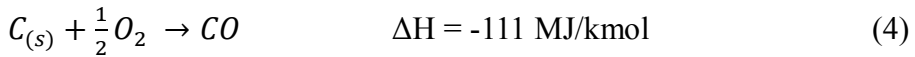
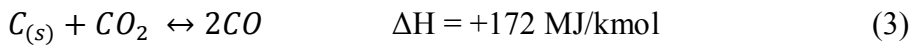
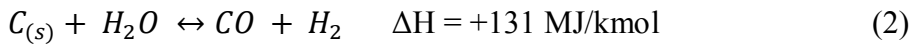
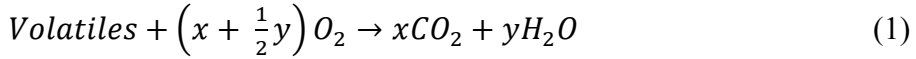
Figure 2-4: Coal handling facility [30]

2.2.2 Gasification Technology overview

The heart of the IGCC process is the gasification unit. During gasification process, solid (coal, biomass, carbonaceous material) or liquid fuels are converted into syngas through sub-stoichiometric reaction with oxygen or air between temperature ranges of 450-1650°C.

Fuel is fed into the pressurized reactor with a controlled and limited supply of high purity oxygen and steam. The chemistry of the gasification process is complex as it is associated with a series of endothermic and exothermic reactions. As the temperature in the gasification unit increases, the de-volatilization reactions took place and the weaker chemical bonds tend to break giving rise to yield oils, phenols, tars and hydrocarbon gases. Consequently, the fixed carbon left after the de-volatilization is gasified with the O_2 , steam, H_2 and CO_2 . The heat generated during the partial oxidation reaction is utilized in breaking the strong chemical bonds in the feed stock and other associated endothermic reactions [31]. All of these reactions results in the production of syngas which is a mixture of carbon-mono oxide (CO), hydrogen (H_2), carbon dioxide (CO_2) and water (H_2O). Syngas usually contains high concentration of CO and H_2 with a fraction of CO_2 and methane (CH_4). The formation of methane is an exothermic process that do not consume the oxygen, therefore, CH_4 concentration is relatively lower in the higher temperature systems. However, the increase in CH_4 concentration in the syngas can enhance the gasification efficiency. Some of the major coal gasification reactions are shown in the equations (1-8). Additional steam

is often added into the gasifier together with coal to increase syngas generation as shown in equation 2.



In this process, 20-30% chemical energy of the fuel is converted into heat to generate syngas whereas the rest 70-80% of it remains in syngas called as syngas efficiency. This energy can be extracted by burning syngas or transforming it to other valuable Fischer-Tropsch (FT) products. Coal gasification processes have been developing for years and currently more than hundreds of gasification system exists [32]. Depending upon the

coal and oxidant movement in the gasifier, three type of gasification technologies exists namely moving bed, fluidized bed and entrained flow bed. The brief explanation of each of the gasifier is given as follows.

2.2.2.1 Moving bed gasifier

It is the simplest and oldest type of gasifier that can be operated at an atmospheric pressure. Moving bed gasifier has four zone i.e. drying, carbonization, gasification and combustion. Coal is fed from top of the gasifier whereas the oxygen/air is introduced from bottom. The large size coal particles move slowly down the gasifier and reacts with the hot gases moving up to vessel. The drying zone is near the top of gasifier where the entering coal is heated and dried resulting in the cooling of the product gas leaving the reactor. As the particles moves down the gasifier, the de-volatilization reactions occur in the carbonization zone. Furthermore, as the coal particle passes through the gasification zone, the reaction between the de-volatilized coal particles with the steam and CO_2 takes place. Finally, the reaction between the char particles and oxygen takes place in the combustion zone which operates at a higher temperature. The gasifier can be operated in either dry-ash mode or the slagging mode. This gasifier offers larger residence time of feedstock and oxidant which results in formation of methane gas in syngas. Due to less

oxidant consumption in gasifier, the efficiency is usually higher. The syngas formed in the gasifier is at a low pressure with a temperature range of 425-650 °C. The temperature of the product gas is usually controlled by the moisture content of the incoming coal. For an instance, the lignite coal that contains higher moisture content would results in lower temperature of the product gas. On the other hand, bituminous coal which usually contains less moisture results in higher syngas temperature leaving the gasifier. Coarse coal particles have to be used to enhance bed permeability and to avoid chemical burning and pressure drop. The schematic of the moving bed gasifier is given in *Figure 2-5*. As the residence time of coal in the moving bed gasifiers is higher than the other gasifiers, the heating value of coal is transformed into the chemical energy of the syngas instead of the thermal energy of gas .Therefore, the cold gas efficiency of syngas from moving bed gasifiers is usually higher than the fluidized and entrained flow gasifiers.

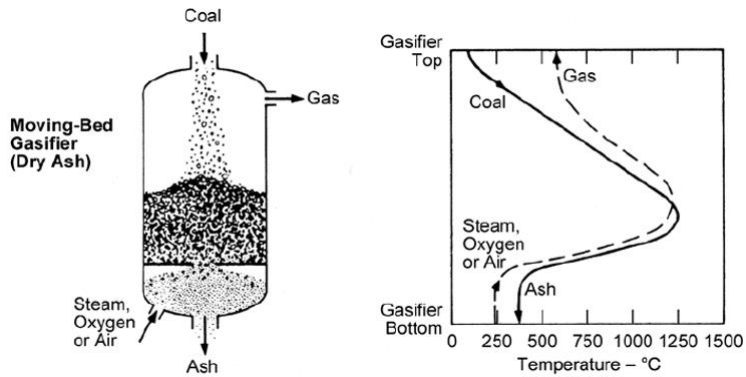


Figure 2-5: Moving bed gasifier

2.2.2.2 Fluidized bed gasifier

Fluidized bed gasifiers usually use high pressure oxygen/steam to suspend coal particles in the reactor bed. These type of gasifiers can be only used if coal is grinded to a very small size (<6 mm) to withstand the fluidization process. Fluidization can be achieved by feeding a high pressure oxidant or steam from the bottom of gasifier, whereas, the coal particles are fed from one side of the reactor. These gasifiers usually operates at high temperatures to achieve 90-95% of carbon conversion. However the temperatures are kept below the ash fusion temperature to avoid clinker formation that may result in de-fluidization. The fluidized bed reactors are usually used for the reactive coals (low rank) and biomass. Due to relatively less temperature than the entrained flow gasifier, some of the char particles remains un-reacted. Therefore,

fluidized bed gasifiers are associated with cyclone separators attached at the top of the gasifier that recycles the entrained char particles with syngas. Ash particles in fluidized bed reactors are collected at the bottom of the gasifier where they encountered with the incoming steam and the recycled gas. The syngas formed in this type of gasifier has a temperature range of 900-1050°C. The fluidized bed gasifiers has certain advantages that includes uniform and moderate temperature, ability to accept wide range of feedstocks, free of tar and phenol and moderate oxidant requirements. As compared to the moving bed gasifiers, these gasifiers offers shorter residence time among the oxidant and the coal particles. Some of the commercial available fluidized bed reactors include Winkler (HTW) and KRW designs. The simplest schematic of fluidized bed gasifier is given in *Figure 2-6*.

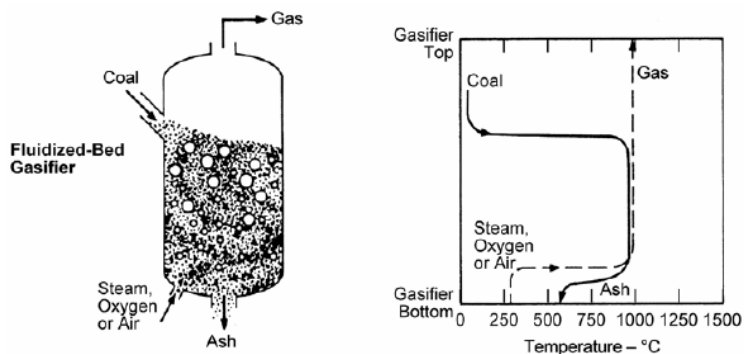


Figure 2-6: Fluidized bed gasifier

2.2.2.3 Entrained flow gasifier

Entrained flow gasifiers are best used in the coal-gasification applications as it allows all types of coals to gasify regardless of their rank and caking characteristics. They can be operated in either dry mode or slurry mode. In dry mode, the fine coal particles react with an oxidant and steam at higher temperature. On the other hand, coal water slurry can also be used to generate syngas. The selection of the operation mode depends on the end product. For an instance, the coal slurry process can generate a significant amount of steam during the gasification process which can be directly used in downstream water gas shift reactors, however, it also increases the oxygen consumption during the gasification process. On the other hand, dry process consumes less oxidant and allows the formation of syngas with higher hydrogen and carbon-monoxide ratio that ultimately increases the heating value of the produced syngas. Also in the dry mode, coal should be dried enough to permit pneumatic transport without any risk of agglomeration or clogging. In some sub-bituminous and lignites, there is too much water that needs a separate drying stage [6]. In the entrained flow gasifiers, the coal and oxidant are fed co-currently from the top of gasifier at higher pressures which results in turbulent flow leading to more than 99.5 %

carbon conversion to syngas. The residence time between the solid and gas particles is just few seconds but the reaction rate is extremely high. The schematic of the entrained flow gasifier is given in *Figure 2-7*.

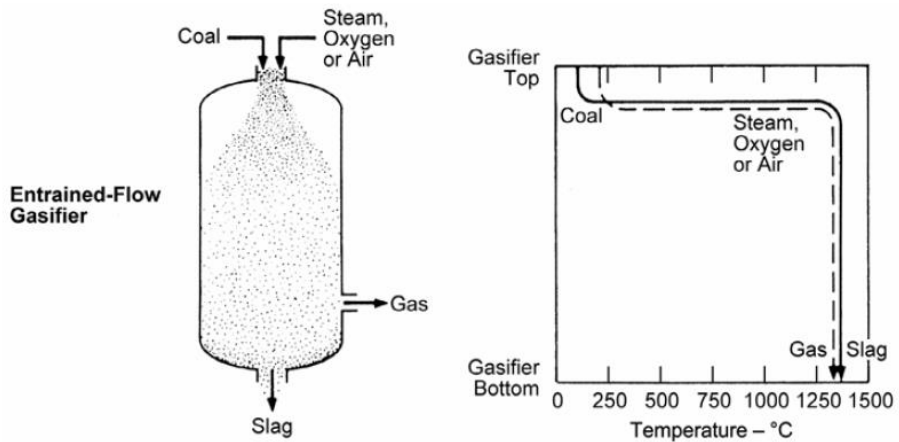


Figure 2-7: Entrained flow gasifier

The higher conversion of the coal particles is due to the fact of extremely small size of coal particles (<100um) and the higher operating temperature and pressure conditions (1600°C and 6.5MPa). The oils, phenols and other undesirable compounds formed in de-volatilization zone are readily decomposed to hydrogen and carbon-monoxide. Some of the key characteristics of the entrained flow gasifiers are as follows:

- Gasification ability irrespective of the coal rank.
- Uniform syngas and reactor temperatures
- Shorter residence time

- Consumes relatively large oxidants
- Increase sensible heat of raw gas
- Ash is obtained as slag
- Molten slag is entrained with syngas

Most of the commercially available gasifiers for IGCC power generation systems are entrained flow. Some of the companies that commercially provide the entrained flow gasification technologies include General Electric (GE), ConocoPhillips, Shell, Prenflo and Noell [33, 34]. *Figure 2-8* also represents the brief comparison between different gasifiers in terms [6].

Category	Moving-bed		Fluid-bed		Entrained-flow
Ash conditions Typical processes	Dry bottom Lurgi	Slagging BGL	Dry ash Winkler, HTW, KBR, CFB, HRL	Agglomerating KRW, U-Gas	Slagging KT, Shell, GEE, E-Gas, Siemens, MHI, PWR
Feed characteristics					
Size	6–50 mm	6–50 mm	6–10 mm	6–10 mm	<100 μm
Acceptability of fines	Limited	Injection through tuyères	Good	Better	Unlimited
Acceptability of caking coal	Yes (with stirrer)	Yes (with stirrer)	Possibly	Yes	Yes
Preferred coal rank	Any	High	Low	Any	Any
Operating characteristics					
Outlet gas temperature	Low (425–650°C)	Low (425–650°C)	Moderate (900–1050°C)	Moderate (900–1050°C)	High (1250–1600°C)
Oxidant demand	Low	Low	Moderate	Moderate	High
Steam demand	High	Low	Moderate	Moderate	Low
Other characteristics	Hydrocarbons in gas	Hydrocarbons in gas	Lower carbon conversion	Lower carbon conversion	Pure gas, high carbon conversion

Figure 2-8: Characteristics of different gasification technologies

2.2.3 Air Separation Unit (ASU)

Coal gasification processes usually require an oxidant and steam to carry out gasification reactions. Gasification can be carried out using air, oxygen or oxygen enriched air. The choice of the oxidant varies depending on the end use of syngas, degree of the system integration, type of gasification technology and the allowable nitrogen in the product gas. Usually, air-blown gasifiers do not need any air separation unit (ASU) but they result in high concentration of N_2 in the syngas. On the other hand, oxygen blown gasification systems have several advantages over the air-blown gasification systems. Usually the syngas produced from oxygen blown gasifiers have the heating value of 250-400 Btu/scf, whereas, the air blown gasifiers produce the syngas of heating value of 90-170 Btu/scf. The syngas with an average heating value can be used instead of natural gas in the gas turbines to generate electricity. Due to less volume of oxidant requirement in case of oxygen blown processes, the size of the gasification unit and the associated auxiliary systems also reduces. Moreover, the cold gas efficiency of syngas is approximately 7-10% higher in case of oxygen-blown processes compared to the air-blown processes. While comparing both the technologies, it has been

seen that air-blown gasification processes offers more operational difficulties in gas cleaning and turbine operation process.

ASU's are the most expensive part of the IGCC projects which together with compressors, turbines and heat exchangers imparts about 10-15% of total plant cost. About 5-7% of the total power generated in IGCC plant is utilized by ASU during air compression. Cryogenic units, pressure swing absorption and polymeric membranes are the few techniques for air separation purposes. Most extensively and large scale air separation units are based on cryogenic air separation technique. Cryogenic plants can have the oxygen production capacity of more than 5000 t/d with the oxygen purity level of above 99% [35]. Pressure swing adsorption units for air separation purposes can be employed for a small scale plants (140t/d) where oxygen purity up to 95% is acceptable [36]. Polymeric membranes are also attaining a lot of research attention but their capacity of oxygen production is still very low. IGCC power plants consumes huge amount of oxygen and nitrogen at elevated pressures so cryogenic air separation technology is usually used. Depending upon the oxygen purity requirements and delivery pressure, the energy consumption of the ASU also varies. ASU can be further divided into

low-pressure (LP) ASU and elevated-pressure (EP) ASU based on their operating pressures[37]. Some of the operating parameters for LP-ASU and EP-ASU are shown in the *Table 2-3*.

Table 2-3: Operating parameters of elevated and low pressure ASU

Component	Pressure (atm)	EP ASU Temperature (°C)	LP ASU Temperature (°C)
N ₂	4 - 7	--	Minus 174 – minus 181
O ₂	4 - 7	--	Minus 159 – minus 167
N ₂	10-14	Minus 153 – minus 148	--
O ₂	10-14	Minus 164 – minus 169	--

The cryogenic air separation unit is usually associated with the main air compressor and a pre-purification unit. Air is compressed to an elevated pressure and passed through a series of molecular sieves to remove moisture and dust particles. It is then cooled to its liquefaction temperature and distilled into two main constituents, oxygen and nitrogen. These separated products can be kept into the liquid form or heated to get vapors as required by the process[36]. The simplified flow scheme of an ASU is shown in *Figure 2-9*.

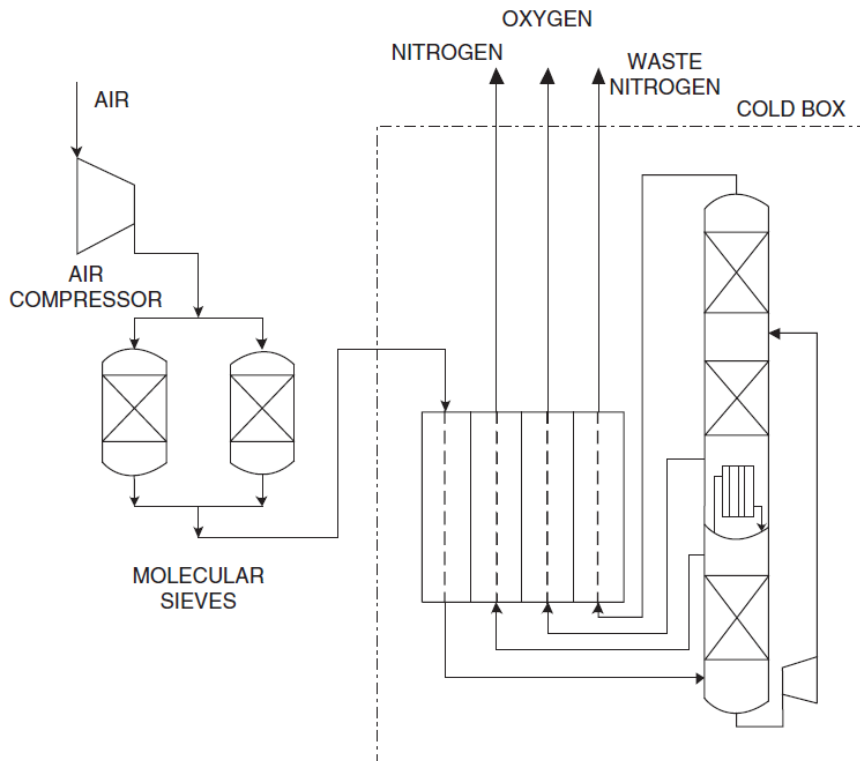


Figure 2-9: Simplified air separation unit (ASU) flow scheme[13]

2.2.4 Syngas cooling

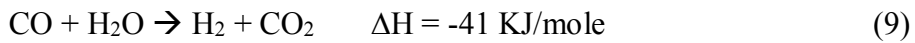
Syngas leaving the gasifier is usually at a temperature a temperature range of 600-1800 °C, so the syngas is cooled for cleanup and meet the downstream process requirements. Two type of methodologies that can be employed for syngas cooling are water quenching and radiant cooling or sometimes can be used in combination. Water quenching is the simplest configuration and requires least capital. The syngas is quenched

with water to decrease the temperature close to 250-270 °C while generating extra steam that could be used in water gas shift reactions, however, this process is considered as least efficient. On the other hand, radiant only design first decreases the syngas temperature to 800-850 °C in the radiant cooler followed by a water quench to decrease the temperature to 200 °C. This methodology offers higher process efficiency compared to the quench only design with an increased process reliability [38].

2.2.5 Water Gas Shift Reactor (WGSR)

Water gas shift (WGS) conversion is a chemical reaction that converts CO and H₂O to an equivalent amount of H₂ and CO₂ in the presence of catalyst. WGS reactions are stoichiometric in nature as shown in Equation (9) however concentration of steam is usually kept high to achieve maximum CO conversion and to maintain reactor bed temperature. Coal gasification power plants leads to high volume of CO in the syngas, so steam requirements are significantly increased in order to maintain the minimum inlet steam/CO ratio. These reactions are exothermic in nature so their equilibrium constant decreases with the increase in temperature thereby low CO conversion is achieved at

elevated temperatures. However these reactions are faster at high temperatures.



Depending upon the H_2S concentration in the syngas, WGS reactions can be carried out in two ways i.e. sweet shift or sour shift. Both of these processes are shown in Figure 2-10. If the sulfur (H_2S) is removed from syngas prior to the WGS reactor, it is called sweet shift conversion whereas if the sulfur (H_2S) is removed after WGS reactor then it is called as sour shift conversion process. Furthermore shift reactions are usually carried out in two reactors i.e high temperature shift reactor (HTS) and low temperature shift reactor (LTS), installed in series with an intermediate heat exchanger to remove heat. Usually 90% conversion of CO is achieved in the HTS reactor whereas the remaining conversion is achieved in LTS.

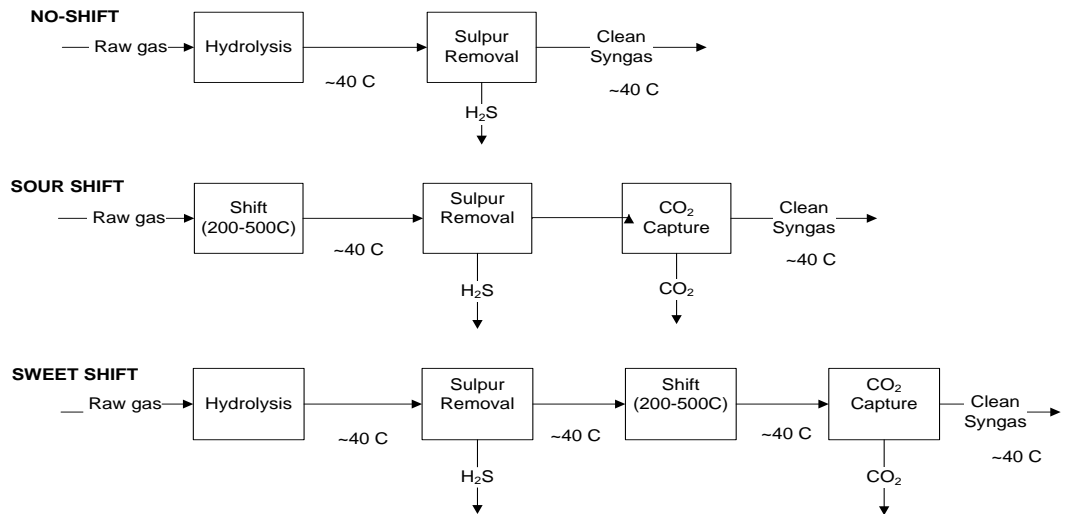


Figure 2-10: Comparison of Sour and Sweet shift catalytic process

WGS reactions are carried out in the presence of catalyst and several types of WGS catalyst are commercially available, however the three most commonly used are shown in *Table 2-4*. The sour shift process is more energy efficient as compared to sweet shift because no alternate heating and cooling is required in the process. In sweet shift process, syngas is cooled to 40°C for sulfur removal and then reheated to 200°C for shift reactions and then again cooled to 40°C for CO₂ removal. Due to alternative heating and cooling requirements for the process conditions, heat losses occur during each transition.

Table 2-4: Catalyst used for Sweet shift and Sour shift reaction

	Active Component	Operating Temperature (°C)	Sulphur content (ppm)
HTS Catalyst	Fe ₃ O ₄ with Cr ₂ O ₃	350-500	< 20
LTS Catalyst	Cu with Zn and Al ₂ O ₃	185-275	< 0.1
Sour Shift Catalyst	Sulphided Co and Mo (CoMoS)	250-500	> 1000

2.2.5 Syngas clean up

Gasification of coal produces syngas that must be treated prior to its utilization. Acid gas removal (AGR) section mainly contains H₂S removal section and the CO₂ removal section. Environmental target of IGCC power plants is 0.0128lb SO₂/MMBtu, which requires the sulfur content in syngas to reduce by 30ppmv [38]. There are several commercially available processes that can be used to remove acid gases. These processes can be differentiated on the type reagents used: chemical solvents, physical solvents or hybrid solvents [38, 39]. Some of the chemical and physical reagents are shown in *Table 2-5* and *Table 2-6*.

Table 2-5: Chemical Reagents used in AGR process

Chemical Reagent	Acronym	Process Licensors
Monoethanolamine	MEA	Dow, Exxon, Lurgi, Union
Diethanolamine	DEA	Elf, Lurgi
Diglycolamine	DGA	Texaco, Fluor
Triethanolamine	TEA	AMOCO
Diisopropanolamine	DIPA	Shell
Methyldiethanolami	MDEA	BASF, Dow, Elf, Snamprogetti, Shell, Union Carbide, Coastal
Hindered amine		Exxon
Potassium	“hot pot”	Eickmeyer, Exxon, Lurgi, Union Carbide

Chemical solvents are more suitable than physical solvents for the processes operating at ambient pressures. The chemical nature of solvents make solution loading and circulation less dependent on the partial pressure of the acid gases. Moreover as the solution is aqueous, co-absorption of hydrocarbons are minimal. For example, in conventional amine unit, the chemical solvents reacts exothermically with an acid gas. They usually makes a weak bond that can be easily broken during regeneration process. Each chemical solvent has its own operating conditions. The absorption temperature is kept below 50°C however the regeneration temperature is usually 130°C. The major advantage of this process is that it allows to remove acid gas to low level

at moderate partial pressure. However main disadvantage of this process includes higher regeneration energy of solvent and re-boiler's heat duty.

Table 2-6: Physical Solvents used in AGR process

Solvent	Trade Name	Process Licensors
Dimethyl ether of poly-ethylene	Selexol	UOP
Methanol	Resticol	Linde AG and
Methanol and toluene	Resticol II	Linde AG
N-methyl pyrrolidone	Purisol	Lurgi
Polyethylene glycol and dialkyl ethers	Sepasolv	BASF
Propylene carbonate	Fluor Solvent	Fluor
Tetrahydrothiophenedioxide	Sulfolane	Shell
Tributyl phosphate	Estasolvan	Uhde and IFP

Physical solvents are organic in nature and have high solubility for acid gases. These solvents work on the basis of Henry's law. Higher the partial pressure of acid gas in syngas, higher will be the absorption. The pressure swing absorption technique is employed where absorption takes place at elevated pressure whereas desorption takes place by reducing pressure in multistage flash drums. Physical solvents operates at lower temperature to compare to the chemical solvents so solvent refrigeration is usually required to enhance the absorption rate. In IGCC

process, acid gases in the syngas are at higher partial pressures so physical solvents are used for their efficient removal. The recent studies showed that the selexol process is the most efficient process for removing acid gases as it requires less energy for removing unit mass of CO₂ [40]. A simplified process flow diagram of the AGR section using selexol process is shown in *Figure 2-11*.

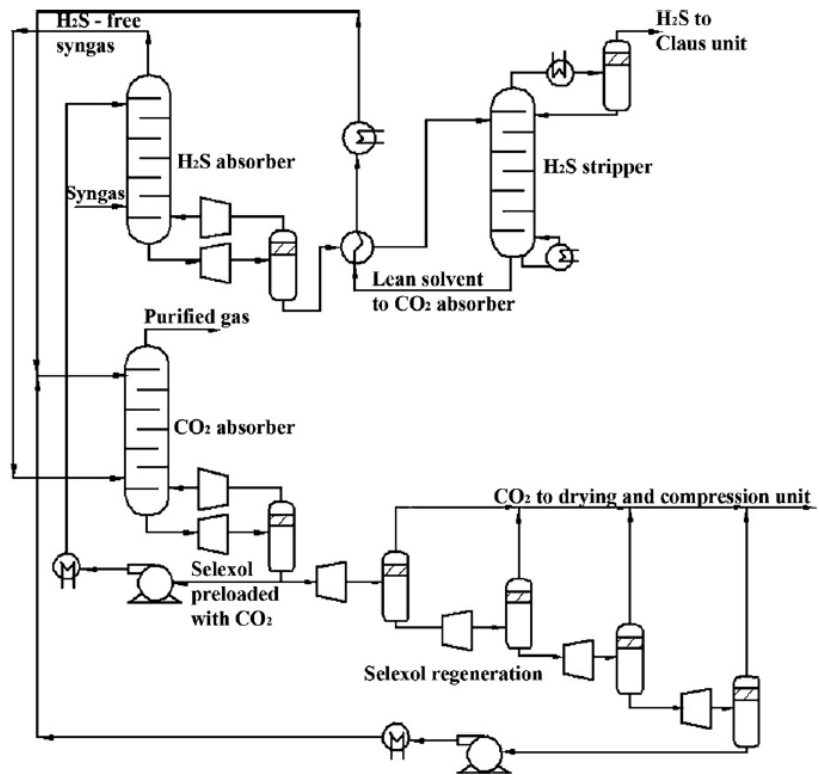


Figure 2-11: Simplified selexol process flow diagram for AGR

2.2.6 Combined Cycle Power Generation

The CC section is responsible for electricity generation where Brayton and Rankine cycles are integrated to achieve higher thermal efficiencies with maximum power output. It comprises of topping gas turbines section and bottoming steam turbine with heat recovery steam generation (HRSG) systems. The simplest flow diagram of CC is shown in *Figure 2-12*. The gas turbine unit consist of combustor, compressor and a gas turbine. The air/oxidant is compressed and introduced into the combustion chamber where syngas combustion takes place. The flue gas produced in combustion chamber with a high pressure is fed to gas-turbine to convert its pressure energy into shaft work. To achieve higher efficiency of the CC, gas turbines are associated with complex heat recovery steam generation cycle (HRSG) section involving multiple pressure boilers and steam turbines. Combined cycles with only

electricity power have thermal efficiencies between 50-60% using advanced gas turbines.

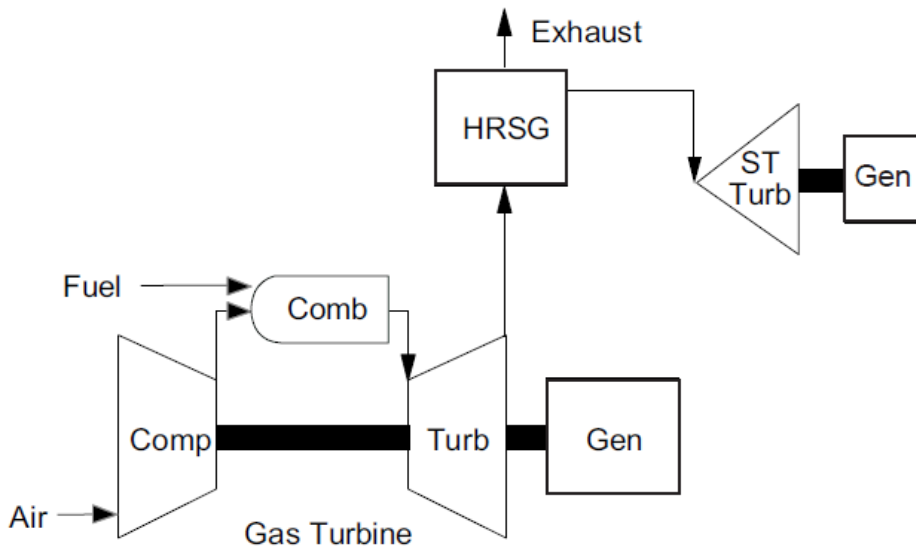


Figure 2-12: Combined Cycle flow diagram

Generally, natural gas combustion turbines have been used in industries as a primary fuel. However, in IGCC power plants, syngas with the varied calorific values ranging from 100 Btu/ft³ to 5000BTU/ft³ are generated. *Table 2-7* highlight various fuels according to their calorific values. Comparing with the natural gas, syngas offers ~50% less calorific value so huge volumes of syngas is required to meet the minimum requirement of the energy input to the gas turbine. Consequently, these

turbines typically have large assemblies and associated equipment for handling large volumes of syngas to maintain process conditions[38]. Moreover keeping in view the economics of process, gas turbine section is one of the most expensive part of an IGCC power plant so advances in gas turbines has a potential to both increase efficiency of power plant and to decrease cost of electricity. Heavy duty “F class” turbines are currently the state of art technologies that are used in refineries and IGCC power plants [41].

Table 2-7: Fuel gas classification and calorific values[42, 43]

Classification by calorific value	Calorific value kcal/nm³ (Btu/scf)	Specific fuels	Primary gas components
Very high	10700-44500 (1200-5000)	Liquefied Petroleum	Propane Butane
High	7100-10700 (800-1200)	Natural gas, SNG, Sour gas	Methane
Medium	2700-7100 (300-800)	Coal Gas (O ₂ blown) Coke Oven gas Refinery gas	H ₂ , CO, CH ₄
Low	900-2700 (100-300)	Coal gas (air blown)	CO, H ₂ , N ₂
Very low	Under 900	Blast Furnace gas	CO, N ₂

The modern gas turbines can withstand the temperature up to 1600°C however typical operating range of temperature for gas turbines is maintained at 1350°C to avoid NO_x production. To increase the life

time of turbine blades, temperature of flue gas entering the gas turbine is controlled by injecting excess air or nitrogen. Moreover moisture content in the flue gas should be maintained less than 12-15% to avoid erosion of turbine blades. Depending upon the gas turbine efficiency and pressure ratio, flue gas comes out of the gas turbine at a temperature range of 450-650°C. It is then passed through the series of heat exchangers and boilers to generate steam. The steam cycle consists of heat recovery steam generation (HRSG) section, steam turbine with alternator, cooling system and an auxiliary system. HRSG is entirely a convective heat exchanger package that consists of tubes having pressurized steam or water on the tube side with an exhaust gas on the shell side. The process involves an economizer that raises the temperature of water close to its boiling point. Economizer is followed by boiler to generate saturated steam which is further followed by super heaters to generate superheated steam.

HRSG section is designed on the basis of pinch point and minimum approach temperature differences to utilize heat efficiently and effectively. The smaller pinch point reflects the higher efficiency of steam cycle however the approach temperature range is kept between 5-12°C. Steam turbines are similar to gas turbines however the working

fluid for either turbine is different. In a steam turbine high enthalpy (high pressure and temperature) steam is expanded in nozzles where the kinetic energy of steam particles is increased at the expense of decreasing pressure. The expansion of steam in steam turbine is performed in several stages associated with steam reheating and moisture removal mechanism prior to enter in the next stage. However in gas turbine, high pressure exhaust of flue gas is passed through turbine blades and its pressure energy is converted into shaft work to generate electricity.

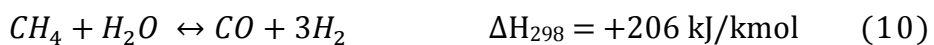
2.3 Overview of Methane Reforming Process

Methane reforming processes for syngas generation is a mature technology and has been used in process industries for the last many decades. Methane reforming is the most economical techniques for the production of H₂ gas. For instance, around 95% of total hydrogen generation in United States is through natural gas reforming [44]. The most extensively used techniques for natural gas reforming involves steam reforming (SMR), partial oxidation (POX) and dry reforming (DMR). Moreover, these techniques can also be used in combination as mixed reforming (SMR+DMR), tri-reforming (SMR+DMR+POX) and auto-thermal reforming (SMR+POX). The selection of a particular

reforming technology depends on many considerations such as feedstock, process parameters, catalyst and downstream product quality requirements. The brief overview of these methodologies is given as follows.

2.3.1 Steam Methane Reforming

Steam methane reforming (SMR) technology is the most widely used technique for commercial production of H₂ gas. SMR is an endothermic process which is carried out by reacting high enthalpy steam with the methane gas at a temperature and pressure range of 700-1000°C and 3-30 bar, respectively, as shown in Equations 10-12. Reforming process is usually carried out in two sequential steps i.e. pre-reforming and reforming. Firstly, the compressed methane is heated and mixed with a high enthalpy steam in a pre-reforming section. Then the mixture is allowed to pass over the nickel based catalyst in the reformer section to generate H₂ [45]. Usually, SMR reactions yield the higher amount of H₂ with an overall H₂/CO ratio of 3:1 in the syngas that could also be used in various poly generation processes involving Fischer-Tropsch (FT) reactions and GTL (gas-to-liquids) techniques.





Typical SMR processes requires an additional heat source for preheating the gas stream to assist the reforming process. Usually SMR processes yield higher H₂/CO ratio, however, the CO generated in the process is further converted into H₂ and CO₂ by water gas shift reactions as mentioned in the previous section. Typical steam methane reformer [46] is represented in *Figure 2-13*.

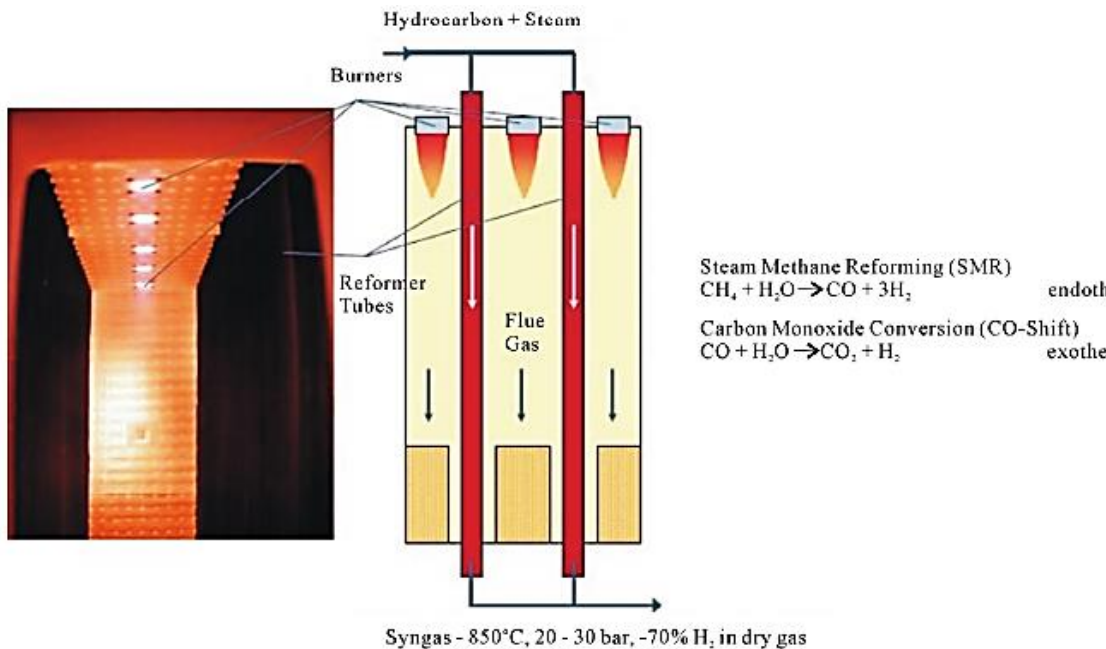


Figure 2-13: Tubular SMR unit [46]

2.3.2 Partial Oxidation

Another commercial technique for syngas reforming is the partial oxidation (POX) of hydrocarbons. The POX of methane occurs when the sub-stoichiometric fuel-air mixture is oxidized or combusted in the limited supply of oxidant (high purity oxygen). Usually, the partial oxidation reactions are exothermic and requires less thermal energy, however, the energy required to produce pure oxygen is an energy intensive process. The partial oxidation reactions produces syngas with a H₂/CO ratio close to 2:1 as given in Equation 13. It can be seen from reactions the slight increase in the oxidant flow rate would lead the process from partial oxidation to complete combustion as shown in equation 14 and equation 15 which can incur process instabilities [47].



While comparing the SMR and POX, it has been seen that POX reactions yield less amount of H₂. Moreover, the co-feeding of CH₄ and O₂

mixtures would also lead to an explosion if the process conditions are not maintained precisely.

2.3.3 Dry Reforming (DMR)

Dry reforming also called as CO₂ reforming is a technique in which carbon dioxide reacts with the hydrocarbon such as methane. Dry reforming yields higher quantity of CO in the product gas with an overall H₂/CO ratio of 1:1. Since CO₂ is available in excess amount and also incurs global warming, the efficient use of this methodology can help in reducing CO₂ emissions while generating syngas. The dry reforming reaction is given in Equation 16.



Dry reforming is an endothermic process [48] and takes place in the presence of catalyst, however, it requires more energy compared to the SMR processes. Moreover, the problems associated with the catalyst deactivation due to carbon deposition also pose operational difficulties.

2.3.4 Auto-thermal Reforming

Auto thermal reforming is the combination of best features of steam methane reforming and partial oxidation reactions [49]. It combines the heat effects of both the reforming techniques by injecting fuel, steam and

oxidant together in the reactor. The heat generated from the partial oxidation reactions are absorbed by the steam methane reforming reactions. This process require less steam for the SMR reactions and practically consumes all the heat generated during partial oxidation (combustion) of fuel.

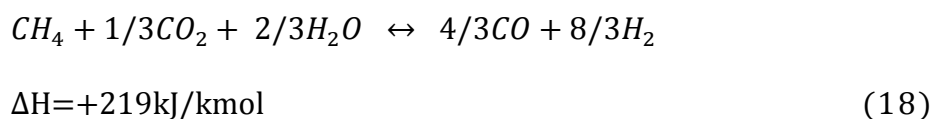


While comparing with the SMR technology, the auto-thermal reformer do not require an external heat source or in-direct heat exchanges which makes its design more compact and reduces the capital cost. Moreover, the simultaneous heat consumption from the POX reactions by SMR reactions also reduces the risk of forming hot spots.

2.3.5 Mixed Reforming

Mixed reforming is a combination of SMR and DMR techniques to generate the syngas with an adjusted H₂ and CO ratios [46]. As both the technologies comprises of endothermic reactions in the presence of noble catalysts, the overall thermodynamic of this mixed reforming methodology is commercially un-favorable. However, the key advantage of using this technique include the CO₂ utilization that can help in reducing greenhouse gas emissions and also it has a potential to reduce

the carbon deposition rate on the catalyst bed which would be otherwise very high in case of standalone DMR process. Moreover, there are certain applications where the H₂/CO ratio in the syngas needs an adjustments which can be achieved without using any other unit (WGSR). Usually, SMR methodology helps in generating higher H₂/CO ratios close to 3:1 which is certainly high for some FT chemical. On the other hand, DMR technique generates the less H₂/CO in the syngas close to 1:1 so the combination of SMR and DMR techniques can be used in achieving the required ratio [50].



2.3.6 Tri-Reforming (TRM)

Tri-reforming (TRM) is the coupling of SMR, DMR and POX techniques. The combination of these three methodologies in a single reactor can provide the desired syngas composition with more energy savings and better control of greenhouse gas emissions [51]. Depending on the end use of the syngas, it can be integrated with the other processes (coal gasification, production of FT chemicals, poly-generation processes, etc.). Recently, TRM technique has been tested on commercial scale in

South Korea by Korean Gas Company (KOGAS) [52]. *Figure 2-14* represents the brief overview of the methane reforming techniques in terms of syngas composition. It can be seen that SMR techniques provides the highest, whereas, DMR techniques provide the least H_2/CO ratios in the syngas [46].

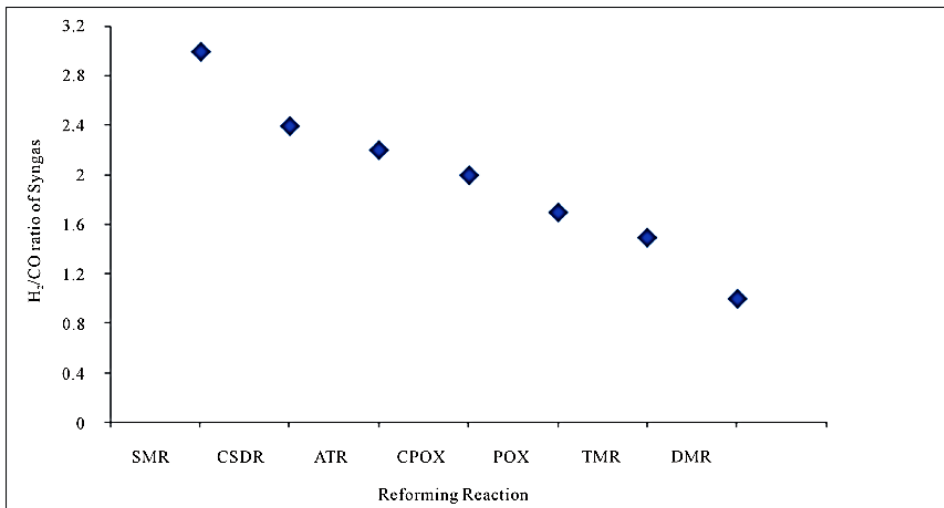


Figure 2-14: H_2/CO ratio of syngas for various reforming techniques

2.4 Summary

IGCC and methane reforming processes have been commercially used for the last many decades to produce both the syngas and electricity. The syngas can be cleaned and processed to generate various FT fuels or can be directly use for power production. IGCC technology mainly utilizes the coal as a raw material for syngas production with low H_2/CO ratios,

whereas, reforming processes requires natural gas to generate syngas with higher H_2/CO ratios. Although standalone NGCC processes utilizing natural gas shows higher thermal efficiencies with the CCS technologies but the higher cost of the natural gas limits its large scale implementation for power generation purposes. Therefore, there is potential to utilize both the coal and natural gas in a single IGCC process to increase the syngas generation capacity while limiting the extensive natural gas consumption. Utilizing coal as the major raw material in a single process may improve the overall economics, whereas, natural gas utilization can enhance both the syngas generation capacity and process performance. Moreover, the process integration and intensification opportunities between the IGCC and natural gas reforming processes can also enhance the overall process reliability and sustainability.

Chapter 3 : Simulation Methodology and Performance Analysis

3.1 Overview & Concept Development

Currently, the most common power generation technologies include ultra-supercritical pulverized coal (USPC), natural gas combined cycle (NGCC) and integrated gasification and combined cycle (IGCC) power plants. However, the efficiency of power plants tremendously drops with the addition of CCS technology to the system. For an instance, NGCC, USPC and IGCC power plants show an efficiency drop of 7.1%, 11.4% and 9%, respectively with a retrofit of CCS technology [53]. The addition of CCS to existing power plants not only affect the performance but also cause an increase in the cost of electricity (COE). For an example, IGCC, NGCC and USPC offer an increase of 39%, 43% and 78%, respectively in the cost of electricity with an addition of a CCS technology [53]. Although, NGCC power plants with CCS technologies have the highest operational efficiencies, yet the increase in COE together with the fluctuating cost of natural gas limits its extensive utilization over the coal based power plants. IGCC has been identified as one of the most viable options among other coal based power plants in terms of lower

environmental impacts with the better control on GHG emissions. It offers higher process efficiencies with lower COE compared to the conventional USPC power plants with CCS technologies [38]. Therefore, improving the performance of IGCC process to make them more reliable and sustainable has been under research for the last many decades. Amirabedin et al. [54] evaluated the performance of IGCC power plants using exergy analysis for various type of coals and compared the results in terms of CO₂ emissions. Kawabata et al. [22] proposed an exergy recuperation technique for enhancing the cold gas efficiency of syngas using exhaust heat from steam and gas turbines in the gasification section. Man et al. [55] compared the IGCC power plants in terms of technical, economic and environmental aspects with CCS and CCU (carbon capture and utilization) technologies for reducing the carbon footprint. Gharaie et al. [56] optimized the operating conditions and integrated the utility system with IGCC for maximizing the power generation capacity. Ferguson et al. [57] and Carbo et al. [25] enhanced the IGCC process performance by improving the heat exchanger network design. Urech et al. [58] and Paduran et al. [40] evaluated the specific heat requirements for various solvents (Selexol, Restisol, Purisol, MDEA) used for CO₂ capture and compared their effect on overall IGCC process performance.

Similarly, co-gasification of coal with other feed stocks and with an option of poly-generation processes helped in improving the reliability and economics of the process [14, 18, 59, 60].

Another technology for syngas generation is the methane reforming process. The most commonly used methane reforming processes include steam reforming (SMR), dry methane reforming (DMR), mixed reforming (SMR + DMR) and auto-thermal reforming (ATR). The selection of a particular reforming technology depends on many considerations such as feedstock, process parameters, catalyst and downstream product quality requirements. Most of the previous studies focused on the standalone modelling and simulation of IGCC and reforming processes for the syngas and power generation. However, little attention has been paid towards their integration in a single process to improve the process performance and/or economics. Process optimization [26, 61], intensification [8, 62] and integration [24] with the already existing technologies can help in developing a more sustainable energy production systems with CO₂ capture that can improve the process economics in terms of COE. Recently, an integration of IGCC and natural gas reforming processes are gaining a lot of attention for increasing the H₂/CO ratio in the syngas. Qian et al [51] coupled the coal

gasification with tri-reforming process to increase the H_2/CO in the syngas for methanol production. Similarly, Yi et al [63] performed the techno-economic assessment of integrating coal gasification and DMR processes for enhancing the syngas production which can be used in various poly generation processes. Adams et al. [7] explored the design routes for integrating IGCC with methane reforming processes and compared them in terms of both process performance and economics. It has been further seen that the integration of coal gasification and reforming processes has a potential to enhance the design robustness and process sustainability [7]. Most of the previous studies referring IGCC integration with reforming processes utilized an additional steam and CO_2 to carry out SMR and DMR reactions, respectively. Also, by integrating gasification and reforming process, process intensification opportunities have not been explored in the previous studies. In this study, the conventional IGCC process model has been developed first followed by development of conceptual design for integrating IGCC and natural gas reforming process. The conceptual model utilizes the process heat and steam from the syngas to assist the reforming process without an external source. Moreover, this study also includes the techno-economic investigation of proposed process and its comparison with the existing

technologies to understand the effect of process intensification on economics in terms of COE.

3.2 Development of Process Models

3.2.1 IGCC Process Model with CO₂ Capture (Case 1)

Case 1 is the conventional IGCC process which is considered as the base case design in this study [38]. The simplified process flow diagram of base case design is shown in *Figure 3-1*. Entrained flow gasification methodology is adapted as it can be operated at high temperature and pressure ranges with an ability to handle wide variety of feedstocks (coal, biomass, liquid fuel) [6]. Syngas produced in the gasification unit is at a very high temperature (~1600°C) and contains high concentration of H₂ and CO. The temperature of the syngas is reduced to 250°C in the radiant and convective heat exchangers to carry out WGS reactions. WGS reactions are also stoichiometric and requires an equivalent amount of steam to convert CO into H₂ and CO₂. However, practically steam/CO ratio is kept higher to avoid carbon deposition on the catalyst bed and to achieve maximum CO conversion [64, 65]. A steam/CO ratio of 2.2 is used in this study to achieve CO conversion of over 99%. WGS reactions are exothermic but their equilibrium constants are affected by the

variation in temperature of syngas. Hence, an additional heat exchanger is installed between WGS reactors to maintain the syngas temperature while generating the additional steam. The shifted syngas passes through the AGR units where the CO₂ and H₂S is removed from the syngas. Built-in columns in Aspen Plus (Radfrac) have been used to simulate the AGR units with the selexol solvent. The separated CO₂ is then further processed and compressed to an elevated pressure for its transport and storage, whereas, H₂S is further treated in a Claus unit to recover elemental sulfur. The syngas leaving from AGR section contains high concentration of H₂ which is directed towards CC section to generate the heat and electricity.

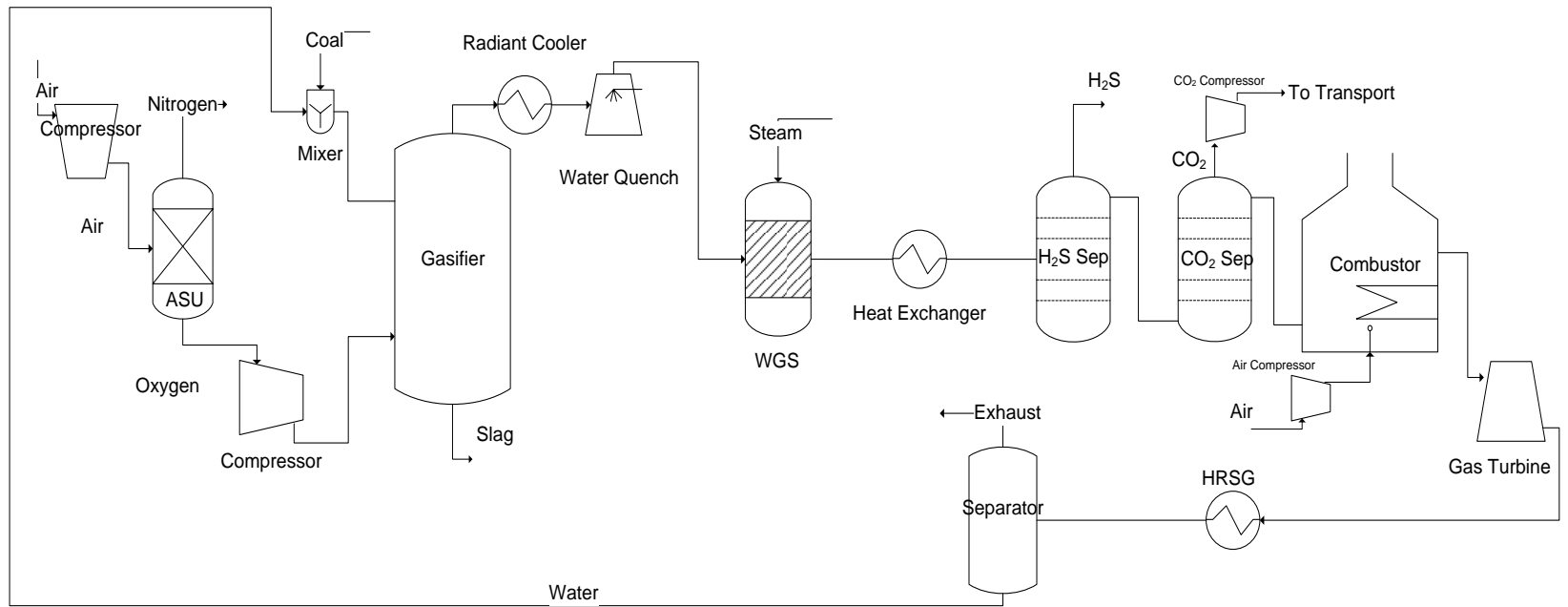


Figure 3-1: Case 1 – Conventional IGCC design for power generation with CO₂ capture

For the validation of model, the composition of syngas obtained from the simulated base case and its comparison with the conventional IGCC process at the gasification and the WGSR section is given Figure 3-2 and Figure 3-3, respectively. The results show that relative difference between the syngas compositions obtained for the simulated base case and the NETL [38] report is not very significant. Therefore, the simulated model for the base case design can be used with confidence for developing the conceptual model of integrating conventional IGCC with the methane reforming process. The specific details of each section is provided in the coming section.

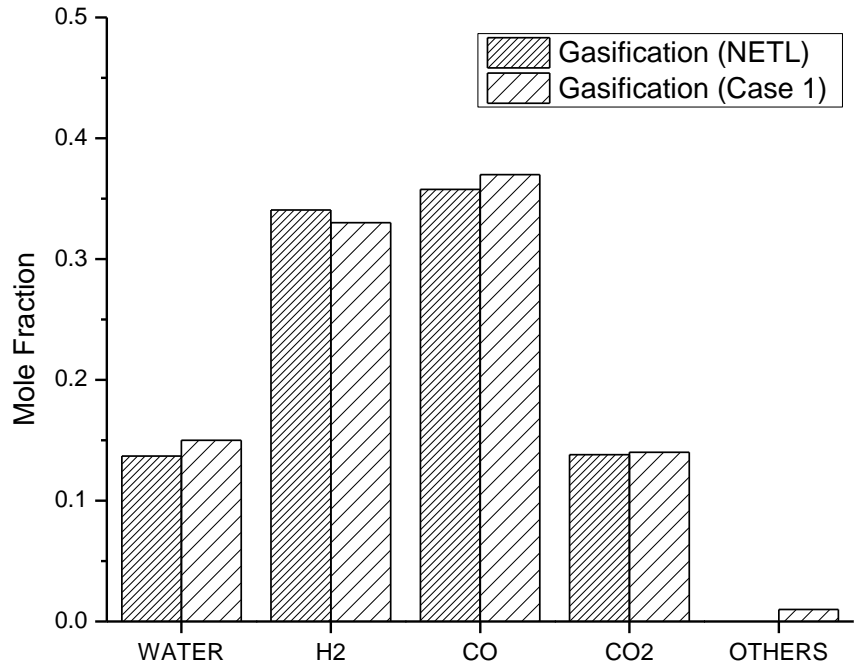


Figure 3-2: Syngas composition at the gasifier for base case (case 1) and its comparison with the NETL report

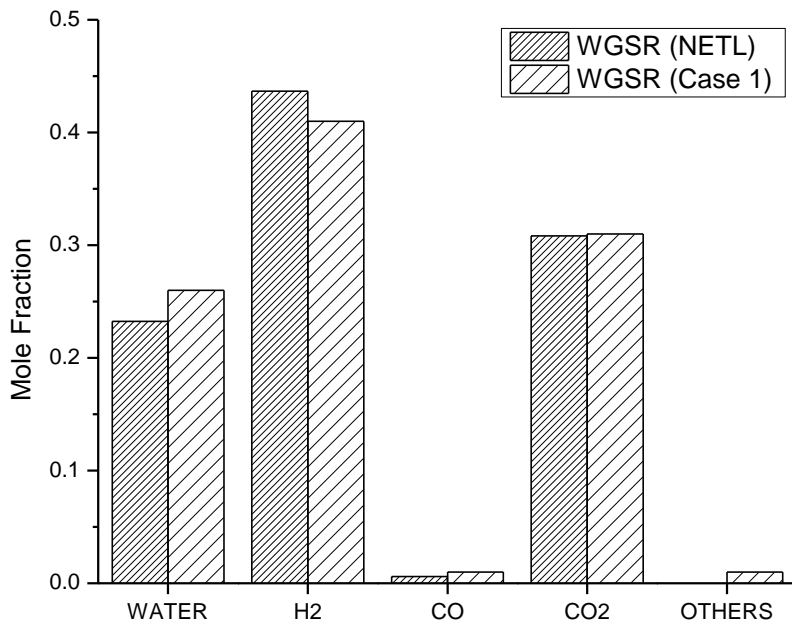


Figure 3-3 : Syngas composition at the WGSR section for base case (case 1) and its comparison with the NETL report

3.2.2 Integration of IGCC and Methane Reforming

Process with CO₂ Capture (Case 2)

Case 2 represents a conceptual design where an IGCC power plant is integrated with the steam reforming unit to increase the syngas generation capacity. In this case, a reforming unit is placed after the gasification unit which is fed with natural gas compressed to the reactor pressure of 32 bar. The process flow diagram of case 2 is shown in Figure 3-4. The developed methane reforming model is first validated with the literature data [66] and then the same model is integrated with the coal gasification process. The *Figure 3-5* shows that the syngas compositions from the developed model are in good agreement with the literature. However, syngas composition will be varied when the reforming unit uses the syngas from the gasification unit instead of only natural gas which contains high concentration of CH₄. Conventionally, in case of standalone reforming process, an additional heat source is required for preheating the gas streams to 700-1000 °C. However, in this case, the syngas generated from the coal gasification unit at a high temperature is sufficient enough to provide the necessary heat to carry out reforming reactions. The syngas temperature from gasifier in this case is first reduced to 1200°C in a radiant cooler followed by its mixing with the

compressed methane gas. The temperature of mixture is maintained at 1150°C to carry out the reforming reactions where the methane and high enthalpy steam reacts in the presence of catalyst to generate H₂ and CO. Theoretically, SMR reactions are stoichiometric but in this study a ratio of 3:1 is maintained between steam and CH₄ to achieve maximum conversion and to avoid carbon deposition on catalyst bed. The temperature of syngas reduces to ~1040°C in the reforming section due to an endothermic process. It can be seen from *Figure 3-6* that the conversion of CH₄ increases as the temperature of the outlet is increased.

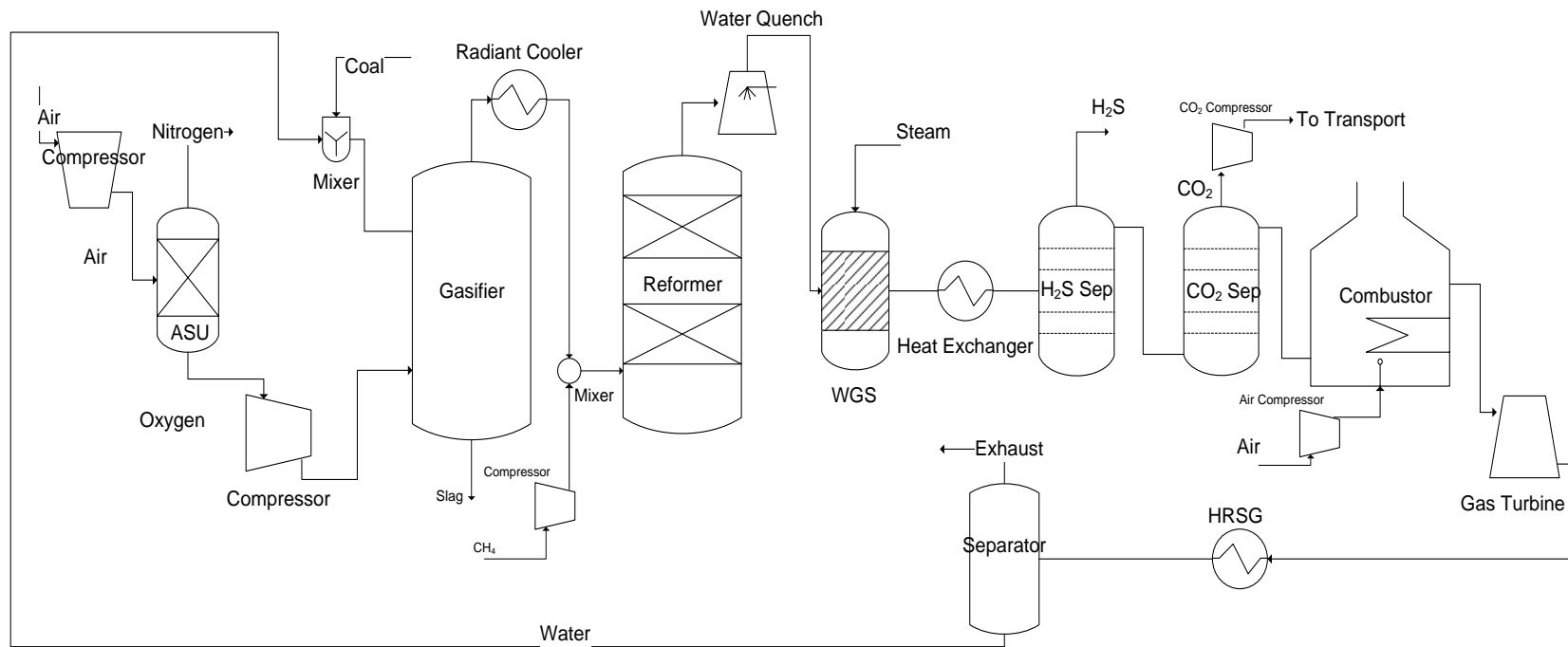


Figure 3-4: Case 2 – Integration of IGCC and methane reforming process for power generation with CO₂ capture

increases as the temperature of the outlet is increased.

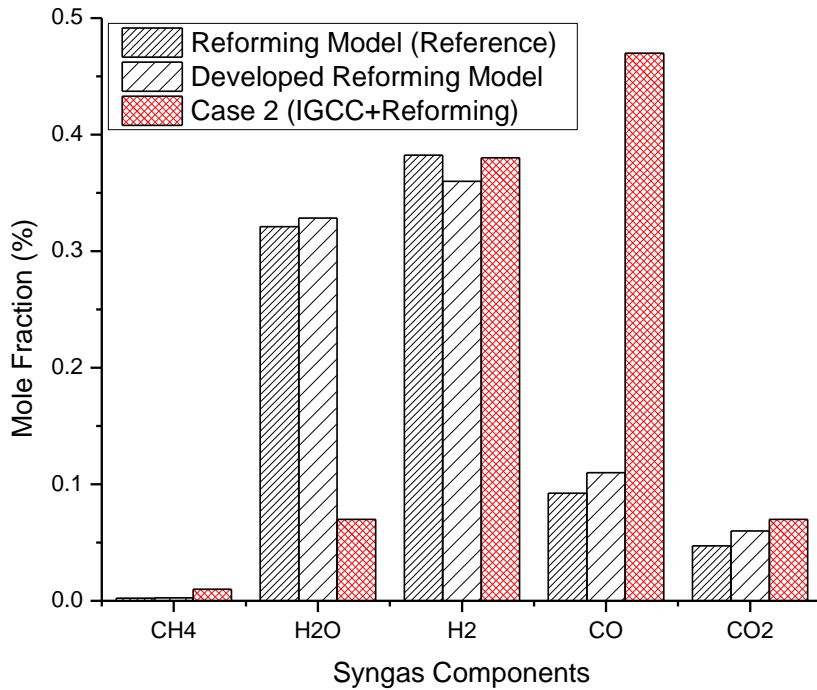


Figure 3-5: Validation of reforming model and its integration with the coal gasification process

The temperature difference between the inlet and the outlet of the reformer remains constant for a specific flow rate of the natural gas and the syngas. Therefore, the inlet and the outlet temperatures of the reforming sections are controlled precisely to attain maximum natural

gas reforming. It can be seen from the results that the H₂ and CO concentration in the syngas tends to increase, whereas, the concentration of CH₄ and H₂O tends to decrease which represents the efficient reforming. The resulting syngas from the reforming section is then followed by the syngas quenching with water to carry out WGS reactions. The rest of the process flow diagram is consistent with the base case design. The CO₂ generated in the process is consequently removed in the CO₂ removal unit and H₂ is directed towards the CC section where it is combusted to generate electricity.

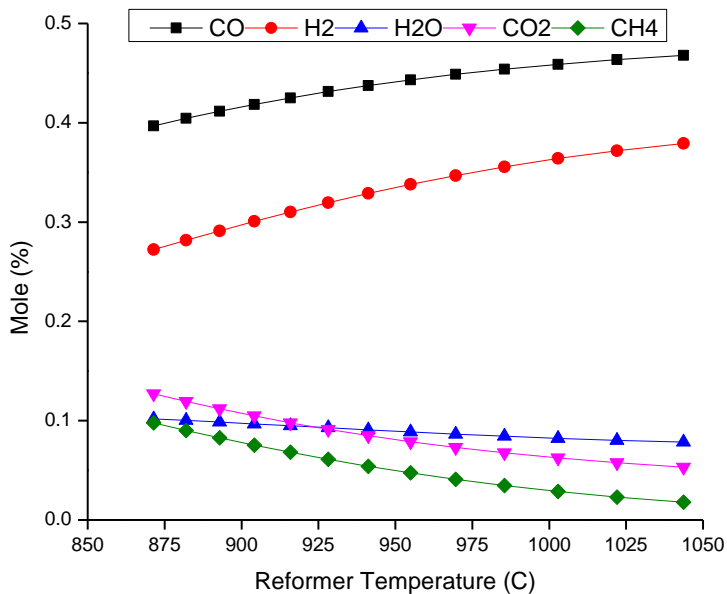


Figure 3-6: Syngas composition at the outlet of reforming unit.

3.2.3 Design basis for model development

The process designs explained in previous sections are simulated using a commercial software i.e. Aspen Plus®. Peng-Robinson equations of state is employed as the thermodynamic package as it can reasonably predict process parameters over wide range of conditions [67]. Coal is an un-conventional component so it is modeled using proximate, ultimate and sulfanal analysis of coal. The composition of coal and natural gas used in the simulation is shown in Table 3-1 and *Table 3-2*, respectively. The composition of syngas at various sections of the base case design is first compared with the literature to analyze the reliability of the simulated model and then the reforming unit is added in the base case with slight tuning of process parameters to develop the case 2.

Coal is wet grinded with water to obtain slurry in various weight fractions. To keep the consistency between case 1 and case 2, coal water slurry ratio of 70:30 (70% coal and 30% water by mass) is used. Coal water slurry and high purity oxygen is fed co-currently to the entrained flow gasification unit at higher pressure to generate high enthalpy syngas. The modelling of gasifier, reformer and WGSR in Aspen Plus is done

using RGibbs reactor which is based on the minimization of the Gibbs free energy.

Table 3-1: Coal composition [38]

Proximity Analysis		
Items	Weight as received (%)	Dry weight (%)
Moisture	11.12	-
Fixed Carbon	44.19	49.72
Volatiles	34.99	39.37
Ash	9.7	10.91
Total	100	100
HHV (kJ/kg)	27,113	30,506
LHV (kJ/kg)	26,151	29,544
Ultimate		
Moisture	11.12	-
Ash	9.7	10.91
Carbon	63.75	71.72
Hydrogen	4.5	5.06
Nitrogen	1.25	1.41
Chlorine	0.29	0.33
Sulfur	2.51	2.82
Oxygen	6.88	7.75

Table 3-2: Natural gas composition and NGCC process performance [38]

Composition	Vol %
CH ₄	93.90%
C ₂ H ₆	3.20%
C ₃ H ₈	0.70%
C ₄ H ₁₀	0.40%
CO ₂	1.00%
N ₂	0.80%
Total	100.00%
Lower calorific value (LHV)	47.76 MJ/kg
NGCC Power Plant Performance	
NGCC Efficiency (Without CO ₂ capture)	50.8 %
NGCC Efficiency (With 90% CO ₂ capture)	43.7 %
CO ₂ emissions (With Capture)	42.27 kg/MW _h
Natural gas flow rate (Case 2)	2.47 kg/sec
NGCC power generation capacity (With CCS)	51.6 MWe

The design assumptions used for each section of the IGCC process along with their modelling techniques are represented in Table 3-3. The performance of the base case (case 1) design and proposed integrated design (case 2) is compared using the standard plant performance and economic indicators.

Table 3-3: Design Assumptions

Unit/Component/ System	Modeling Unit	Parameters
Coal Flow Rate	Mixer	38.51 kg/sec 70% slurry ratio (70% coal and 30% water)
Gasification Reactor	R _{Yield} , R _{Gibbs} (Reactor)	Flow regime: Entrained Flow Ash type: Slag Temperature: 1550°C Pressure: 32 bar Pressurization mode: Slurry Pump Carbon Conversion~ 98%
Reformer	R _{Gibbs} (Reactor)	Natural gas flow rate: 2.47 kg/sec H ₂ O:CH ₄ = 3:1 Nickel based catalyst
Air Separation Unit (ASU)	HeatX, Compr	Oxygen Purity 99.5% (vol) Power Consumption: 245 kW/t

Shift Conversion (WGS)	RGibbs Reactor	Sour Catalyst (Co-Mo) 2 Adiabatic reactors Steam/CO: ~2.2 CO conversion ~ 99%
H ₂ S removal Section	RadFrac	Selexol Solvent H ₂ S removal ~ 99.9% Absorber Stages: 25 Regeneration Stages: 22 Solvent Regeneration : Thermal
CO ₂ removal Section	RadFrac	Selexol Solvent CO ₂ removal = 90% Absorber stages: 20 Solvent Regeneration: PSA Flashing:(13.78, 3.44, 1.01, 0.3) bar
Pump Efficiency	Pump	85%
Compressor Efficiency	Compr	82%
Steam Turbine Eff (Isentropic)	Compr	87.50%
Gas Turbine Eff (Adiabatic)	Compr	GE 7FA
		85%
CO ₂ Delivery Pressure	Compr	100 bar
Heat Recovery Steam Generation (HRSG)	HeatX, Compr	12.52 / 2.9 / 0.45 (MPa)

3.3 Performance Analysis

3.3.1 Evaluation of the process performance

Case 1 is a conventional IGCC process design where the heating value of syngas typically depends on the operational conditions of the gasifier. For instance, O/C ratio is an important parameter which control the syngas composition and its heating value [68]. On the other hand, addition of reforming unit after the gasification unit in case 2 design generates an additional syngas compared to that of case 1 design. Usually the gasification processes favors higher yield of CO with H₂/CO ratio between 0.35 and 0.8. On the other hand, the design for case 2 produces higher heating value syngas as a result of higher yield of H₂ content from the addition of reforming process. Therefore, an integration of gasification and reforming process can generate a wide range of syngas composition required for the downstream application. The methane reforming process utilizes high enthalpy steam from the gasifier to convert CH₄ to H₂ while maintaining the reformer's temperature and pressure. The composition of syngas along with its heating value at the inlet of WGS reactors for both processes is represented in *Figure 3-7*. It can be seen that H₂ concentration in the case 2 is higher than case 1 which

consequently increases the heating value of syngas and generates more power during the combustion process. The composition and flow rate of streams at the outlet of various sections of power plant is also given in *Table 3-4* for both the processes.

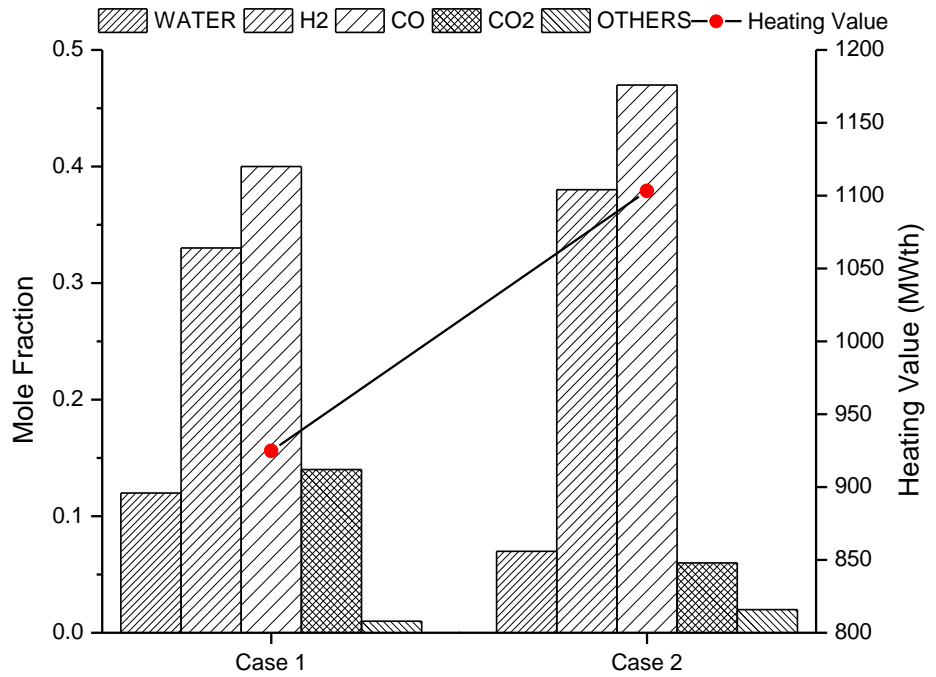


Figure 3-7: Composition and heating value (MWth) of syngas at WGS inlet for case 1 and case 2.

Table 3-4: Stream flow rates during each section of the process

	Coal	Oxygen (Gasifier)	Gasifier	Reformer		Shift Conversion	
	Case1/Case2	Case1/Case2	Case1/Case2	Case 1	Case 2	Case 1	Case 2
Mass Flow (kg/hr)	138635	90868	267611	-	277170	514859	555734
Mole Flow (kmol/hr)	-	2840	14136	-	15732.1	27748	31188.4
Mol %							
H ₂	-	-	0.33	-	0.38	0.41	0.43
CO	-	-	0.40	-	0.47	0.01	0.01
CO ₂	-	-	0.14	-	0.06	0.31	0.25
H ₂ O	-	-	0.12	-	0.07	0.26	0.30
O ₂	-	0.99	-	-	-	-	-
CH ₄	-	-	-	-	0.01	-	-
N ₂	-	0.01	-	-	-	-	-
Others	-	-	0.01	-	0.01	0.01	0.01

	AGR Removal Section		Oxidant (Air)		Flue Gas (Gas Turbine)	
	Case 1	Case 2	Case1	Case 2	Case1	Case 2
Mass Flow (kg/hr)	42764	54503.07	798265	1900880	1417179	2209940
Mole Flow (kmol/hr)	11878	14164.03	27669	65887.5	53774	82139
Mole %						
H ₂	0.95	0.95	-	-	-	-
CO	0.01	0.02	-	-	-	-
CO ₂	0.03	0.03	-	-	0.01	0.01
H ₂ O	-	-	-	-	0.14	0.16
O ₂	-	-	0.21	0.21	0.12	0.11
CH ₄		0.01				
N ₂	-	-	0.79	0.79	0.73	0.72
Others	0.01	-	-	-	-	-

The performance of the base case design and proposed integrated design is compared using the standard plant performance and economic indicators. The mathematical formulations for calculating net power generation capacity, ancillary power consumption and process performance are given as follows:

Net Power Generation

Net power generation shows the net electrical capacity of a power plant which is calculated by subtracting the ancillary power from the gross power generated in the process as shown in Equation 19.

Net Power = Gross power

$$(\text{MWe}) - \text{Ancillary Power}(\text{MWe}) \quad (19)$$

Ancillary Power Consumption

Ancillary power represents the total electrical consumption in all the sub-sections of the process as represented by Equation 20.

Ancillary power

$$= \sum \text{Power consumed by plant sub systems} \quad (20)$$

Net Electrical Efficiency

Net electrical efficiency (η_{net}) of a power plant represents its performance in terms of energy conversion as shown in Equation 21.

$$\eta_{\text{net}} = \frac{\text{Gross power output (MW}_e\text{)} - \text{Ancillary power (MW}_e\text{)}}{\text{Feed stock heating value (MW}_{\text{th}}\text{)}} * 100 \quad (21)$$

Since, the flowrate of syngas is higher in case 2 due to an additional natural gas reforming process, the net flow rate of syngas through the combustion section increases. Due to higher syngas combustion rate, the corresponding flue gas flow rate through the gas turbine increases which results in higher electricity generation. The power generated from the gas turbine section in case 1 and case 2 is calculated as 338.1 MW_e and 404.13 MW_e, respectively. Moreover, the higher concentration of H₂ in the syngas for case 2 also generates more heat during its combustion which consequently increases the steam cycle power generation capacity. The steam cycle power generation capacity for case 1 and case 2 is calculated as 195.94 MW_e and 365.11 MW_e, respectively. However, the results show that case 2 utilizes 18.3% more energy compared to the case 1. The power consumption in case 1 and case 2 is calculated as 168.45 MW_e and 199.24 MW_e, respectively. The breakdown of power consumption at various sections of the process for both cases is shown in *Figure 3-8*.

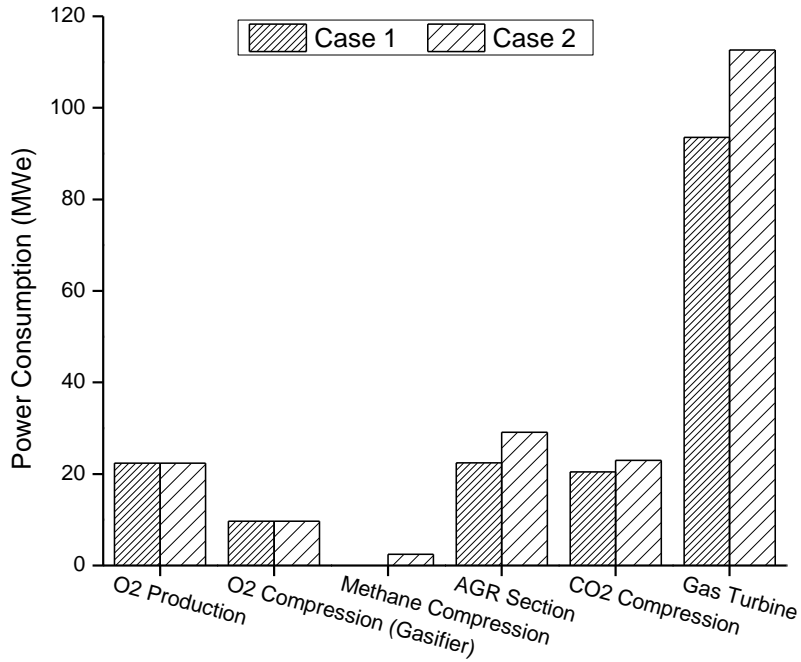


Figure 3-8: Power consumption break down for case 1 and case 2

The results showed that the most highly power consuming unit in both the processes are the compressors associated with the gas turbine section, air separation unit for O₂ production and feeding to the gasification unit. As the coal slurry flow rate is same in both the cases, the same amount of O₂ is required for the gasification process and thus requires the same energy for the O₂ production and compression. On the other hand, case 2 contains an additional reforming unit which consumes 2.45 MW_e of

power for natural gas compression. As the flow rate of natural gas is not very large, the power consumption by the natural gas compression do not significantly affect the overall power capacity. However, the addition of reforming process in case 2 generates more syngas which consequently increases the power consumptions of both the AGR removal and CO₂ compression sections. Finally, the net power generation capacity and efficiency of case 1 and case 2 is calculated as (375.08 MW_e, 472.92 MW_e) and (35.93 %, 40.70 %), respectively. *Figure 3-9* provides the summary of the power generation and consumption for both the cases along with their process performances.

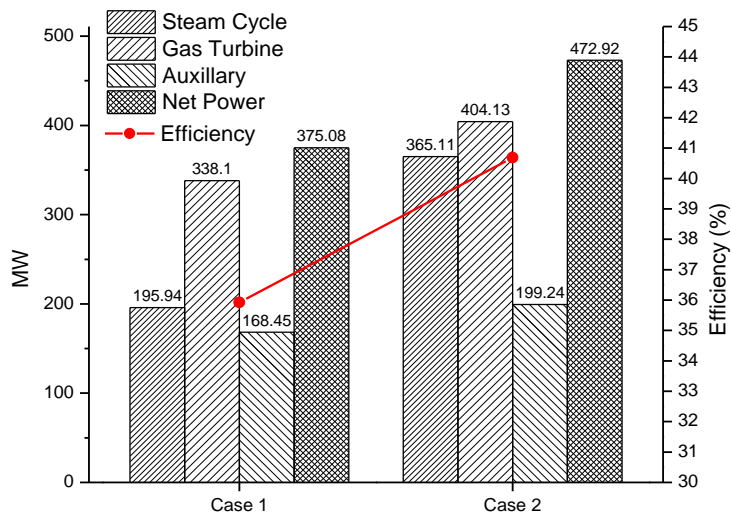


Figure 3-9: Electricity generation from steam and gas turbine sections

Integration of IGCC and reforming process (Case 2) utilizes both the coal and natural gas as a feedstock in comparison to the case 1 that only requires coal for its operation. As natural gas used in case 2 is also an important utility so it is important to compute the corresponding NGCC power plant performance in addition to conventional IGCC process for the fair evaluation of analysis. In case of NGCC, high pressure gas is directly combusted in the gas turbine to produce electricity. On the other hand, the syngas available after the WGSR section in IGCC process is utilized in the combined cycle to generate power. Therefore, the process equipment requirement for the NGCC and IGCC technologies is different and result in different process economics. A standard NGCC plant doesn't include either gasifier not WGSR which decreases the capital cost of the plant compared to the IGCC plant. However, relatively higher and fluctuating prices of natural gas limits its extensive consumption over coal based power generation processes. A typical NGCC plant with CO₂ capture has a fuel cost contribution of above 60% per unit cost of electricity. An IGCC plant, on the other hand, has a fuel cost contribution of around 20% per unit of electricity produced [38]. Therefore, the case 2 design has been proposed with an additional reforming unit to utilize small volumes of natural gas to enhance both

the syngas generation capacity and process performance of the IGCC process. In order to fairly compare the base case design with the proposed design, a standalone NGCC process with the same fuel flowrate as used in case 2 in addition to the standalone IGCC process is evaluated. Table 3-2 also highlights some of the process performance indicators for the NGCC power plant with and without CCS technology. The flowrate of natural gas in case 2 is specified as 2.47 kg/sec on the basis of steam to CH₄ ratio of 3:1 for an efficient reforming process. With natural gas flowrate of 2.47 kg/sec, the power generation capacity of standalone NGCC is calculated as 51.6 MW_e. Therefore, the cumulative net power and efficiencies of both the systems (NGCC + IGCC) is calculated to be 426.68 MW_e and 36.8%, respectively. It can be seen from the results that IGCC integration with the methane reforming process exhibits 4.7% and 3.9% higher process efficiency compared to conventional IGCC and the cumulative standalone processes, respectively. Figure 3-10 compares the performance of case 1 and case 2 design along with the collective IGCC+NGCC standalone design. It can be seen from the results that case 2

design offers the highest power generation capacity and efficiency among all the case studies.

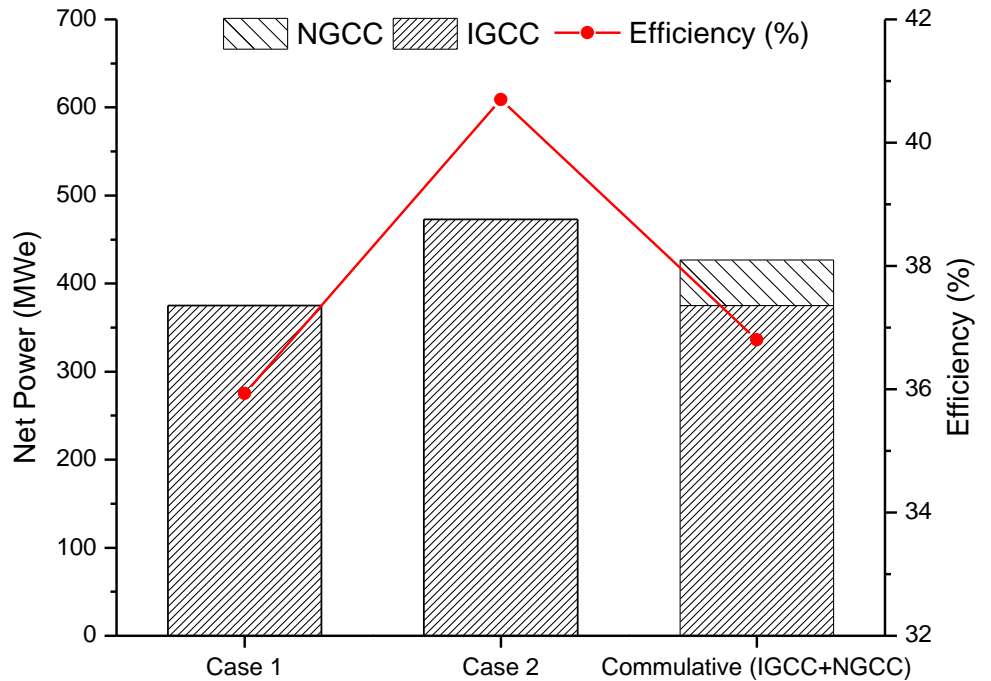


Figure 3-10: Comparison of net power generation (MWe) capacity and efficiency of all cases.

3.3.2 Assessment of CO₂ specific emissions

One of the other important environmental quality control indicator is the CO₂ specific emission analysis. Specific CO₂ emissions (SE_{CO₂}) are calculated as an un-captured CO₂ emitted mainly in kg/h for each MW of energy generated as shown in Equation 22.

$$SE_{CO_2} = \frac{\text{Emitted CO}_2 \text{ flow rate (kg/h)}}{\text{Net Power Output (MWe)}} \quad (22)$$

Specific CO₂ emissions represents the process performance in terms of environmental impacts. All the results in this study have been tuned to capture 90% of CO₂ in the AGR section. In power generation industries, CO₂ emissions are evaluated as a function of electricity generation. From CO₂ specific emissions analysis, annual CO₂ emissions can be computed for any power plant. The CO₂ specific emissions can vary for different processes with the same power generation capacities because of difference in CO₂ loss rates among various sub sections of the process. CO₂ specific emissions evaluated for case 1 and case 2 is 87.74 and 80.26 kg/MW_h, respectively. While comparing the results, it has been seen that case 2 design not only offers the less SE_{CO₂} but also higher performance compared to case 1 design.

3.3.3 Performance comparison with Literature

The assessment of conceptual design's reliability is always a difficult task due to lack of availability of industrial data. IGCC technology exhibits complex integration of various processes compared to the PC and natural gas based power plants that limits its large scale demonstration and commercialization. Therefore, an alternative methodology of comparing the simulation results with the already published scientific literature is considered. *Table 3-5* represents the comparison of process performance and CO₂ specific emissions for both the cases with the other reference studies. The results shows that the efficiency and specific emissions calculated for case 1 design is close to the results published in the literature [6, 25, 38, 40, 53, 58, 69]. On the other hand, case 2 design offers an IGCC integration with the natural gas reforming process with CCS technology. The results for the case 2 design not only offers the higher process efficiency but also the least CO₂ specific emissions compared to the case 1 design.

Table 3-5: Performance comparison with literature

	Case 1	Case 2	NETL [38, 53, 69]	Others [6, 25, 40, 58]
Gasification Pressure (bar)	32	32	56	30-65
Gasification Temp (°C)	1550	1550	1316	1250-2000
Gasifying Agent	O ₂	O ₂	O ₂	O ₂
WGS (Steam/CO)	2.2	2.2	2.0	1.0-2.4
Syngas Combustion Temp (°C)	1370	1370	1371	<1600
Solvent Type	Selexol	Selexol	Selexol	Selexol
CO ₂ capture (%)	90	90	90	90
Net Power with CCS (MW _e)	375.08	472.92	640.25	200-850
η with CO ₂ capture (%)	35.93	40.7	32.5	32-36
η without CO ₂ capture (%)	44.5	47.28	38.2	42-45
CO ₂ specific emissions (kg/MW _h)	87.74	80.26	93	79-82

3.3.4 Sensitivity Analysis

3.3.4.1 Effect of coal water slurry ratio on the process performance

Sensitivity analysis has been performed to observe the variation in efficiency and net power generation capacity of power plant for different coal water slurry ratios. It is observed that decreasing coal water slurry ratio to 60:40 (60% coal and 40% water by mass) in case 1 decreases both the heating value of the syngas and the net power generation capacity. Heating value of the syngas is associated with cold gas efficiency as shown in the Equation 23.

$$\eta_{CG} = \frac{LHV_{gs} * V_{gas}}{LHV_{fuel} * m_{fuel}} * 100(\%) \quad (23)$$

Figure 3-11 shows the variation in heating value and syngas composition for all the case studies with 70% and 60% coal water slurry ratios at the inlet of WGSR section.

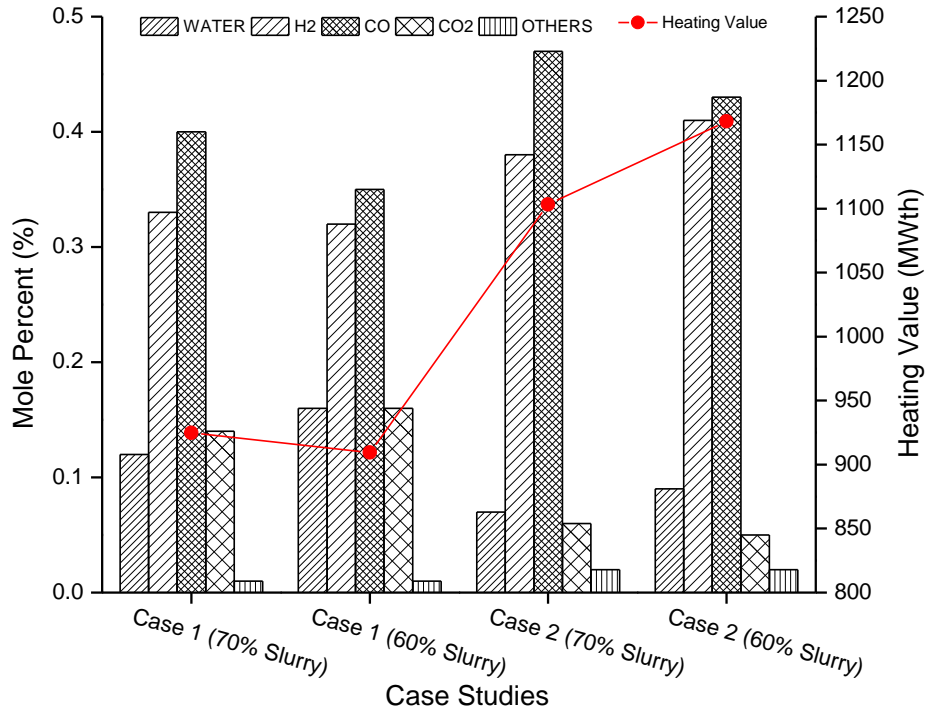


Figure 3-11: The effect of coal water slurry ratio on syngas composition and heating values (Inlet of WGSR)

It can be seen from results that the decrease in coal percentage (60%) in case 1 decreases the concentration of H₂ and CO in the syngas while increasing the steam and CO₂ concentration. Due to the decrease in the heating values, process efficiency of case 1 also reduces to 35.77%. This slight decrease in the process efficiency is due to the fact of utilizing more O₂ for the gasification process. However, decreasing the coal water

slurry ratio in case 2 helps in improving the process performance. As case 2 contains the reforming unit, the high steam generation in the gasification process can help in converting more CH₄ to the H₂ that helps in increasing the heating value of the syngas. It can be seen from results that decreasing the coal water slurry ratio increase the H₂ concentration in the syngas. Due to an increase the heating value of syngas, the process performance of case 2 is improved to 41.9%. The brief overview of varying the coal water slurry ratio and its effect on process performance for all the case studies is provided in the *Table 3-6*.

Table 3-6: Overview of coal water slurry ratio on process performance

		η_{GC}	Heating value (MW _{th})	Net Power (MW _e)	Efficiency (η)
Case 1	70% slurry	88.57	924.7	375.08	35.93
	60% slurry	87.11	909.49	373.4	35.77
Case 2	70% slurry	94.94	1103.19	472.92	40.7
	60% slurry	95.96	1168.17	510.13	41.9

Keeping in view the operational complications, higher coal content in the slurries tends to increase wear and tear of the pumps that lead towards higher operational and maintenance costs. Therefore it is preferred to

keep the coal water slurry ratio low in order to avoid frequent failures which supports the conceptual design of case 2 with lower coal content.

3.3.4.2 Effect of O₂ purity on the process performance

ASU is considered as one of the highly energy intensive unit used for O₂ production. The energy required to produce O₂ tends to increase as the purity of the O₂ increases. The required level of O₂ purity depends on the end use of the syngas and the employed CCS technology. Sensitivity analysis has been performed on the O₂ production energy with respect to the O₂ purity and its effect on the overall process performance. *Figure 3-12* shows that the increase in O₂ purity affects both the net power generation and process efficiency. The results show that the net power generation reduces from 381.52 MWe to 375.08 MWe and 479.36 MWe to 472.98 MWe for case 1 and case 2, respectively. Moreover, the efficiency drop of 0.61% and 0.55% has been observed for case 1 and case, respectively. It has been seen from results that there is a slight drop in net power generation and efficiency as the purity is increased from 95% to 99.5%. Therefore, most of the commercial IGCC systems operates at 95% purity.

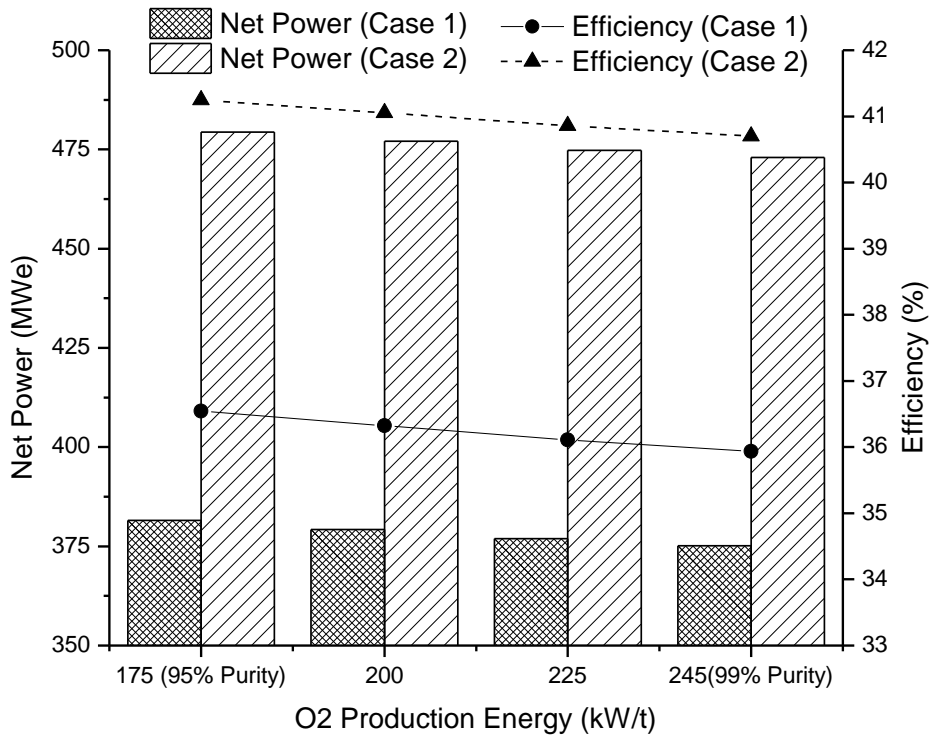


Figure 3-12: Effect of O₂ purity on the process performance

3.3.4.3 Effect of coal rank (Bituminous, Lignite) on the process performance

The process performance of IGCC power plants are greatly affected by the quality of the coal. Recently, Botero et al. [70] and Chen et al. [71] compared the performances of an IGCC process with different ranks of coal. Usually, bituminous coals are preferred for IGCC processes due to

their higher heating values and higher carbon content. However, the coal reserves around the world shows higher percentage of lower rank coals which include the lignite. Sensitivity analysis is performed on both the case studies to determine the effect of coal rank on the process performance. The results showed that the decrease in the coal rank from bituminous to lignite leads to the decrease in the concentration of both the H₂ and CO in the syngas that ultimately affects the heating value of the generated syngas. It can be seen in *Figure 3-13* that the cold gas efficiency and the heating value of syngas exhibits the direct relationship. It has been further seen from the results the use of low rank coal enormously affect the process performance of both case 1 and case 2. It can be seen from *Figure 3-14* that the net power generation capacity drops from 375.07 MWe to 249.39 MWe and 472.92 MWe to 350.14 MWe for case 1 and case 2, respectively. Furthermore, the drop of 10.84% and 11.49% process performance is observed for case 1 and case 2, respectively, while using the lignite coal. Although, the process performance of case 1 and case 2 drops with the use of low rank coal but the case 2 design still shows the 4.12% higher process performance compare to the case 1 design.

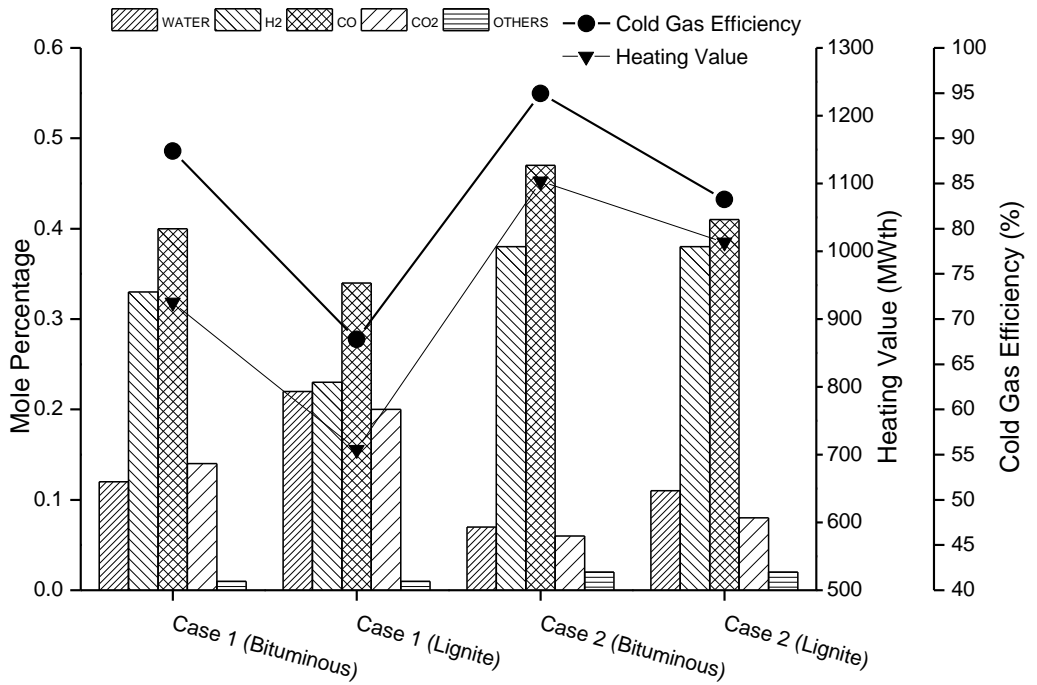


Figure 3-13: Effect of coal rank on syngas heating values for case 1 and case 2

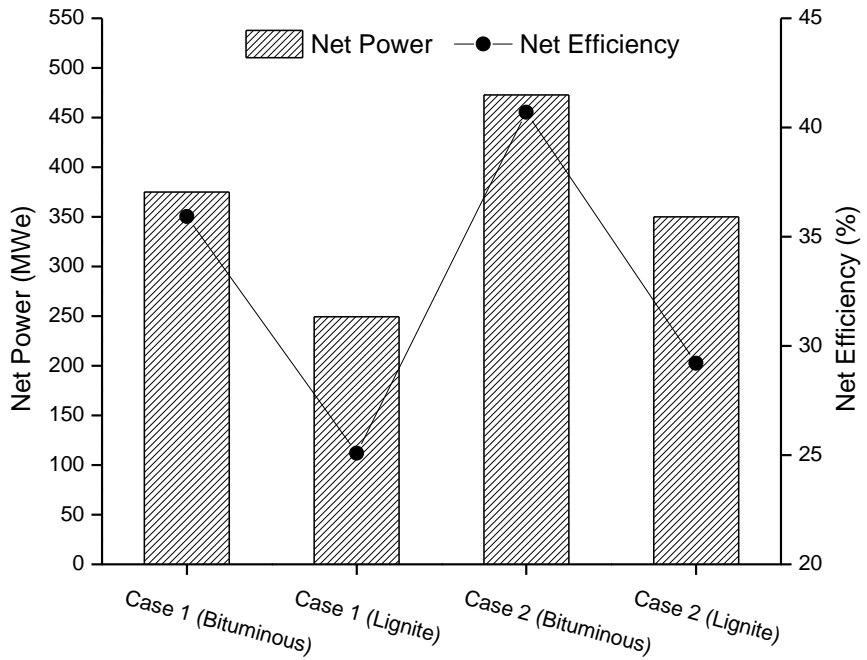


Figure 3-14: Estimation of process performance for case 1 and case 2 for different coal ranks

3.3.4.4 Impact of CO₂ capture rate on the process performance

The CO₂ capture and pressurization units are considered as the key processes of the overall CCS process. The rate of CO₂ capture can greatly affect the net power generation capacity and efficiency of the power plants. Sensitivity analysis has been performed in order to analyze the impact of CO₂ capture percentage (0-90%) on the net power generation and plant's efficiency. *Figure 3-15* shows the variation in plant efficiency with CO₂ capture percentage. Both case 1 and case 2 showed the same trend of decrease in efficiency with percentage increase in CO₂ capture. The results showed that the power generation capacity of case 1 and case 2 can be increased from (375.07MWe to 410.73 MWe) and (472.92MWe to 512.11MWe), respectively, if the CO₂ capture percentage is decreased from 90% to 0%. Moreover, the process efficiencies can be increased up to 3.41 and 3.37 points for case 1 and case 2, respectively, if the CO₂ capture rate is reduced to 0%. It can be seen from results that the case 2 behaves quite efficiently for different ranges of CO₂ capture and showed the highest process performance among the two cases. While comparing the process performance of case 2 with the other conventional PC process

[38], it has been seen that case 2 showed even higher efficiency with 90% capture compared to the USPC power plants with 0% capture of CO₂.

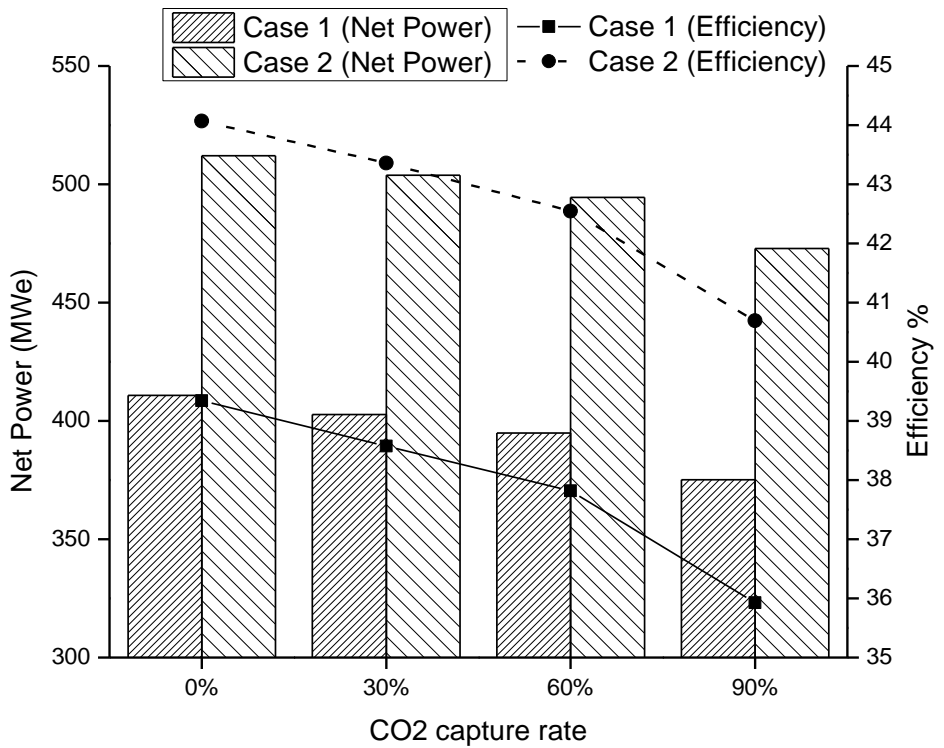


Figure 3-15: Effect of CO₂ capture rate on the process performance

3.4 Summary

In this study, two process models have been developed and compared in terms of process performance. Case 1 represents the conventional IGCC process, whereas, case 2 represents a conceptual design of integrating IGCC with the methane reforming process. The results showed that the net power generation capacity and efficiency of case 1 and case 2 is calculated as (375.08 MW_e, 472.92 MW_e) and (35.93 %, 40.70 %), respectively. Some plant performance indicators have been used to determine the CO₂ emissions with and without the CCS technology. CO₂ specific emissions calculated for case 1 and case 2 is 87.74 and 80.26 kg/MW_h, respectively. It has been seen from results that the process efficiency tends to decrease with an increase in CO₂ capture rate. Moreover, the comparative analysis showed that the case 2 design with 90% CO₂ capture rate have higher process efficiency than the USPC power plants even with 0% of CO₂ capture which makes its design more sustainable. Moreover, sensitivity analysis (coal water slurry ratio, O₂ concentration, and coal rank) has been performed to determine the reliability of both the processes in changing circumstances. The results showed that the increase in water content in the slurry decreases the syngas efficiency in case 1, however, the increase in steam content in

syngas increases the methane reforming capacity for case 2 which ultimately increases both the heating value and cold gas efficiency of the syngas. The results also showed that case 2 design provides an opportunity of using higher water content in the slurries while improving the process performance. The O₂ production from ASU is also an energy intensive process so the sensitivity analysis is performed to determine the energy requirements to generate 95% and 99.5% pure O₂. It has been seen from results that the increase in O₂ concentration from 95% to 99.5 % increase the overall energy consumption, however, it only affects the process performance with in the range of 0.5-1%. Furthermore, the sensitivity analysis performed for different ranks of coal showed that the use of lignite coals reduces the process performance by 10.84% and 11.49% points for case 1 and case 2, respectively, compared to the base case design that utilizes the bituminous coal. Though, the decrease in process efficiencies have been observed for both case studies while using low rank coals, still the case 2 design offers 4.12% higher efficiency compared to the case 1 design. Comparing all the plant performance indicators, it has been seen that the case 2 offers better performance compared to the case 1 design. Additionally, the case 2 design also provides an opportunity to use both coal and natural gas to generate

higher heating value syngas that can be used in various poly generation processes to generate FT chemicals.

Chapter 4 : Economic Analysis

4.1 Capital Expenditure Calculation (CAPEX)

The commercial implementation of IGCC technology for power generation demands for a high cost competition with the already existing technologies. Currently, both the CAPEX (capital cost) and O&M (operational-and-maintenance cost) required for IGCC power generation systems are higher than the USPC and NGCC power plants with CO₂ capture [38, 53]. Due to an involvement of various sub-systems in the IGCC process, there is no general rule to directly estimate the CAPEX and O&M cost. The investment required for IGCC power plants depends on various factors i.e. size of plant, power generation capacity, efficiency, raw material consumption and un-certainties associated with the system. For an instance, gasification and air separation technology is provided by various vendors (Shell, GE, Siemens, etc.) and (Air Liquide, Linde, etc.) having their own characteristics and specific costs. Due to the afore-mentioned factors, IGCC process still cannot be considered as a standardized commercial technology with well-established cost models.

Capital cost of the plant is a function of equipment size, material of construction and operating conditions. Therefore, it can be expressed in terms of power law of capacity as mentioned in Equation 24 where C_E – equipment cost with capacity Q and cost index I_E ; C_B – base case cost of equipment with capacity Q_B and cost index I_B ; M – constant value ranging from 0.48 to 0.87 however average value of 0.6 is mostly used [72].

$$C_E = C_B \times \left(\frac{Q}{Q_B}\right)^M \times \frac{I_E}{I_B} \quad (24)$$

Specifying the flow rates of each stream and sizing all the equipment, the CAPEX for case 1 and case 2 has been calculated using the literature [40, 72-75] as shown in *Table 4-1*.

Table 4-1: Capital cost estimation

Plant Sub-System	Units	Case 1 (M€)	Case 2 (M€)
Reformer	MMCFD of H ₂	0	45.60
Solid Handling Facility	tonne of coal/hr	36.38	36.38
Gasification Island	tonne of coal/hr	146.12	146.12
Syngas processing unit	tonne of syngas/hr	36.21	37.64
Acid Gas Removal Unit	tonne of CO ₂ /hr	87.18	89.89
Air Separation Unit	tonne of O ₂ /hr	73.52	73.52
CO ₂ Processing And Drying	tonne of CO ₂ /hr	22.18	22.82
Sulfur Removal Unit	tonne of Sulfur/hr	43.06	43.06
Power Island	MW _e	284.51	341.70
Offsite Unit and Utilities	Equipment Cost (25%)	182.29	209.19
Total Installed Cost	M€	911.46	1045.94
Contingency	Installed Cost (15%)	136.72	156.89
Land Cost	Installed Cost (5%)	45.57	52.30
Total Investment Cost	M€	1093.75	1255.12
Total Cost per MW _e (gross)	M€/MW _e	1.41	1.19
Total Cost per MW _e (net)	M€/MW _e	2.93	2.06

For comparing the CAPEX of both case studies in terms of power generation capacities, gross and net investment indexes were used. Total investment cost (TIC) is used as an economic indicator to estimate the gross and net investment required for each MW of energy generated as given in Equation 25 and Equation 26 below.

$$\text{TIC per MW (gross)} = \frac{\text{Total Investment Cost}}{\text{Gross Power Output}} \quad (25)$$

$$\text{TIC per MW (net)} = \frac{\text{Total Investment Cost}}{\text{Net Power Output}} \quad (26)$$

The total investment required for an IGCC power plant is divided into two sections namely onsite investment costs and off-site investment costs. On-site investment includes the cost of equipment, installation cost, piping and valves, civil structures, engineering and consultation fee. The off-site costs include road network, workshops, offices, storage facilities and medical services. To keep the economic analysis consistent for all the cases, utility cost, land cost and contingency costs are taken as 25%, 15% and 5% of the total installed cost respectively.

As the flow rate of coal water slurry is same in both the cases, the CAPEX associated with solid handling facility, gasification section and syngas processing unit remains same. However, case 2 demands for an additional 45.60 M€ for the reforming section which accounts for 5% increase in the total installed cost. As reforming section increases the syngas generation capacity, the CAPEX for both AGR and CO₂ processing unit consequently increases. Moreover, an increased flow rate of both the syngas and flue gas through the CC section increases the power island cost and total installed cost by 20.1% and 6.27%, respectively for the case 2 design compared to the case 1 design. The

total investment cost required for case 1 and case 2 is calculated as 1093.75 and 1255.12 M€'s, respectively. Moreover, *Table 4-1* also shows the total investment cost required for each MW of power generated for both the cases. The TIC/MW_{net} calculated for case 1 and case 2 is 2.93 and 2.06 M€'s, respectively. Although the CAPEX of case 2 is higher than the base case design, yet its higher process efficiency reduces the TIC/MW_{net} by 29.7 %.

4.2 Operational Expenditure Calculation (OPEX)

Operational and maintenance (O&M) cost is also an important economic indicator that represents fixed and variable overheads of the plant. O&M cost of plant varies according to the complexity and frequent failures of rotating equipment in power plants. It is calculated in terms of actual working hours of the plant throughout the year. For calculating operational and maintenance cost, some economic assumptions [72-74] are taken into account as shown in *Table 4-2*. Maintenance cost is taken as 3.5% of the total installed cost of the equipment whereas management cost is taken as 30% of the total labor cost.

Table 4-2: Economic Assumptions

Coal Price	34.35 \$/t = 0.038 €/kg
Natural Gas	5 €/GJ
Cooling Water price	0.01 €/t
Boiler Feed Water (5 % recharge)	0.40 \$/m ³ = 0.33€/m ³
Selexol Price (2% Blowdown)	6500 €/t
Waste Disposal	10 €/t
Annual Operating Hours	7500
Plant construction time	3 Years
Plant Life	25 Years
Maintenance	3.5% of OPEX
Discount rate	8%
Administration	30% Labor Cost
Labor Cost (120 person)	50,000 €/ Person

O&M expenditure can be further categorized into fixed O&M (maintenance, labor and administration) and variable O&M (raw materials, solvents and catalyst recharging). The detailed comparison of O&M expenditure required for case 1 and case 2 is given in *Table 4-3*. It can be seen that O&M cost for case 1 and case 2 is calculated as 140.08 and 168.10 M€/year respectively. The results show that fixed O&M cost of case 2 is approximately 12% higher than that of the case 1. Moreover, case 2 design also utilizes an additional natural gas and catalyst for the reforming process which increases 23.23% of its variable O&M cost. However, while comparing the O&M costs in accordance with the net

power generation capacities, case 2 shows a reduction of 26.32% in cost compared to the case 1 design which in turn represents its higher process efficiency.

Table 4-3: Operational and maintenance cost estimation

O&M cost	Units	Case 1	Case 2
Fixed O&M cost			
Maintenance Cost	M€/year	31.90	36.61
Labor Cost	M€/year	6.00	6.00
Administrative, support & overhead cost	M€/year	1.80	1.80
Total Fixed O&M cost	M€/year	39.70	44.41
Total Fixed O&M Cost (Net MW _e)	M€/MW _e	0.11	0.07
Variable O&M cost			
Natural Gas	M€/year	-	15.94
Coal	M€/year	39.56	39.56
Boiler Feed Water (BFW)	M€/year	55.73	62.90
Solvent (Selexol)	M€/year	0.80	0.96
WGS Catalyst	M€/year	1.36	1.38
Reforming Catalyst	M€/year	-	0.02
Waste Disposal	M€/year	2.94	2.94
Total variable O&M Cost	M€/year	100.38	123.70
Total variable O&M Cost (Net MW _e)	M€/MW _e	0.27	0.20
Total Fixed and Variable Cost	M€/year	140.08	168.10
Total Fixed and Variable Cost (Net MW_e)	M€/MW _e	0.37	0.28

4.3 Project life and payback time

It is also important to consider the cumulative cash flow of a project which gives an overview about the payback time and overall return on investment. In this study, the plant construction and operational life time is considered as three years and twenty five years, respectively. However, the working capital recovery time is fixed as one year.

Figure 4-1 represents the cumulative cash flow for both the cases. It can be seen from the results that not only the payback time of case 2 is less than the case 1 design but it also offer higher return on the investment.

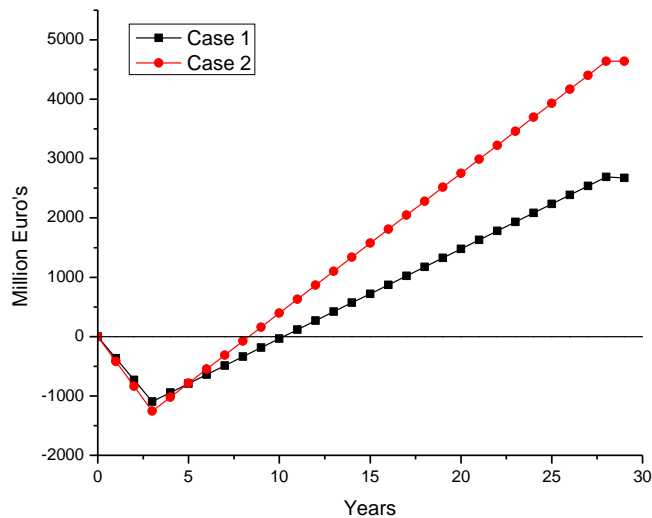


Figure 4-1: Investment payback time and cumulative cash flow estimation for case 1 and case 2.

4.3 Estimation of cost of electricity (COE)

The main purpose of any power plant is to produce electricity at an economical price. The cost of electricity (COE) may vary with the power plant type (with or without CCS technology), raw material (coal, natural gas, etc.) and the associated maintenance costs. Similarly, levelized cost of electricity (LCOE) is also an important economic indicator for estimating the cost of electricity during the life time of the plant. It provides electricity cost estimation by relating power generation capacity with the CAPEX and O&M expenditure required over the life time of the project. *Figure 4-2* shows the comparison between both cases in terms of CAPEX and O&M requirements along with their expected LCOE. It can be analyzed that the O&M expenditure and net electricity production capacity of a power plant are the main influencing factors for determining the LCOE. Despite the fact of higher CAPEX and O&M requirements in case 2 design, the LCOE calculated for case 2 is lower than case 1 due to its higher electricity generation capacity. The LCOE calculated for case 1 and case 2 is 70.57 and 66.47 €/MWh, respectively. During an actual operation of power plant, LCOE may be subjected to a range of un-certainties.

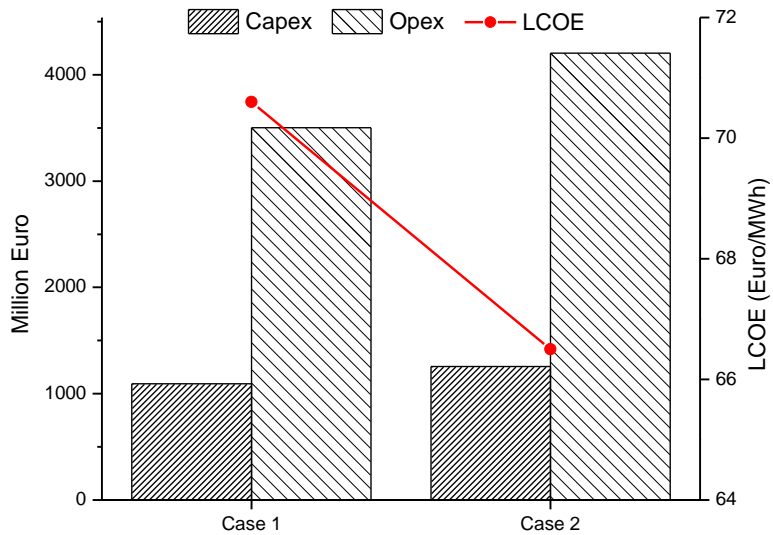


Figure 4-2: Investment required and LCOE estimation for case 1 and case 2.

Therefore, sensitivity analysis has been also performed to evaluate the influence of various factors on the LCOE. The influence of CAPEX (+/- 15%), O&M expenditure (+/- 5%), availability (+/- 5%), fuel price (+/- 15%) and discount rate (+/- 2%) has been evaluated for both cases as shown in *Figure 4-3*. It can be seen from the results that O&M expenditure, availability and the discount rate have a great influence on the LCOE even at low variations. The gasification technology especially for power generation is intimidating for the industry because of high capital and operating costs. In order for the IGCC technology to progress,

the cost of electricity produced using IGCC technology needs to be reduced by efficiency enhancement, process integration and other technological advancements.

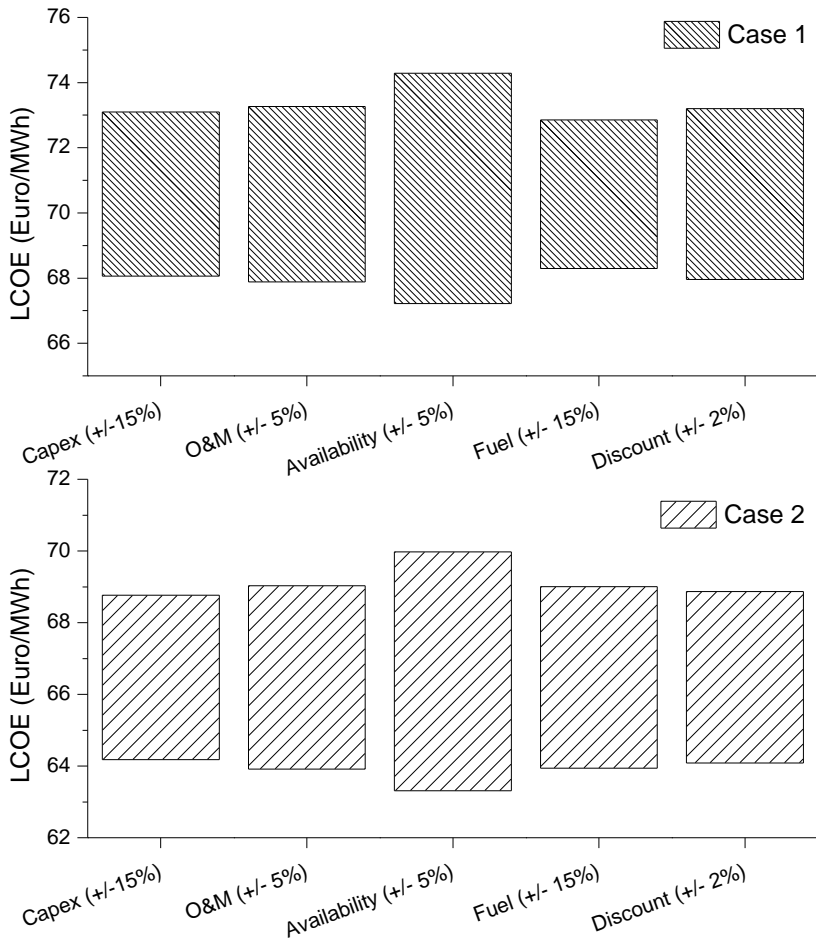


Figure 4-3: Sensitivity analysis of some un-certainty factors influencing LCOE.

This study focused on process intensification technique to enhance process performance and economics. Analyzing the fuel cost trends of the last few decades, the cost of coal is relatively less and stable compared to the natural gas price which is more prone to price fluctuations. Sensitivity analysis has been also performed to evaluate the effect of fuel prices on the overall economic performance. The base case fuel prices have been presented in the *Table 4-2*. The results showed that the fuel prices directly affects the O&M cost of power plants which ultimately impacts the LCOE. The effect of variation in fuel prices (+/- 15%) on the O&M cost for the case 1 design is shown in *Figure 4-4*.

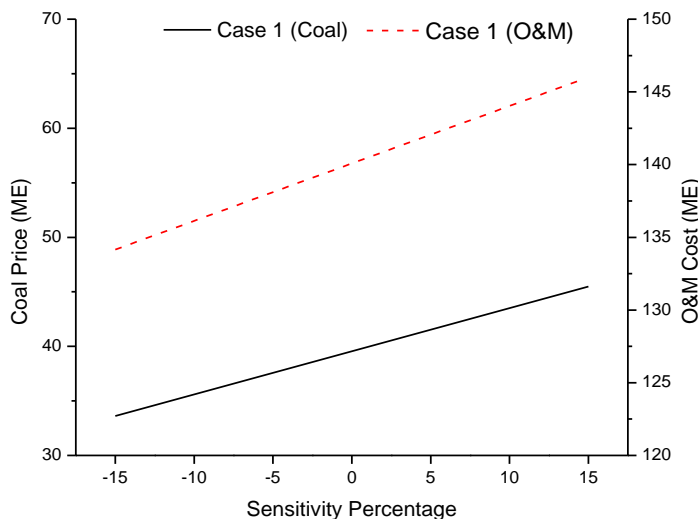


Figure 4-4: Effect of fuel prices on the process economics of case 1

The results show that the O&M cost increases with an increase in coal prices and vice versa. Moreover, the detailed sensitivity analysis have been performed on the fuel prices for the case 2 design as it utilizes both natural gas and coal. The results for the gas and coal price fluctuations on the economic performance have been shown in *Figure 4-5*.

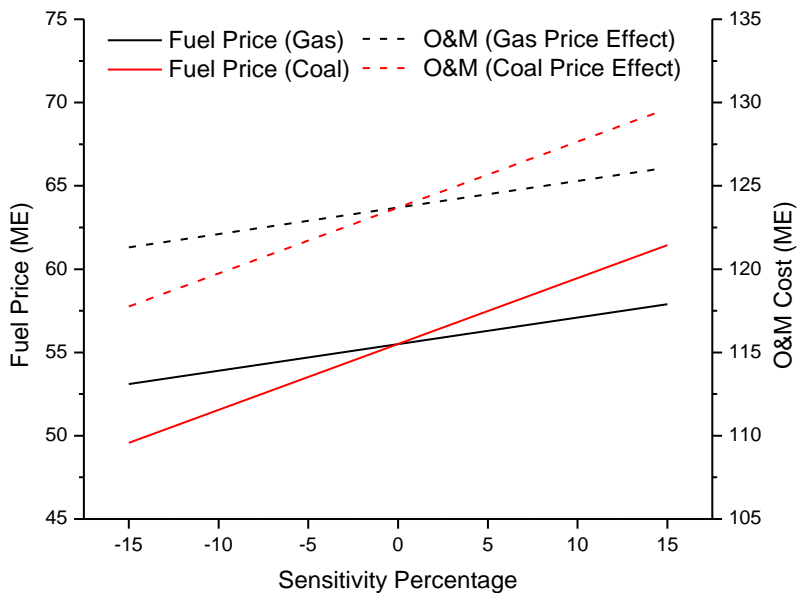


Figure 4-5: Effect of coal and natural gas prices on O&M cost of case 2

It can be seen from the results that a direct relationship exhibits between the fuel prices and O&M cost. An increase in the gas and coal price increases the overall O&M cost of the process and vice versa.

4.4 Cost of CO₂ capture.

CO₂ avoided and removal costs are considered as an important economic indicators to analyze process performance of power generation systems with CCS technologies. CO₂ avoided and removal costs can be calculated using Equation 27 and Equation 28, respectively.

$$CO_2 \text{ avoided cost} = \frac{LCOE_{with\ CCS} - LCOE_{without\ CCS}}{CO_2 \text{ emissions}_{without\ CCS} - CO_2 \text{ emissions}_{with\ CCS}} \quad 27$$

$$CO_2 \text{ removal cost} = \frac{LCOE_{with\ CCS} - LCOE_{without\ CCS}}{CO_2 \text{ removed}} \quad 28$$

The CO₂ avoidance cost calculated for case 1 and case 2 is 36.23 and 27.97 €/tonne, respectively. On the other hand, CO₂ removal cost calculated for case 1 and case 2 is 26.99 and 20.45 €/tonne, respectively. Usually, the CO₂ removal cost is lower than the avoided cost due to an extra energy requirements for operating CO₂ capture systems which increase the overall CO₂ emissions [76]. CO₂ avoidance and removal cost for both the cases along with their LCOE is given in *Table 4-4*. The results shows that the case 2 design offers 22.8% and 24.2% less CO₂ avoidance and removal cost, respectively, compared to the case 1 design.

Table 4-4: CO₂ capture and avoided cost

	Units	Case 1	Case 2
LCOE	€/MW _h	70.57	66.47
CO ₂ Specific emission	kg/MW _h	87.74	80.26
CO ₂ avoidance cost	€/tonne	36.23	27.97
CO ₂ removal cost	€/tonne	26.99	20.45

4.5 Summary

In this study, the economic analysis has been performed on the conventional IGCC process (case 1) and an integrated IGCC with reforming process (case 2) using some important economic indicators. The results showed that the total investment cost (TIC) required for case 1 and case 2 is calculated as 1093.75 and 1255.12 M€'s, respectively. Moreover, the TIC/MW_{net} calculated for case 1 and case 2 is 2.93 and 2.06 M€'s respectively. The results showed that the TIC for case 1 is lower than the case 2, however, the TIC required for each MW of energy generated for case 2 is 29.7% less than the case 1 design. As the main purpose of the power plants is to generate electricity so the results are also compared in terms of levelized cost of electricity (LCOE). The LCOE calculated for case 1 and case 2 is 70.57 and 66.47 €/MW_h, respectively. It has been from results that due to the higher power

generation capacity of case 2 design, it has a potential to reduce the LCOE by 5.81% compared to the case 1 design. Moreover, economic analysis has been performed to evaluate the CO₂ capture cost, cumulative cash flow of the projects and the investment payback time for both cases. It has been seen from results that the case 2 design not only requires the less CO₂ capture and avoidance costs compared to the case 1 but also exhibits higher rate of return on the investment with the less payback time.

Chapter 5 : CO₂ Topside Injection Process

5.1 Introduction

Carbon capture and storage (CCS) is one of the technologies to handle greenhouse gases in order to limit their global warming impact. CCS consists of a number of processes in series starting from CO₂ capture, its transportation and storage at a safe location, generally a geological site. CCS is not a new concept, oil and gas industry in the US has been capturing and transporting CO₂ through thousands of kilometer pipelines for the purpose of enhanced oil recovery (EOR) process as early as 1970s. At that time, the objective of CO₂ injection into the geological site was mainly attributed with enhancing the oil production for economic reasons. However, with further progress in research relating the CO₂ emissions with the climate change impact, CO₂ injection into the storage site has an added aspect of permanent CO₂ storage to limit its atmospheric emission levels. The requirement to control the CO₂ emission level, more geological sites including depleted oil and gas reservoirs, enhanced coal bed storage and saline aquifers have been explored where CO₂ can be safely stored for long duration of time. All the CO₂ in the US and Canada used for the EOR application has been

transported through pipelines in the supercritical phase ($P > 7.382$ MPa, $T > 31.04$ °C) due to economic reasons. However, other transportation methods and thermodynamic conditions may be competitive, especially when the storage site is off-shore and installation of a pipeline requires a reasonable capital cost. In such a situation, CO₂ transport in liquid phase using ships can be an alternative choice. The well bottom reservoir conditions are dictated by its location and geology. However, the CO₂ injection parameters are not constrained by the reservoir conditions but by the topside delivery conditions.

One of the potential offshore storage locations in South Korea is Ulleung basin that is located 60 km away from the East coast in the East Sea. Two integrated CCS projects (KCCS-1 and KCCS-2) currently at an evaluation stage plan to transport 1.0 Mtpa of CO₂ by ship from a post-combustion capture facility to the Ulleung basin. Some studies investigated the transport scenarios from various capture sites to the Ulleung basin. Yoo et al. [77] performed a feasibility study on the liquid CO₂ transport to Ulleung basin using shipping. They concluded that the CO₂ transport using ship even for the shorter distance is recommended because of flexible operation. Kang et al. [78] estimated the CO₂

transport cost in South Korea for both the pipeline and ship transport. They found the cost to be approximately US\$21/tCO₂ and US\$23/tCO₂ for the pipeline and ship transports, respectively for a transport capacity of 3 Mt CO₂ per year.

Most of the recent studies focusing on ship transportation of CO₂ set their research boundary upstream of an injection system. On the other hand, studies investigating the storage mechanism in the EOR field or other geological locations assumed the fixed CO₂ conditions from the literature. The purpose of this study is to evaluate the design of CO₂ injection system for an off-shore storage site where CO₂ is available in the liquid phase at the vessel. Though, LCO₂ unloading from the ship and its injection in the well represents a small section of an overall CCS chain, nevertheless, it is a critical part from an operational point of view that should not be overlooked.

The injection system comprise of pressurizing and heating equipment that can maintain conditions required at the reservoir wellhead. The temperature and pressure conditions required at reservoir wellhead are reservoir specific for each injection site, however, heating and pumping is always required. The injection system can be either equipped on the

ship or installed on the off-shore platform. Few studies have investigated the design and operation of an injection system. Aspelund et al. [79] suggested the pressurizing and heating of LCO₂ to 60 bar and – 45 °C respectively on the ship and an additional pumping and heating on the platform. You et al. [80] proposed to utilize the cold energy of liquid CO₂ before injection by making use of a Rankine cycle. They also evaluated the exergy efficiency and performed the life-cycle cost for the injection system. A detailed liquid CO₂ injection modelling study was conducted by Krogh et al (Krogh et al., 2012). They simulated the case studies for Snohvit and Sleipner projects using OLGA and Aspen HYSYS® software. Another knowledge sharing report [81] proposed to pump the liquid CO₂ to the required wellhead condition in three stages by first pumping the liquid CO₂ from 7 bara to 21.01 bara, then to 46.01 bara and finally 155 – 400 bara depending on the reservoir conditions. This study [81] recommended to have a vaporization unit on the ship to partly vaporize liquid LCO₂ and return it back to the CO₂ vessel in order to avoid sudden temperature drop. Seo et al. (2016) proposed the pumping and heating of liquid CO₂ from 6 bar and -52 °C to 100 bar and 15 °C.

All the above mentioned studies considered the liquid CO₂ at the thermodynamic conditions of 6-7 bara and -50 - 53 °C assuming large CO₂ transport volumes. However, currently there are no commercial ships which transport liquid CO₂ at such cryogenic conditions and only small size ships up to 1,500 m³ are being used for CO₂ transport at (-27 °C, 16 bar). Tanker trucks mainly used for bulk transportation of CO₂ store liquid CO₂ in cryogenic vessels and conditions of liquid CO₂ is typically at 20 bar and -20 °C. For example, in case of Shenhua CCS pilot project, insulated tank trucks were used to transport liquid CO₂ at -20 °C and 20 bar to the storage site located 17 km away from the capture site [82]. Decarre et al.[83] studied the liquefaction and transport of CO₂ at thermodynamic conditions of (-50 °C, 7 bar) and (-30 °C, 15 bar). They concluded that the (-30 °C, 15bar) case offers the least CAPEX and OPEX from the outlet of the capture plant to the inlet of the temporary storage (conditioning, transport and liquefaction). All the previous studies assumed pure CO₂ stream available from the liquefaction plant into the vessel storage. However, in actual plants, some ppm of water content and other impurities may be left even after the dehydration and impurity removal processes.

The purpose of this study is to design a top side CO₂ injection system which can unload the liquid CO₂ available at -20 °C and 20 bara considering all the design and operational constraints of a liquid CO₂ injection system. The thermodynamic conditions required at the injection system need an assessment from topside process point of view, since existing technology will be used during the initial phase of CO₂ transport development and implementation. The liquid CO₂ conditions of -20 °C and 20 bara also suggest that it will require less heating and pumping energy to achieve the required well head conditions compared to that if the liquid CO₂ is available at -52 oC and 7 bara. This study compares the performance of two thermodynamic operating conditions and evaluate them in terms of performance and economics. This study also aims to fill the study gaps from the previous researches. For example, all the previous studies assumed the CO₂ stream as a pure liquid CO₂, however, practically this may not be possible since some amount of water is left in the CO₂ stream posing a threat of hydrate formation. In this study, we incorporate the CO₂ vapor return line to the pressure vessel which is an important aspect from safety point of view. This paper also investigates the application of two-stage rankine cycle to utilize the cold energy available from liquid CO₂ which can help to improve the overall

efficiency of the injection system compared to that of the base case design.

5.2 Process Design

5.2.1 Base Case

In line with other reference studies, base case design consists of simple pressurization and heating the liquid CO₂. Figure 5-1 shows the process flow diagram for the base case design. Liquid CO₂ available at -20 °C and 20 bara is pumped out from the storage vessel and then heated using sea water as a heating medium.

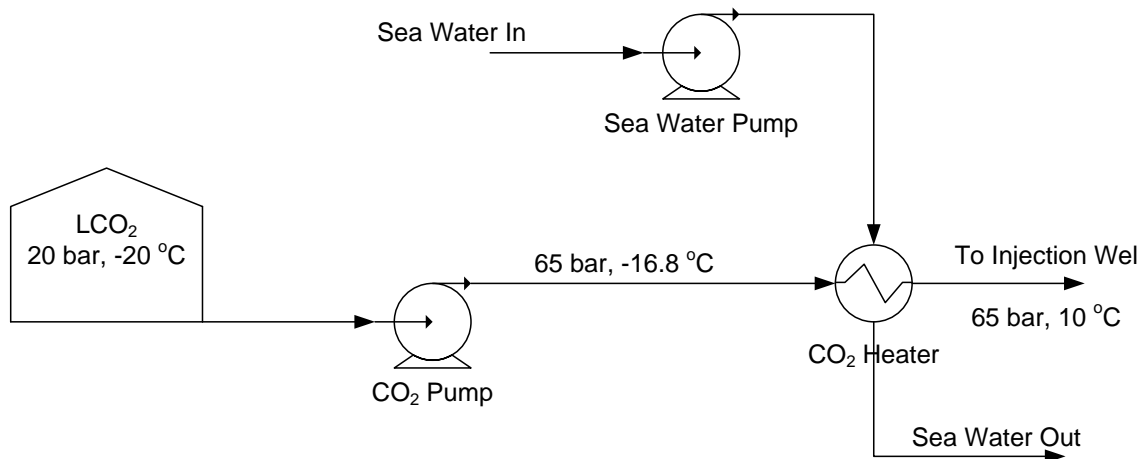


Figure 5-1: Base Case Design for CO₂ Injection

The pump increases the pressure to 65 bara before heating the liquid CO₂ to a well head temperature of 10 °C. The base case design is very similar

to the design of Shenhua CCS pilot project which consisted of a booster pump and an electric heater to increase the pressure and temperature of liquid CO₂. The temperature and pressure at the reservoir well head was increased to 0 °C and 60 bar respectively for the CO₂ injection. The project successfully injected 300 kt of CO₂ over the duration of 3 years [82]. The base case specifications used in this study are listed in Table 5-1.

Table 5-1: Base case specification

	Value	Unit
Feed flow rate	114	t/h
Temperature	-20	°C
Pressure	20	bara
Composition		
CO ₂	0.9999	mol %
H ₂ O	100	ppm
Sea water temperature	16.6	°C
Storage depth	1000	m

The well head pressure is chosen considering the pressure due to CO₂ head at the well bottom, well bottom reservoir pressure and reservoir fracture pressure. The BHIP will be limited to some fraction of the reservoir fracture pressure, as it would be undesirable to fracture the wellbore environment in a CO₂ storage operation. In the absence of field data, the fracture pressure can be estimated from a correlation presented by Heller and Taber [84]:

$$G_f = \gamma - \beta e^{-\alpha d}$$

$$P_f = G_f d$$

where, G_f is the fracture gradient (Pa/m); α , β and γ are coefficients with the values $4.36 \times 10^{-4} \text{ m}^{-1}$, 9.24 kPa/m, and 22.62 kPa/m, respectively; and, p_f is the fracture pressure at depth (Pa). Once the BHIP is known, the wellhead pressure needed to generate the BHIP can be calculated. Given the depth of reservoir, reservoir temperature is calculated assuming a geothermal and pressure gradient of 0.011 C/m and 1.26 psi/m respectively for the Ulleung basin. Therefore, a well head injection pressure of 65 bar is set as a base case value for a storage depth of 1000 m.

Figure 5-2 shows the operating pressure range. It seems that at deeper storage locations, there is more allowable pressure variation range which can allow us to have lesser number of wells. The area between fracture pressure (P_f) line and reservoir pressure (P_r) line is the available area for varying the operational well bottom pressure (P_{wb}). In figure (Well Pressure), P_{co_2} represents the pressure due to CO_2 head at specific depth and P_{head} represents that pressure which must be available at the well head to inject CO_2 in reservoir.

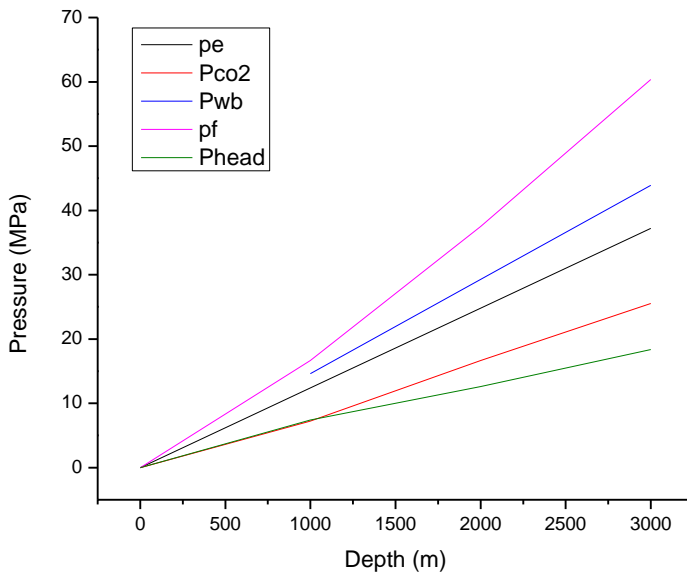


Figure 5-2: Relation between wellhead pressure and depth

Well head temperature of 10 °C is chosen to avoid any hydrate formation in the injection well or at the well outlet. Hydrates are the crystalline solid structures that can form in the presence of free or dissolved water at low temperatures and high pressure conditions. Such crystalline precipitates can damage the mechanical equipment or cause blockage in the injection well [85]. *Figure 5-3* shows the region of hydrate formation on the PT diagram assuming free water content in the CO₂. Hydrates can form in the stream if the operating conditions are on the left side of CO₂ hydrate curve.

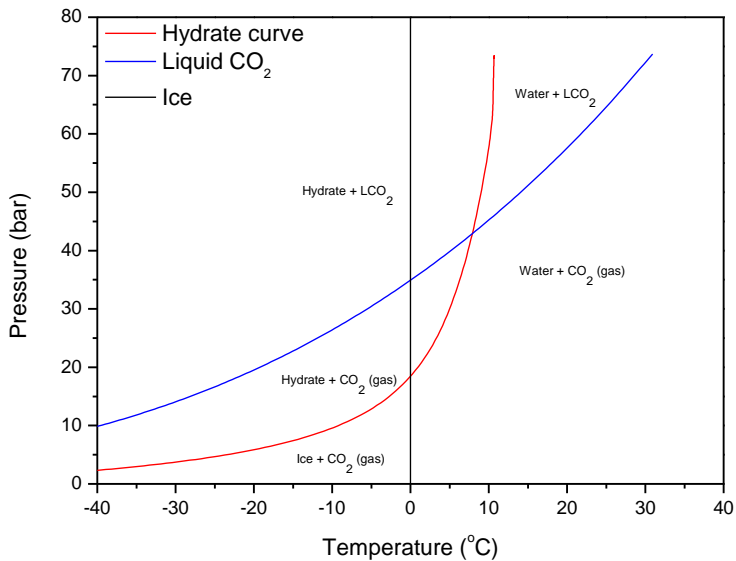


Figure 5-3: CO₂ hydrate curve assuming free water content

5.2.2 2-Stage Rankine Cycle

In pumping and heating the liquid CO₂ from -20 °C to 10 °C, CO₂ cold energy is wasted. The amount of unutilized cold energy while heating the liquid CO₂ from -20 °C to 10 °C amounts to almost 69.2 kJ/kg which corresponds to a power output of 19.2 kWh per ton of CO₂. This study proposes a design which can utilize the CO₂ cold energy for power generation instead of wasting it in the sea water. The proposed topside system in this study employs a two stage pumping of liquid CO₂ while recovering the cold energy using two stage rankine cycle. *Figure 5-4* shows the process flow diagram for the 2-stage rankine cycle design. A small fraction of liquid CO₂ from the storage tank outlet is first heated to generate CO₂ vapor which is subsequently separated from the liquid CO₂ and sent back to the storage tank. The amount of vaporized CO₂ is less than 1 % of the stream flowrate, therefore, a small compressor or blower will suffice the need to return the CO₂ vapor back to the LCO₂ tank. The vapor return line is required to maintain the liquid CO₂ tank pressure. The required vapor return flowrate to the storage tank can be calculated using the mass balance around the storage tank. The separated liquid CO₂ from the flash drum is pumped to a pressure of 65.2 bar. The mechanical inefficiency from the pump increases the LCO₂ temperature to around -

16 C which then exchanges heat with the two-stage rankine cycle. The liquid CO₂ get warmed to – 4 C after the second stage of rankine cycle. The required well head conditions (65 bar and 10 °C) are finally achieved by heating the liquid CO₂ stream using the sea water as a heating medium.

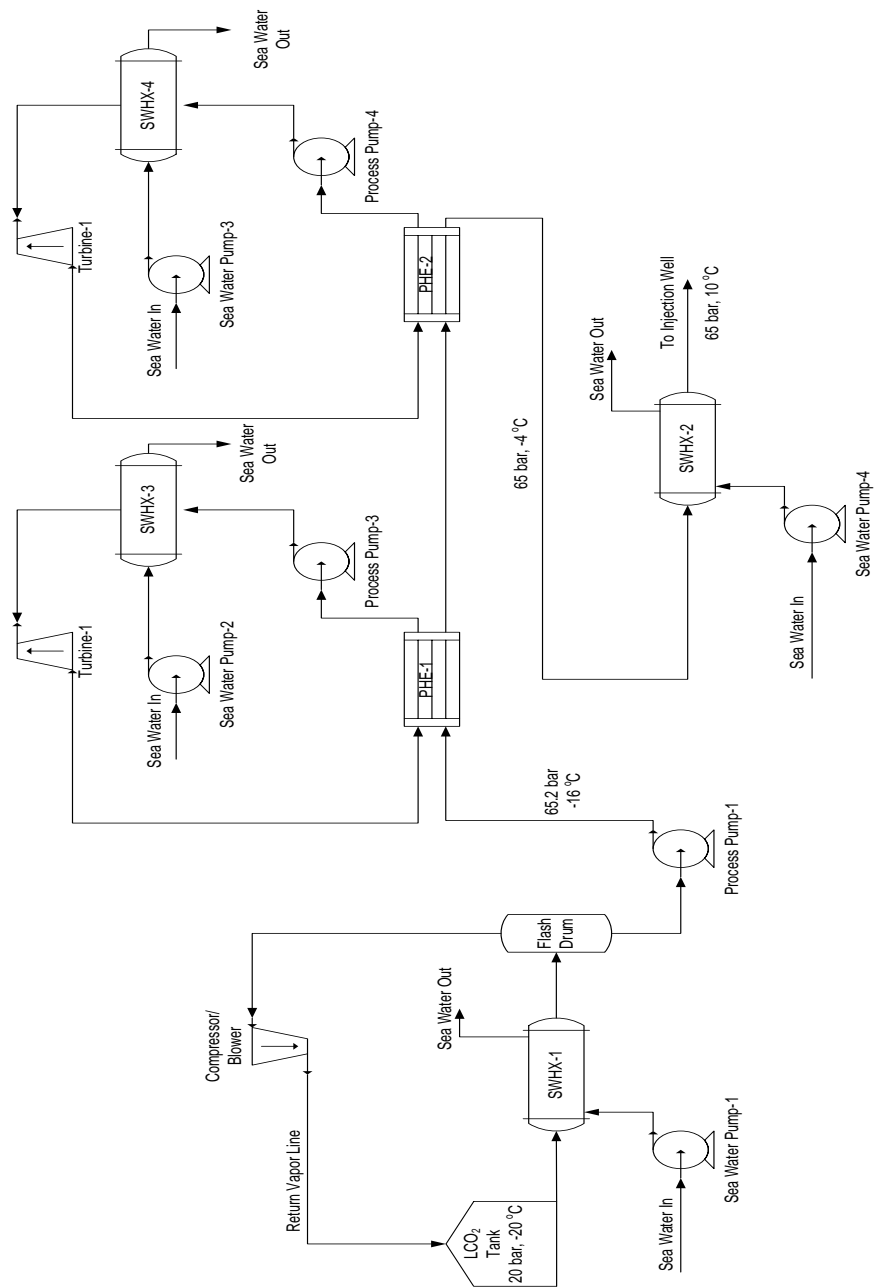


Figure 5-4: 2-Stage NH₃ Rankine cycle

Figure 5-5 shows the P-h diagram for the process along with the base case design. The figure shows that both the base case design and 2-stage rankine cycle injection design follows a very similar path on the P-h diagram.

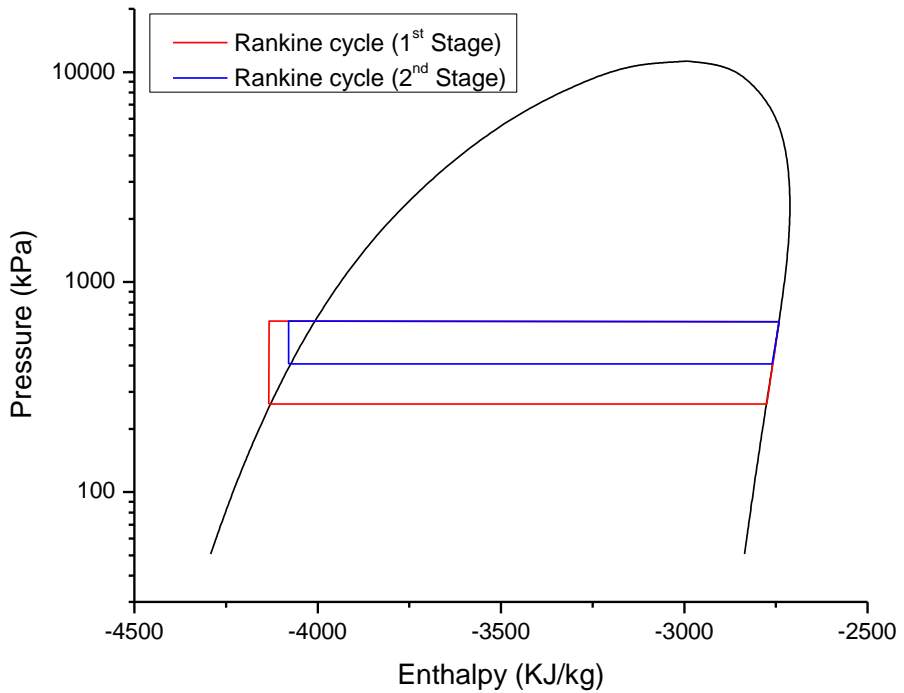


Figure 5-5: Ph diagram of 2-Stage Ammonia Rankine Cycle

The working fluid employed in both the stages of rankine cycle is ammonia because of its highest power generation performance, easy

availability and environment friendly characteristics compared to other working fluids. The rankine cycle is a closed loop thermodynamic cycle that converts heat into the electrical power. The amount of work produced per unit mass of ammonia from the two stages of rankine cycle is approximately 105 kJ and 46.5 kJ respectively. *Figure 5-5* shows the P-h diagram for the two stage rankine cycle. The liquid ammonia is first pumped (1a → 1b) and then heated (1b → 1c) using the sea water to vaporize it completely. The ammonia vapors at high pressure then goes through the turbine (1c → 1d) to generate mechanical work which can be converted to electrical power. The low pressure ammonia vapors are finally condensed (1d → 1a) by using the cold energy from the liquid CO₂ in a closed loop cycle.

5.3 Results and Discussion

5.3.1 Energy Analysis

The net power consumption for the base case and 2-stage rankine cycle for the design injection capacity of 1 Mt CO₂ per year is 496.6 kW and 217.7 kW respectively. The power break down analysis for both the designs is shown in Table 5-2.

Table 5-2: Energy analysis of the top side injection system

	Base Case	2-Stage Rankine cycle
Liquid CO ₂ Pump (kW)	333.01	164.71
Sea Water Pump (kW)	163.67	33.95
Ammonia Pump (kW)	-	0.33
Vaporizer (kW)	-	54.23
Turbine Output (kW)	-	35.51
Net Power Consumption (kW)	496.68	217.71
Specific Power Consumption (kWh/ton of CO ₂)	4.33	1.90

The results show that the 2-stage rankine cycle design consume approximately 56% less power compared to that of the base case design. The reduced net power consumption in case of 2-stage rankine cycle design is achieved mainly by the use of liquid CO₂ cold energy for the power generation using rankine cycle. Although, the incorporation of 2-stage rankine cycle and vaporizer involves more equipment compared to the base case design, however, the overall exergy losses are significantly reduced which resulted in lower net power consumption. The results

show that the net specific power consumption for the base case and 2-stage rankine cycle design is 4.33 and 1.90 kWh per ton of CO₂ injected respectively.

5.3.2 Economic Analysis

2-stage rankine cycle design have more number of equipment compared to the base case design as evident from the process flow diagram. Although the proposed design offer better performance in comparison to the base case design, however, the additional equipment employed in the 2-stage rankine cycle requires the evaluation of process economics. Therefore, the economic analysis has been performed to determine the CAPEX, OPEX and per unit injection cost for the two designs. For the purpose of economic evaluation, Aspen Process Economic Analyzer (APEA) V9.0 has been used to evaluate the capital cost of the equipment. APEA not only estimates the equipment cost, but also asses the piping, civil, steel, instrumentation, electrical, insulation, paint and contingencies associated with the equipment cost. The project life in this study is assumed to be 10 years and the cost of electricity is assumed to be 0.077 \$/kWh. Figure xx (Base case 20bar) shows the cost break down in terms of CAPEX and OPEX. The CAPEX for 2-stage rankine cycle

design is higher compared to the base case design because of an additional equipment implemented in the process. The CAPEX of the base case design approximately contributes 67 % of the total annual cost. On the other hand, CAPEX of the 2-stage rankine cycle design attributes to around 85 % of the total annual cost. The specific cost per unit ton of CO₂ injected for both the design is approximately US\$ 1.03 for a project life of 10 years. It is well understood that the total project life affects the per unit injection cost. Table 5-3 shows the capital cost estimation of each equipment for the two designs. The most expensive equipment common among all the designs is the liquid CO₂ storage tank. Pressurized spherical tank (d = 16 m) for cryogenic application has been assumed for the purpose of cost analysis. The diameter of the spherical tank considerably affects the total cost of the tank.

Table 5-3: Capital cost estimation for the base case and 2-stage rankine cycle design

	Base Case	2-Stage Rankine Cycle
LCO2 Storage Tank (\$)	2111400	2111400
Vaporizer (\$)	-	27000
Flash Drum (\$)	-	49400
CO ₂ Pumps (\$)	149700	149900
Sea water Pumps (\$)	168500	68900
Ammonia Pumps (\$)	-	8500
Turbines (\$)	-	174000
Condenser (\$)	-	46400
Evaporators (\$)	-	47600
Final Heat Exchanger (\$)	56200	43300
Total Capital Cost (M\$)	7.00	9.00

5.3.4 Process Comparison

Most of the previous research studies assumed the liquid CO₂ to be available at -52 °C and 7 bara because of high transport density. The density of liquid CO₂ at -52 °C and 7 bara is approximately 1162 kg/m³ compared to 1031 kg/m³ at -20 °C and 20 bara. This study compared the two thermodynamic conditions to evaluate their impact on the performance and cost of injection process. A similar 2-stage rankine cycle design is developed for the thermodynamic vessel conditions of -52 °C and 7 bara as shown in *Figure 5-6*. Same well head conditions of 65 bar and 10 °C are maintained for both the designs to have a consistent comparison.

Figure 5-7 shows the comparison between two designs in terms of energy consumption and generation. The pumping power required to raise the liquid CO₂ pressure in case of 7 bara design is approximately 15 % more compared to the 20 bara process due to high ΔP required to achieve well head pressure condition. In case of 7 bara design, the collective water pumping power of all the pumps is 10 times more compared to the 20 bara design because of more water consumption in the process. The vaporizer employed in the process to produce small quantity of vapor for

maintaining vessel pressure consumes 3.5 times more power compared to that required in the 20 bara process because of severe cryogenic conditions in 7 bara process.

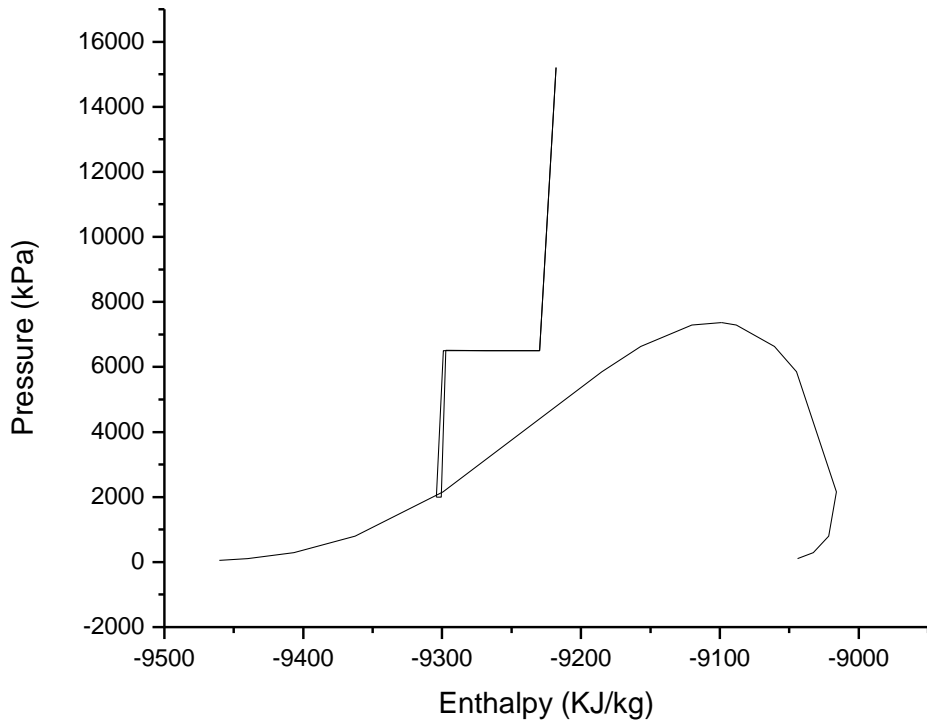


Figure 5-6: Comparison of base case and the improved case

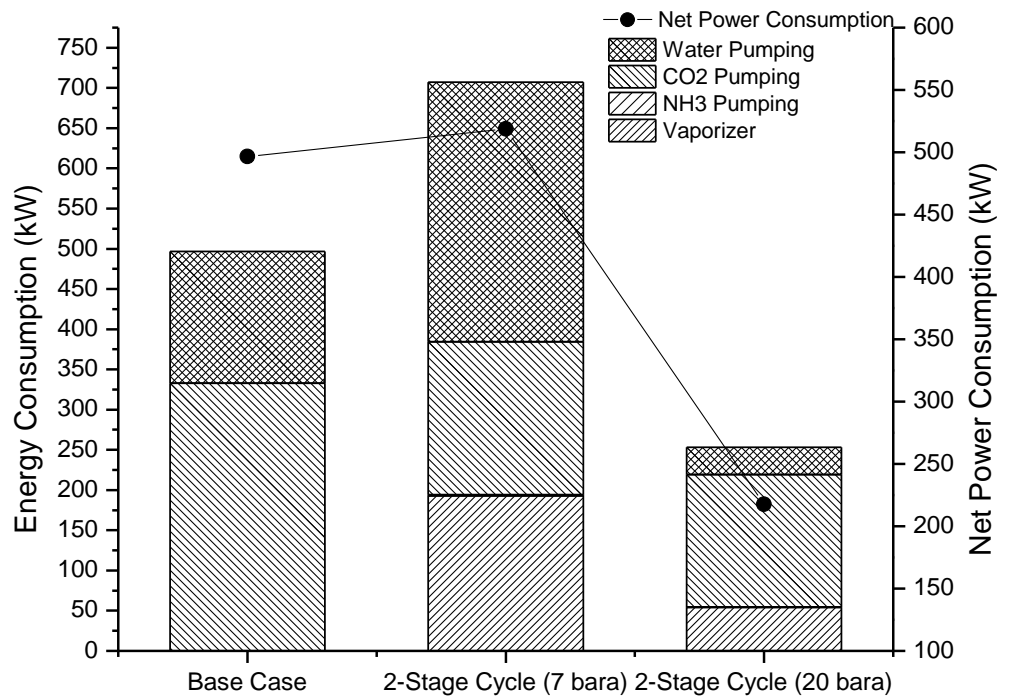


Figure 5-7: Energy Consumption of the Processes

Since more cold energy is available from the 7 bara process, therefore, rankine cycle produces 5.3 times more power compared to 20 bara process for the same CO₂ flowrate. The results show that the net specific

power consumption for the two conditions (7 bara and 20 bara) is 4.52 and 1.90 kWh per ton of CO₂ injected respectively. Economic comparison has been performed to investigate the impact of operating conditions on the CO₂ injection process. *Figure 5-8* shows the economic comparison of two vessel conditions in terms of CAPEX and OPEX. The results show that the CAPEX for both the conditions is almost same since equipment involved in both the processes is the same.

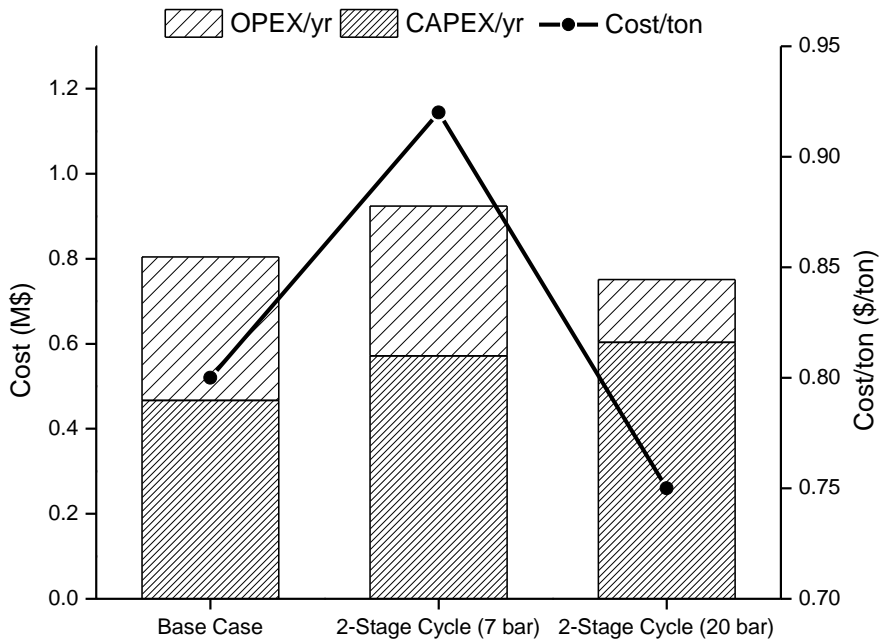


Figure 5-8: Cost Estimation and Economic Analysis

However, the OPEX for 7 bara design condition is approximately 2.4 times high compared to that of the 20 bara conditions. The high OPEX is attributed from the high operational energy requirement of the process as discussed above. The specific cost per unit ton of CO₂ injected for the two design conditions (7 bara and 20 bara) came out to be 0.80 \$ and 0.75 \$ respectively.

5.4 Sensitivity Analysis

5.4.1 Well Head Temperature

To ensure the safe operation of injection system, well head temperature of 10 °C is calculated as a base value. Depending on the reservoir temperature, water content in the CO₂ stream and available sea water temperature at the storage site, well head temperature can vary which can impact the energy consumption of the injection system. Therefore, a sensitivity has been performed to see the impact of well head temperature on the specific energy consumption for the two designs. *Figure 5-9* shows the effect of well head temperature on the specific energy requirement for the two cases. The results show that more energy is required to maintain a higher well head temperature. A high well head

temperature will ensure no hydrate formation but at the cost of more operational energy. However, other methods are also possible where a lower well head temperature can be maintained without the risk of hydrate formation. For example, hydrate inhibitors can be used to limit the hydrate formation provided the water content in the CO₂ stream is below certain level.

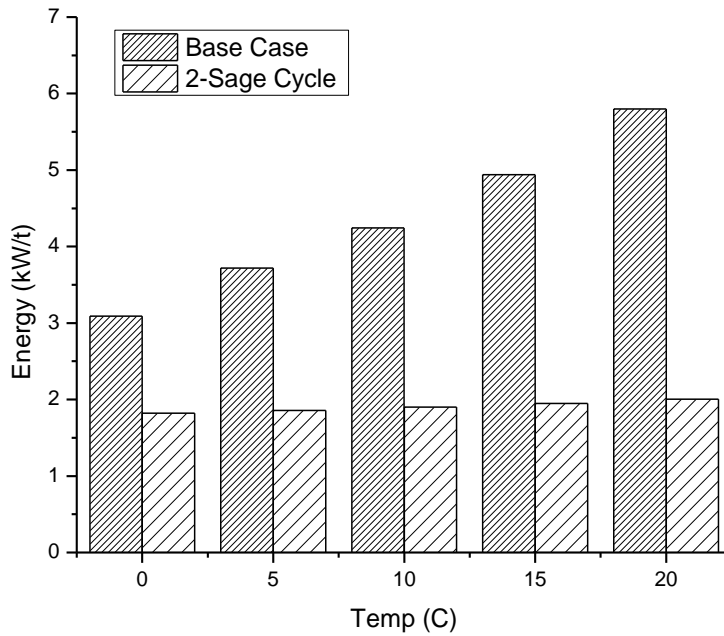


Figure 5-9: Relation between well head temperature & specific energy

5.4.2 Sea Water Temperature

An assumed base value of 16.6 °C is used for the sea water temperature. However, sea water temperature is a site specific parameter and can change depending on the location and season of the year. Therefore, a sensitivity has been performed in order to investigate the effect of sea water temperature on the energy consumption of each design. For a fixed liquid CO₂ flowrate, any change in sea water temperature will affect the ΔT across the heat exchanger. *Figure 5-10* shows the effect of variation in sea water temperature on the specific energy requirement for the two cases. The results show that as the sea water temperature increases, the specific energy requirement decreases for both the designs. This is due to the fact that as the sea water inlet temperature increases, ΔT increases causing the water pump energy requirement to decrease because lower water flow rate can satisfy the required heat duty between the hot and cold fluid.

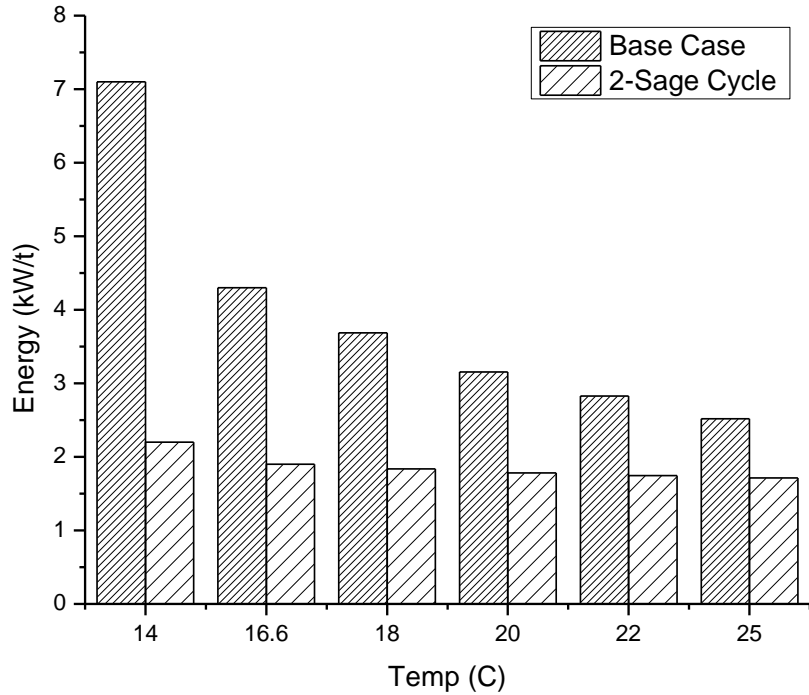


Figure 5-10: Effect of sea water temperature on the specific energy requirements

5.4.3 CO₂ Stream Composition

Water content in the liquid CO₂ stream is an important parameter that can affect the performance of the injection process and hence the associated operational costs. The base value assumed a water content of 100 ppm in the CO₂ stream, however, this may vary depending on the CO₂ capture plant, upstream conditioning and regulatory requirement. Therefore, a

sensitivity has been performed to analyze the effect of water content on the required specific energy of injection process. Figure 5-11 shows the specific power requirement for both the designs with variation in the CO₂ stream water content. It seems from the results that when the water content is available in the CO₂ stream at a ppm level, the specific energy requirement doesn't get effected significantly.

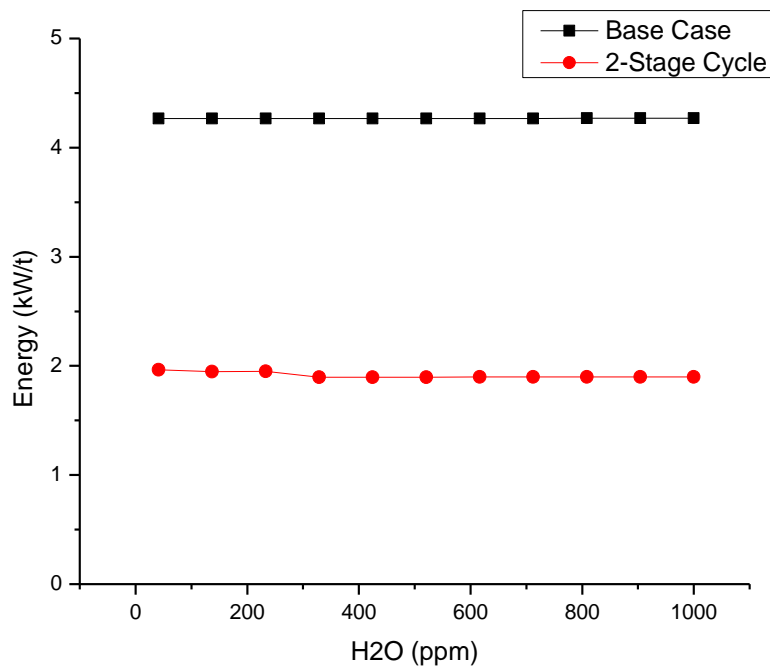


Figure 5-11: Effect of water content in CO₂ stream on specific power requirements

5.4.4 Project Life

Project life is one of the important economic parameters which determines the feasibility of any project at the initial phase of design. Based on the project life of 15 years, the results in the economic analysis showed that the specific injection cost per ton of CO₂ for the base case and 2-stage rankine cycle is almost the same. However, these costs can vary significantly depending on the total project life. A sensitivity has been performed to analyze the impact of project life on the specific injection cost. *Figure 5-12* shows the effect of total project life on the specific cost per unit ton of CO₂ injected and CAPEX and OPEX contribution. The results show that as the project life increases above 10 years, the unit cost of 2-stage rankine cycle design decreases compared to the base case design. The results also show the importance of economies of scale as the unit cost of both the design decreases with an increase in project life. Also, the CAPEX contribution to the total annual cost decreases and OPEX contribution to annual cost increases with an increase in the number of project years.

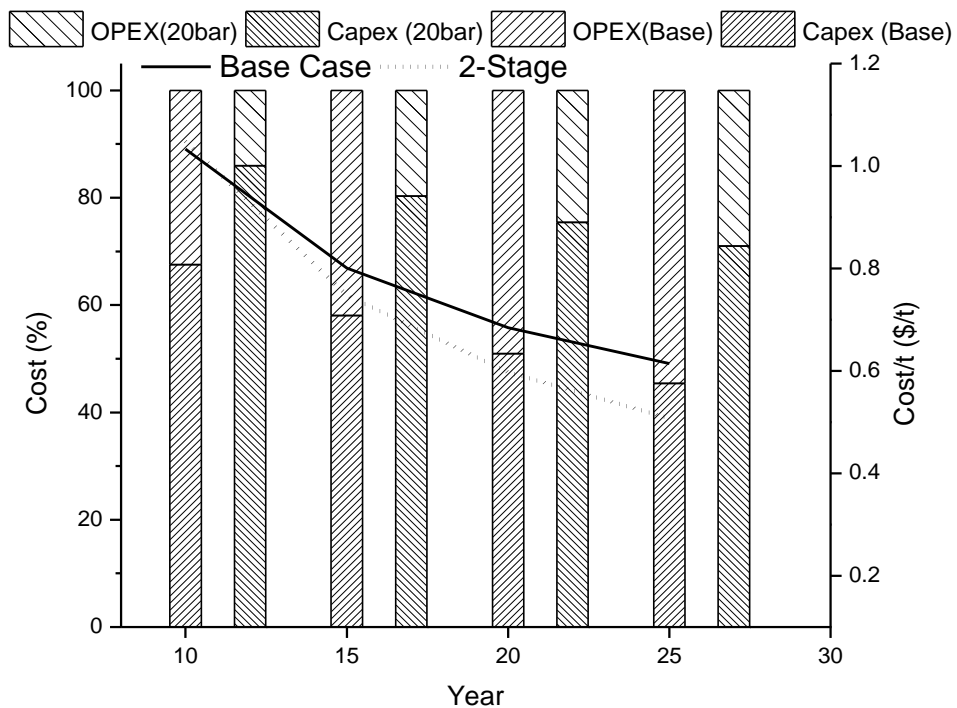


Figure 5-12: Project life and its effect on the specific cost of CO₂ injection

5.5 Summary

Carbon capture and storage (CCS) is one of the dominant technologies to tackle the global warming issue. The transport of CO₂ for geological storage is economically feasible by ship when the storage site location is off-shore and installment of an off-shore pipeline requires a huge capital cost. Ship transportation requires the captured CO₂ to be in liquid phase under pressurized thermodynamic conditions. The injection of liquid CO₂ into the geological reservoir involves pressurization and heating in order to maintain the safe well head operating conditions. This study presents improved design for CO₂ injection that can reduce the power requirement compared to the base case design. The base case and alternative designs are simulated using Aspen HYSYS® in order to decide the process design variables. The study employed two-stage rankine cycle in order to extract the cold energy available from the liquid CO₂ before its injection into the reservoir. The alternative design also proposed to utilize a vapor return line in order to maintain the vessel pressure within safe limits by performing a dynamic simulation. If the LCO₂ is available at -20 °C and 20 bara, the net specific power consumption for the base case and alternative design at 4.33 and 1.90 kWh per ton of CO₂ injected, respectively. The results showed that the

2-stage rankine cycle design consume approximately 56% less power compared to that of the base case design. Moreover, the economic analysis showed that the specific cost of CO₂ injection is 0.80 \$/t and 0.75 \$/t for the base case and alternative case, respectively. Finally, a sensitivity analysis has been done in order to investigate the effect of some important variables (sea water temperature, well head temperature, CO₂ stream composition and project life) in the study.

Chapter 6 : Concluding Remarks

6.1 Conclusions

IGCC power plants are considered as one of the best option for electricity generation with large scale implementation of CCS technology. On the other hand, NGCC power plants offers higher process performance compared to IGCC process with CCS technologies. However, the fluctuating cost of natural gas limits its extensive implementation over coal based power plants. Therefore, an integration of coal gasification and natural gas reforming has been proposed to enhance the process performance while limiting the natural gas consumption. Two case studies have been developed and compared to analyze both the process efficiencies and economics. Case 1 is based on the conventional IGCC process, whereas, case 2 is developed by integrating the conventional IGCC with methane reforming process. The net electricity generation capacity and efficiency for case 1 and case 2 is calculated as (375.08 MW_e, 472.92 MW_e) and (35.93%, 40.70%), respectively. While comparing the results, it has been seen that case 2 design offers nearly 4.7% higher efficiency compared case 1 design with CO₂ capture. The process economics analysis showed that the case 2 design requires a

higher CAPEX and O&M throughout the project life compared to the case 1 design. However, due to the higher power generation capacity and process performance of case 2 design, it has a potential to reduce the LCOE by 5.81% compared to the case 1 design. Moreover, case 2 design not only requires the less CO₂ capture and avoidance costs compared to the case 1 but also exhibits higher rate of return on the investment with the less payback time. With the higher efficiency and least SE_{CO₂}, case 2 has been considered as the most feasible option for electricity production at an economical price compared to the case 1 design.

To complete the CCS chain with the power generation systems, the CO₂ injection system has been also developed in this study. The injection of liquid CO₂ into the geological reservoir involves pressurization (65bara) and heating (10 °C) in order to maintain the safe well head operating conditions. This study presents an improved design mechanism for CO₂ injection that can utilize the cold energy available from the liquid CO₂ to operate the two-stage NH₃ rankine cycle. The results showed that the 2-stage rankine cycle design consume approximately 56% less power compared to that of the base case design. Moreover, the economic analysis also showed that the specific cost of CO₂ injection can be reduced up to 6.2% using the improved design. Finally, a sensitivity

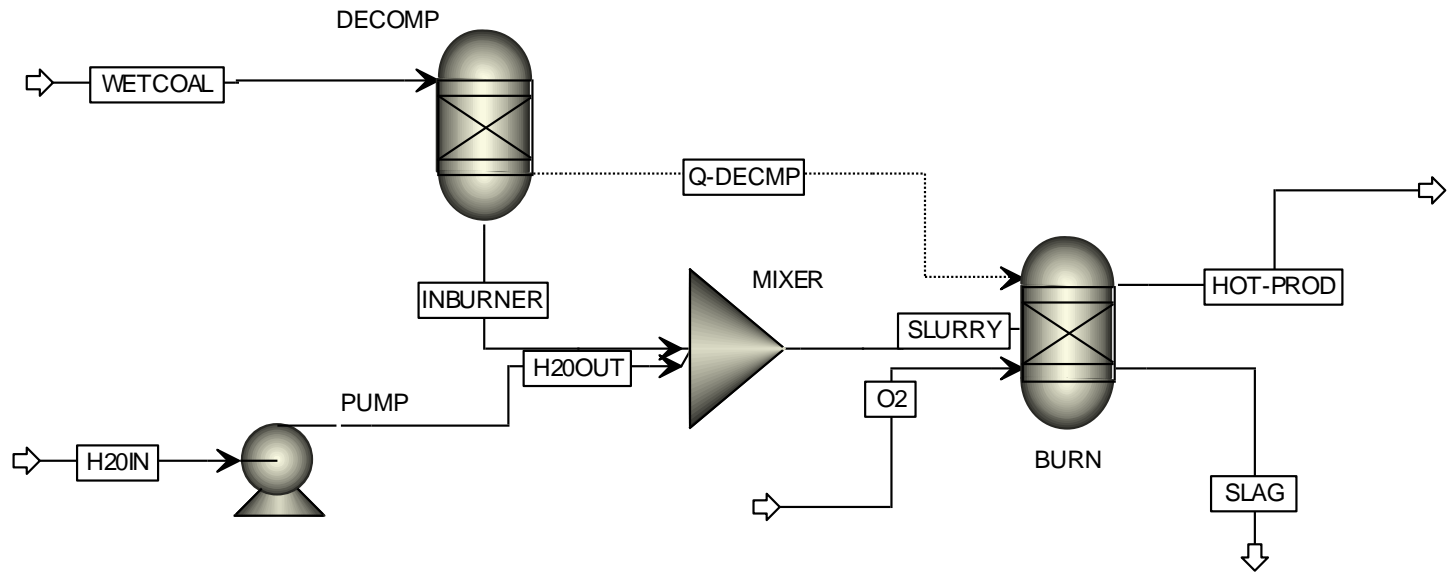
analysis has been also performed in order to investigate the effect of some important variables on the process performance and economics.

6.2 Future Works

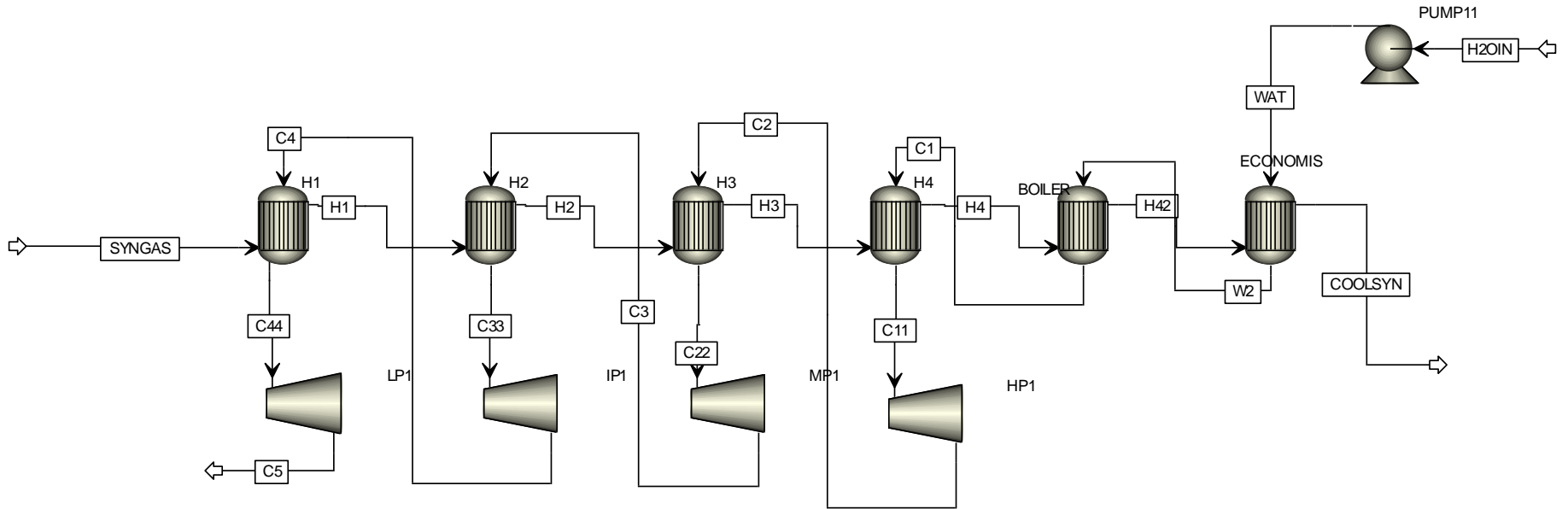
Although there is a lot of literature available for standalone gasification and reforming process, yet there are only few studies available on their integration. There are several topics that can be suggested for the future work. First, the process integration of these two process may not only explore the options for process integration but also for the process intensification. The conceptual design results highlighted the higher process efficiency compared the conventional IGCC and coal fired power plants with the CCS techniques. Therefore, further process optimization and fine tuning of process variables can increase the design robustness. Secondly, the process integration of IGCC and reforming processes can be used to manipulate both the H₂/CO ratios and syngas heating value which can be utilized in generating various Fisher Tropsch chemicals. Third, suggested conceptual design has a potential to enhance the hydrogen gas production compared to the conventional energy intensive processes. The future requirements of hydrogen gas for power generation can significantly enhance the reliability of the suggested

design. Therefore, the co-production of both the hydrogen and electricity in the single process can be studied in more detail to enhance the process economic and making the process more sustainable. Last but not least, the conceptual design of integrating the coal gasification and methane reforming processes can pose some operational difficulties, so the risk and hazard based analysis including HAZOP studies should be performed for the commercial implementation of the conceptual design for power generation with CO₂ capture.

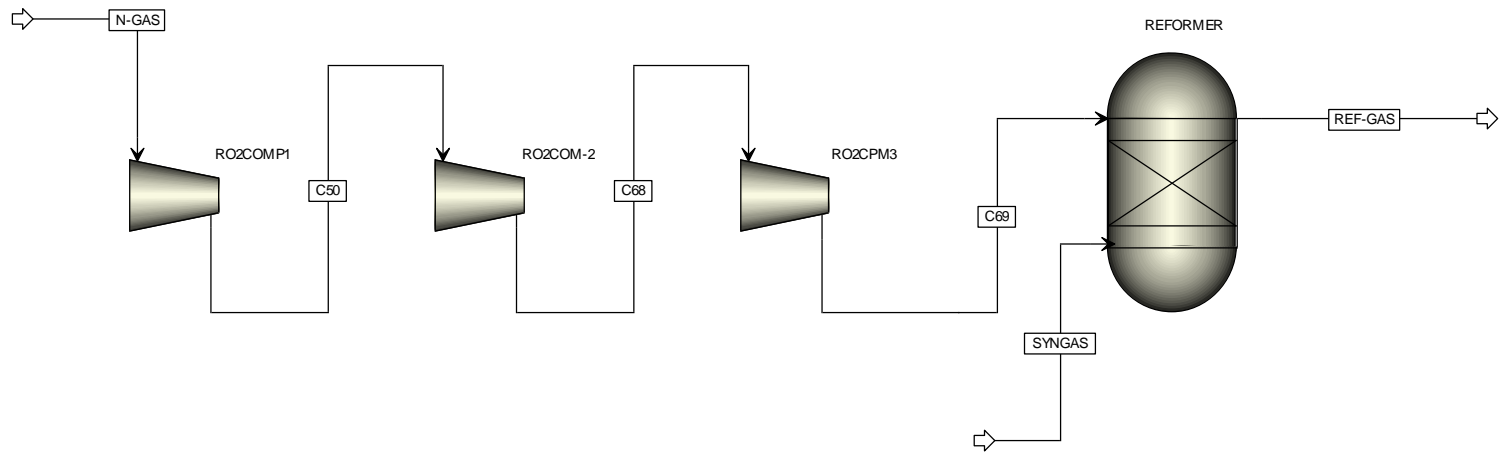
APPENDIX



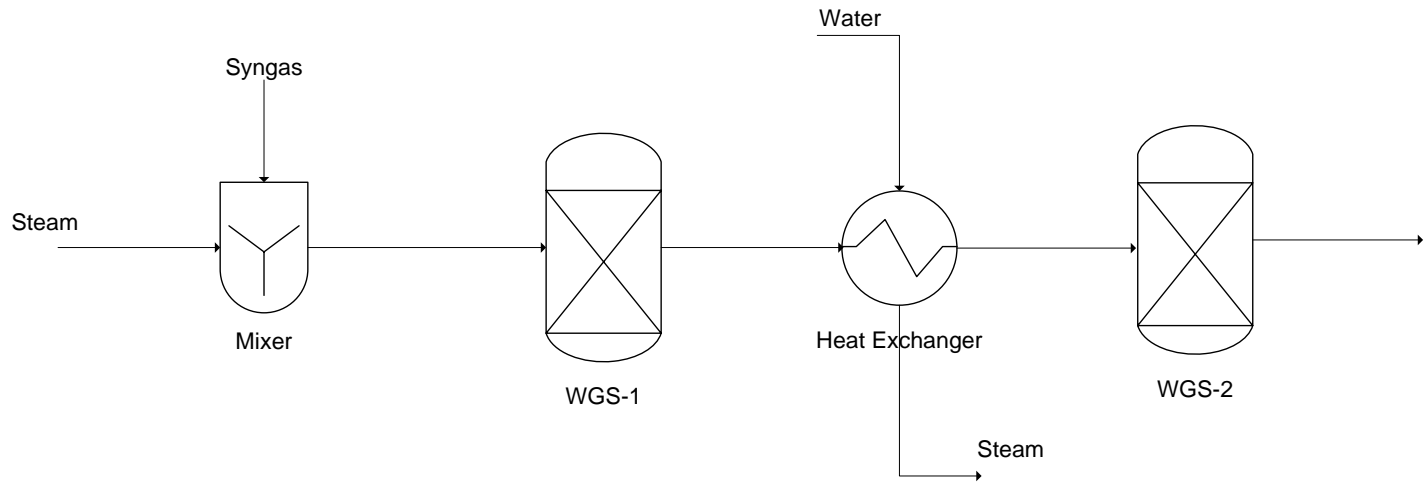
Process Flow Model Entrained Flow Gasification Island



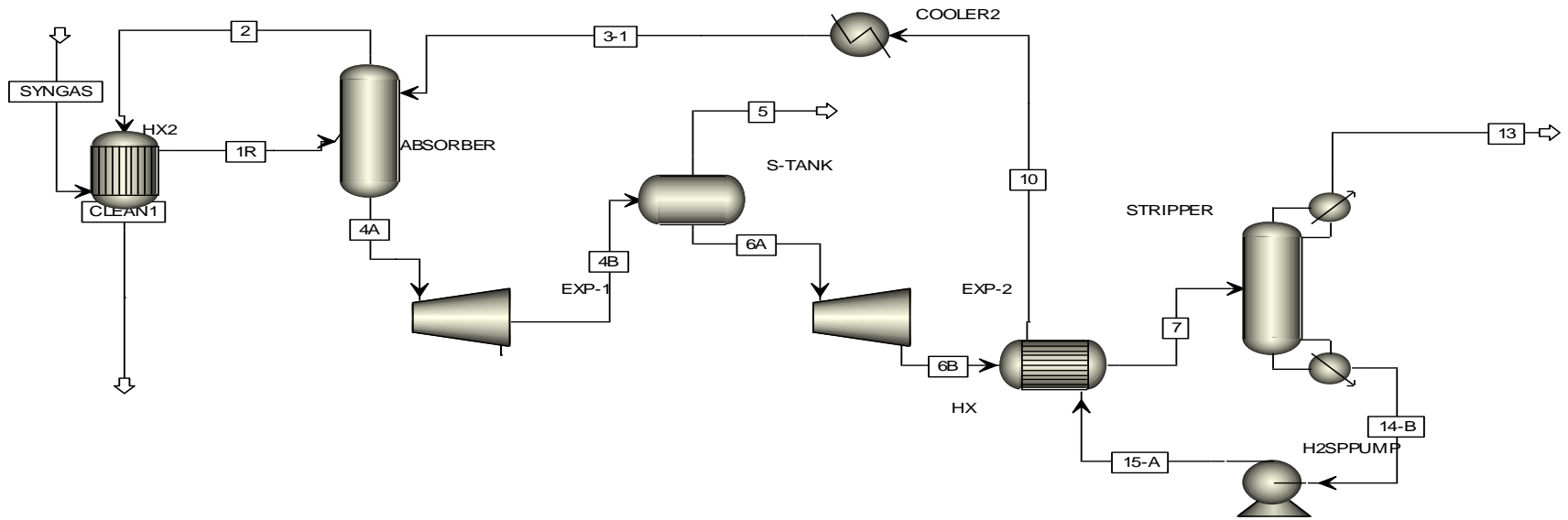
Process Flow Diagram of Heat Recovery Steam Generation (HRSG)



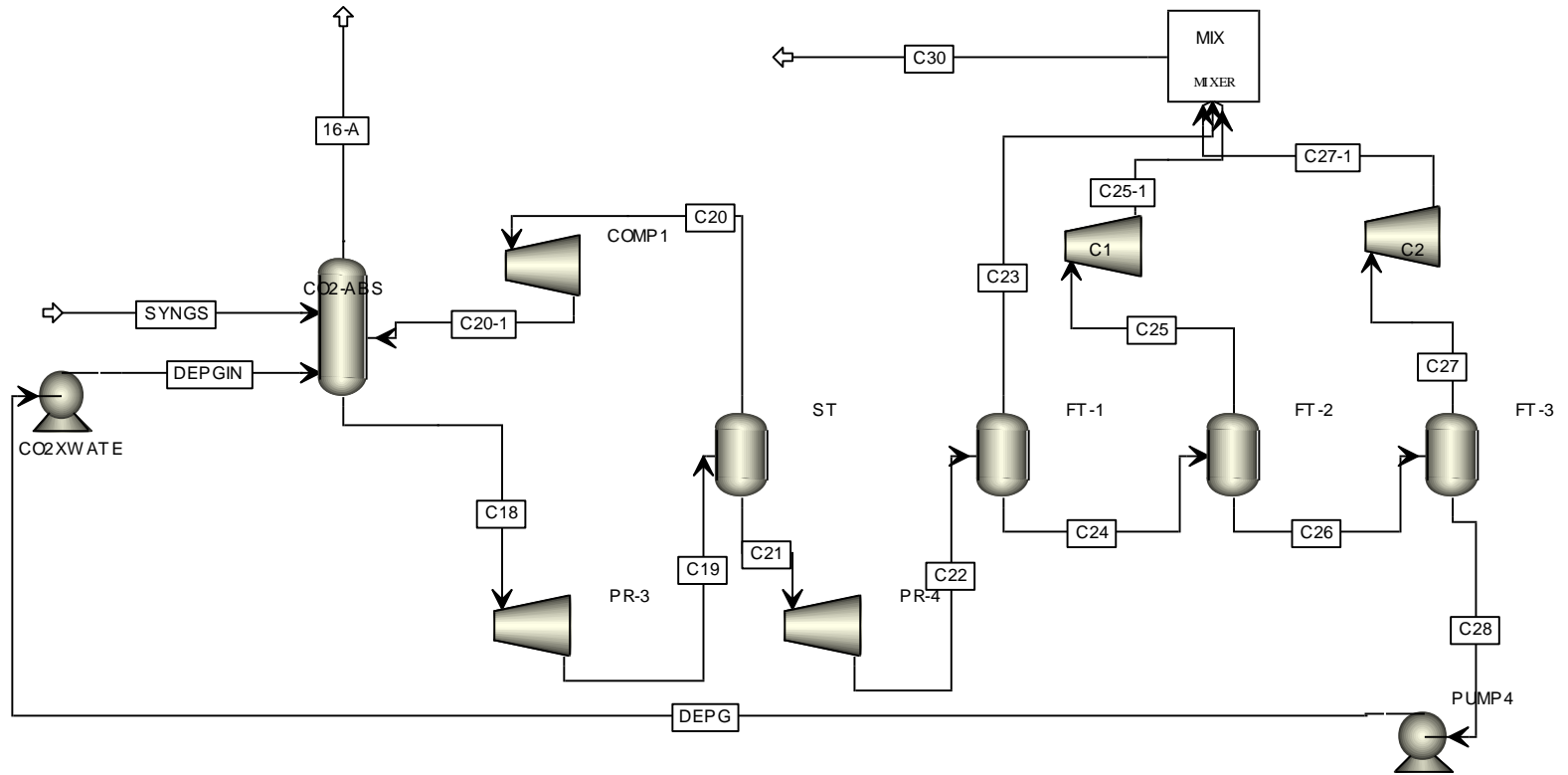
Process Flow Diagram of Reforming Section



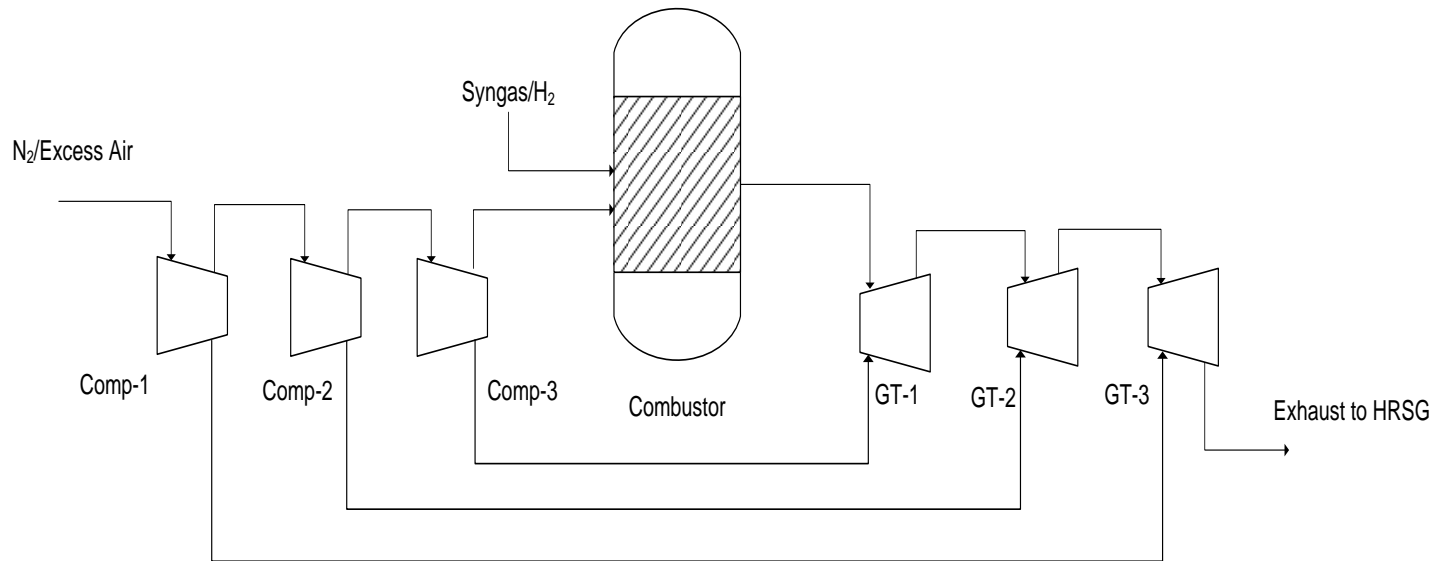
Process Flow Diagram of Water Gas Shift (WGS) Reactors



Process Flow Diagram of H₂S Removal (Selexol Process)



Process Flow Diagram of CO₂ Removal (Selexol Process)



Simplified Flow Diagram Gas Turbine Cycle

Nomenclature

MW_e = Mega Watt (electrical)

MW_{th} = Mega Watt (thermal)

MWh = Mega Watt hour

η = Efficiency

M€ = Million Euro

Abbreviations and Acronyms

AGR: Acid gas Removal

ASU: Air separation unit

ATR: Auto-thermal reforming

CAPEX: Capital expenditure

CC: Combined cycle

CCS: Carbon dioxide capture and storage

CCU: Carbon capture and utilization

COE: Cost of electricity

DRM: Dry reforming of methane

FT: Fischer Tropsch

GHG: Greenhouse gas

GTL: Gas to liquids

GU: Gasification unit

HP: High pressure

HRSG: Heat recovery steam generation

IEA: International Energy Agency

IGCC: Integrated gasification and combined cycle

IP: Intermediate pressure

IPCC: Intergovernmental Panel on Climate Change

LCOE: Levelized cost of electricity

LP: Low pressure
MMCFD: Million cubic feet per day
NGCC: Natural gas combined cycle
O&M: Operation and maintenance
OPEX: Operational expenditure
PC: Pulverized coal
SE: Specific emissions
SMR: Steam methane reforming
TIC: Total investment cost
USPC: Ultra-supercritical pulverized coal
WGSR: Water gas shift reactor

References

1. Change, I.P.o.C., *Climate Change 2014: Mitigation of Climate Change*. Vol. 3. 2015, Cambridge University Press.
2. International Energy Agency (IEA), 2015 edition, CO₂ emissions from fuel combustion, France.
3. Edenhofer, O., R. Pichs-Madruga, Y. Sokona, E. Farahani, S. Kadner, K., A.A. Seyboth, I. Baum, S. Brunner, P. Eickemeier, B. Kriemann, J. Savolainen, S. Schlömer, C. von Stechow, T. Zwickel and J.C., and M. (eds.). IPCC, 2014, *Climate Change 2014: Mitigation of Climate Change*. Contribution of Working Group III to the Fifth Assessment Report of the Intergovernmental Panel on Climate Change, C.U. Press, New York.
4. International Energy Agency (IEA), 2014, *World Energy Investment Outlook*, France.
5. IEA, 2011, *World Energy Outlook*, France.
6. Higman, C. and M. Van der Burgt, *Gasification*. 2011, Gulf professional publishing.
7. Adams, T.A. and P.I. Barton, *Combining coal gasification and natural gas reforming for efficient polygeneration*. *Fuel Processing Technology*, 2011. **92**(3): p. 639-655.
8. Ahmed, U., U. Zahid, Y.S. Jeong, C.-J. Lee, and C. Han, *IGCC process intensification for simultaneous power generation and CO₂ capture*. *Chemical Engineering and Processing: Process Intensification*, 2016. **101**: p. 72-86.
9. Gemayel, J.E., A. Macchi, R. Hughes, and E.J. Anthony, *Simulation of the integration of a bitumen upgrading facility and an IGCC process with carbon capture*. *Fuel*, 2014. **117**: p. 1288-1297.
10. Ahmed, U., C. Kim, U. Zahid, C.-J. Lee, and C. Han, *Integration of IGCC and methane reforming process for power generation with CO₂ capture*. *Chemical Engineering and Processing: Process Intensification*, 2017. **111**: p. 14-24.
11. <http://www.gasification-syngas.org/resources/the-gasification-industry/>.
12. Rousaki, K. and G. Couch. IEA Clean Coal Center, 2000, *Advanced Clean Coal Technologies and Low Value Coals*, United Kingdom.
13. Higman, C. and M.V. Burgt, *Gasification*. 2008, Gulf Professional: USA.

14. Ng, K.S., N. Zhang, and J. Sadhukhan, *Techno-economic analysis of polygeneration systems with carbon capture and storage and CO₂ reuse*. Chemical Engineering Journal, 2013. **219**: p. 96-108.
15. Cormos, A.M., C. Dinca, and C.-C. Cormos, *Multi-fuel multi-product operation of IGCC power plants with carbon capture and storage (CCS)*. Applied Thermal Engineering, 2014. **74**: p. 20-27.
16. Folger, P. Congressional Research Service, 2013, Carbon Capture: A Technology Assessment,
17. (DOE), D.o.E. National Energy Technology Laboratory (NETL), 2005, Power Plant Water Usage and Loss Study, USA.
18. Cormos, C.C., F. Starr, and E. Tzimas, *Use of lower grade coals in IGCC plants with carbon capture for the co-production of hydrogen and electricity*. International Journal Of Hydrogen Energy, 2010. **35**(2): p. 556-567.
19. Fortes, M.P., A.D. Bojarski, E. Velo, J.M. Nougues, and L. Puigjaner, *Conceptual model and evaluation of generated power and emissions in an IGCC plant*. Energy, 2009. **34**(10): p. 1721-1732.
20. Urech, J., L. Tock, T. Harkin, A. Hoadley, and F. Maréchal, *An assessment of different solvent-based capture technologies within an IGCC-CCS power plant*. Energy, 2013. **64**: p. 268-276.
21. Padurean, A., C.C. Cormos, and P.S. Agachi, *Pre-combustion carbon dioxide capture by gas-liquid absorption for Integrated Gasification Combined Cycle power plants*. International Journal of Greenhouse Gas Control, 2012. **7**: p. 1-11.
22. Kawabata, M., O. Kurata, N. Iki, A. Tsutsumi, and H. Furutani, *System modeling of exergy recuperated IGCC system with pre- and post-combustion CO₂ capture*. Applied Thermal Engineering, 2013. **54**(1): p. 310-318.
23. Ferguson, S., G. Skinner, J. Schieke, K.C. Lee, and E.V. Dorst, *High efficiency integrated gasification combine cycle with carbon capture via technology advancements and improved heat integration*. Energy Procedia, 2013. **37**: p. 2245-2255.
24. Lee, J.J., Y.S. Kim, K.S. Cha, T.S. Kim, J.L. Sohn, and Y.J. Joo, *Influence of system integration options on the performance of an integrated gasification combined cycle power plant*. Applied Energy, 2009. **86**(9): p. 1788-1796.
25. Carbo, M.C., J. Boon, D. Jansen, H.A.J. van Dijk, J.W. Dijkstra, R.W. van den Brink, and A.H.M. Verkooijen, *Steam demand reduction of water-gas shift reaction in IGCC power plants with pre-combustion CO₂ capture*. International Journal of Greenhouse Gas Control, 2009. **3**(6): p. 712-719.

26. Emun, F., M. Gadalla, T. Majozi, and D. Boer, *Integrated gasification combined cycle (IGCC) process simulation and optimization*. Computers & Chemical Engineering, 2010. **34**(3): p. 331-338.
27. Shastri, Y. and U. Diwekar, *Stochastic Modeling for Uncertainty Analysis and Multiobjective Optimization of IGCC System with Single-Stage Coal Gasification*. Industrial & Engineering Chemistry Research, 2011. **50**(9): p. 4879-4892.
28. Kunze, C. and H. Spliethoff, *Modelling, comparison and operation experiences of entrained flow gasifier*. Energy Conversion and Management, 2011. **52**(5): p. 2135-2141.
29. Perry, R.H. and D.W. Green, *Perry's chemical engineers' handbook*. 1999, McGraw-Hill Professional.
30. Ask, T.E., D.K. Hartsock, J.E. Davidson, and G.W. Schanche. DTIC Document, 1991, The Economics and Application of Coal Water Fuel in Army Heat Plants,
31. Rubin, E.S., *Implications of future environmental regulation of coal-based electric power*. Annual review of energy, 1989. **14**(1): p. 19-45.
32. O'Brien, J.N., J. Blau, and M. Rose, *AN ANALYSIS OF THE INSTITUTIONAL CHALLENGES TO COMMERCIALIZATION AND DEPLOYMENT OF IGCC TECHNOLOGY IN THE US ELECTRIC INDUSTRY*. 2004.
33. Rosenberg, W.G., D.C. Alpern, and M.R. Walker, *Deploying IGCC in this decade with 3 party covenant financing*. 2004, Belfer Center for Science and International Affairs, John F. Kennedy School of Government, Harvard University Cambridge.
34. Chen, C., *A technical and economic assessment of CO2 capture technology for IGCC power plants*. 2005, Carnegie Mellon University.
35. <http://www.netl.doe.gov/research/Coal/energy-systems/gasification/gasifipedia/commercial-oxygen>.
36. Higman, C. and M.V.D. Burgt, *Gasification 2nd edition*. 2008, Gulf professional publishers: USA.
37. Jones, D., D. Bhattacharyya, R. Turton, and S.E. Zitney, *Optimal design and integration of an air separation unit (ASU) for an integrated gasification combined cycle (IGCC) power plant with CO2 capture*. Fuel Processing Technology, 2011. **92**(9): p. 1685-1695.
38. Woods, M.C., P. Capicotto, J. Haslbeck, N. Kuehn, M. Matuszewski, L. Pinkerton, M. Rutkowski, R. Schoff, and V. Vaysman. National Energy Technology Laboratory (NETL), 2007, Cost and Performance Baseline for Fossil Energy Plants, USA.

39. Metz, B., O. Davidson, H.d. Coninck, M. Loos, and L. Meyer. Cambridge university press,2005, Carbon capture and storage, New York.
40. Padurean, A., C.-C. Cormos, and P.-S. Agachi, *Pre-combustion carbon dioxide capture by gas–liquid absorption for Integrated Gasification Combined Cycle power plants*. International Journal of Greenhouse Gas Control, 2012. **7**: p. 1-11.
41. Systems, G.P. 2003, IGCC gas turbines for refinery applications, New York.
42. Foster, A., H. Von Doering, and M. Hilt, *Fuels flexibility in heavy-duty gas turbines*. GE Company, 1983.
43. Energy, G., *Specification for Fuel Gases for Combustion in Heavy-Duty Gas Turbines*. 2007.
44. <https://energy.gov/eere/fuelcells/hydrogen-production-natural-gas-reforming>.
45. Mondal, K.C. and S. Ramesh Chandran, *Evaluation of the economic impact of hydrogen production by methane decomposition with steam reforming of methane process*. International Journal of Hydrogen Energy, 2014. **39**(18): p. 9670-9674.
46. Ghoneim, S.A., R.A. El-Salamony, and S.A. El-Temtamy, *Review on Innovative Catalytic Reforming of Natural Gas to Syngas*. World Journal of Engineering and Technology, 2016. **4**(01): p. 116.
47. Lavoie, J.-M., *Review on dry reforming of methane, a potentially more environmentally-friendly approach to the increasing natural gas exploitation*. Frontiers in chemistry, 2014. **2**.
48. Noureldin, M.M., N.O. Elbashir, and M.M. El-Halwagi, *Optimization and selection of reforming approaches for syngas generation from natural/shale gas*. Industrial & Engineering Chemistry Research, 2013. **53**(5): p. 1841-1855.
49. Liu, J.A., *Kinetics, catalysis and mechanism of methane steam reforming*. 2006, Worcester Polytechnic Institute.
50. Park, N., M.-J. Park, S.-C. Baek, K.-S. Ha, Y.-J. Lee, G. Kwak, H.-G. Park, and K.-W. Jun, *Modeling and optimization of the mixed reforming of methane: maximizing CO₂ utilization for non-equilibrated reaction*. Fuel, 2014. **115**: p. 357-365.
51. Qian, Y., Y. Man, L. Peng, and H. Zhou, *Integrated Process of Coke-Oven Gas Tri-Reforming and Coal Gasification to Methanol with High Carbon Utilization and Energy Efficiency*. Industrial & Engineering Chemistry Research, 2015. **54**(9): p. 2519-2525.

52. Chung, J., W. Cho, Y. Baek, and C. Lee, *Optimization of KOGAS DME process from demonstration long-term test*. Transactions of the Korean hydrogen and new energy society, 2012. **23**(5): p. 559-571.
53. Global CCS Institute, 2009, Strategic analysis of the global status of carbon capture and storage. Report 2: Economic Assessment of Carbon Capture and Storage Technologies, Australia.
54. Amirabedin, E., M.Z. Yilmazoğlu, and Ş. Başkaya, *Exergetic evaluation of an integrated gasification combined cycle power plant simulated by seven different types of Turkish lignite*. Turkish Journal of Engineering and Environmental Sciences, 2013. **37**(1): p. 42-55.
55. Man, Y., S. Yang, D. Xiang, X. Li, and Y. Qian, *Environmental impact and techno-economic analysis of the coal gasification process with/without CO₂ capture*. Journal of Cleaner Production, 2014. **71**: p. 59-66.
56. Gharaie, M., M. Jobson, M.H. Panjeshahi, N. Zhang, and R. Smith, *Techno-economic optimization of IGCC integrated with utility system for CO₂ emissions reduction—Maximum power production in IGCC*. Chemical Engineering Research and Design, 2013. **91**(8): p. 1403-1410.
57. Ferguson, S., G. Skinner, J. Schieke, K.-C. Lee, and E. van Dorst, *High Efficiency Integrated Gasification Combined Cycle with Carbon Capture via technology advancements and improved heat integration*. Energy Procedia, 2013. **37**: p. 2245-2255.
58. Urech, J., L. Tock, T. Harkin, A. Hoadley, and F. Maréchal, *An assessment of different solvent-based capture technologies within an IGCC-CCS power plant*. Energy, 2014. **64**: p. 268-276.
59. Pérez-Fortes, M., A.D. Bojarski, E. Velo, J.M. Nougués, and L. Puigjaner, *Conceptual model and evaluation of generated power and emissions in an IGCC plant*. Energy, 2009. **34**(10): p. 1721-1732.
60. Cormos, A.M., C. Dinca, and C.C. Cormos, *Multi-fuel multi-product operation of IGCC power plants with carbon capture and storage (CCS)*. Applied Thermal Engineering, 2015. **74**: p. 20-27.
61. Biagini, E., A. Bardi, G. Pannocchia, and L. Tognotti, *Development of an entrained flow gasifier model for process optimization study*. Industrial & Engineering Chemistry Research, 2009. **48**(19): p. 9028-9033.
62. Lima, F.V., P. Daoutidis, and M. Tsapatsis, *Modeling, optimization, and cost analysis of an IGCC plant with a membrane reactor for carbon capture*. AIChE Journal, 2016.

63. Yi, Q., J. Feng, Y. Wu, and W. Li, *3E (energy, environmental, and economy) evaluation and assessment to an innovative dual-gas polygeneration system*. Energy, 2014. **66**: p. 285-294.
64. Casero, P., F.G. Peña, P. Coca, and J. Trujillo, *ELCOGAS 14MWth pre-combustion carbon dioxide capture pilot. Technical & economical achievements*. Fuel, 2014. **116**: p. 804-811.
65. Mansouri Majoumerd, M., S. De, M. Assadi, and P. Breuhaus, *An EU initiative for future generation of IGCC power plants using hydrogen-rich syngas: Simulation results for the baseline configuration*. Applied Energy, 2012. **99**: p. 280-290.
66. Strait, M., G. Allum, and N. Gidwani, *Synthesis Gas Reformers*. 2003, Ceng.
67. Wang, Y., J. Wang, X. Luo, S. Guo, J. Lv, and Q. Gao, *Dynamic modelling and simulation of IGCC process with Texaco gasifier using different coal*. Systems Science & Control Engineering, 2015. **3**(1): p. 198-210.
68. Xie, H., Z. Zhang, Z. Li, and Y. Wang, *Relations among Main Operating Parameters of Gasifier in IGCC*. Energy and Power Engineering, 2013. **5**(04): p. 552.
69. Black, J., J. Haslbeck, A. Jones, W. Lundberg, and V. Shah. DOE/NETL, 2011, Cost and Performance of PC and IGCC Plants for a Range of Carbon Dioxide Capture,
70. Botero, C., R.P. Field, R.D. Brasington, H.J. Herzog, and A.F. Ghoniem, *Performance of an IGCC Plant with Carbon Capture and Coal-CO₂-Slurry Feed: Impact of Coal Rank, Slurry Loading, and Syngas Cooling Technology*. Industrial & Engineering Chemistry Research, 2012. **51**(36): p. 11778-11790.
71. Chen, C. and E.S. Rubin, *CO₂ control technology effects on IGCC plant performance and cost*. Energy Policy, 2009. **37**(3): p. 915-924.
72. Seider, W.D., J.D. Seader, D.R. Lewin, and S. Widagdo, *Product and Process Design Principles (Synthesis, Analysis and Evaluation), 3rd Edition*. 2010, John Wiley & Sons (Asia) Pte Ltd.
73. Cormos, C.C., *Integrated assessment of IGCC power generation technology with carbon capture and storage (CCS)*. Energy, 2012. **42**(1): p. 434-445.
74. Majoumerd, M.M., M. Assadi, and P. Breuhaus. *Techno-Economic Evaluation of an IGCC Power Plant With Carbon Capture*. in *ASME Turbo Expo 2013: Turbine Technical Conference and Exposition*. 2013. American Society of Mechanical Engineers.

75. Gandrik, A., R. Wood, M. Patterson, and P. Mills, *HTGR-Integrated Hydrogen Production via Steam Methane Reforming (SMR) Economic Analysis*. Document ID: TEV-954. INL, 2010.
76. Metz, B., *Carbon dioxide capture and storage: special report of the intergovernmental panel on climate change*. 2005, Cambridge University Press.
77. Yoo, B.-Y., D.-K. Choi, H.-J. Kim, Y.-S. Moon, H.-S. Na, and S.-G. Lee, *Development of CO₂ terminal and CO₂ carrier for future commercialized CCS market*. International Journal of Greenhouse Gas Control, 2013. **12**: p. 323-332.
78. Kang, K., C. Huh, S.-G. Kang, J.-H. Baek, and H.J. Noh, *Estimation of CO₂ pipeline transport cost in south korea based on the scenarios*. Energy Procedia, 2014. **63**: p. 2475-2480.
79. Aspelund, A., M. Mølnevik, and G. De Koeijer, *Ship transport of CO₂: technical solutions and analysis of costs, energy utilization, exergy efficiency and CO₂ emissions*. Chemical Engineering Research and Design, 2006. **84**(9): p. 847-855.
80. You, H., Y. Seo, C. Huh, and D. Chang, *Performance analysis of cold energy recovery from CO₂ injection in ship-based carbon capture and storage (CCS)*. Energies, 2014. **7**(11): p. 7266-7281.
81. Vermeulen, T., *Knowledge Sharing Report-CO₂ Liquid Logistics Shipping Concept (LLSC)*. Overall Supply Chain Optimization, Global CCS Institute. Available on (October 12, 2012): <http://cdn.globalccsinstitute.com/sites/default/files/publications/19011/co2-liquid-logistics-shipping-concept-llsc-overall-supply-chain-optimization.pdf> June, 2011. **21**.
82. Zhang, K., J. Xie, C. Li, L. Hu, X. Wu, and Y. Wang, *A full chain CCS demonstration project in northeast Ordos Basin, China: Operational experience and challenges*. International Journal of Greenhouse Gas Control, 2016. **50**: p. 218-230.
83. Decarre, S., J. Berthiaud, N. Butin, and J.-L. Guillaume-Combecave, *CO₂ maritime transportation*. International Journal of Greenhouse Gas Control, 2010. **4**(5): p. 857-864.
84. Heller, J. and J. Taber. *Influence of reservoir depth on enhanced oil recovery by CO₂ flooding*. in *Permian Basin Oil and Gas Recovery Conference*. 1986. Society of Petroleum Engineers.
85. Yang, S., S. Hamilton, R. Nixon, and R. De Silva, *Prevention of Hydrate Formation in Wells Injecting CO₂ into the Saline Aquifer*. SPE Production & Operations, 2015. **30**(01): p. 52-58.

Abstract in Korean (국문초록)

IGCC 란 대규모 CO₂ 포집 및 저장 기술(CCS)을 결합한 높은 열 효율을 갖는 사전 연소 기술이다. 한편 NGCC 발전기술은 CCS 기술을 사용하는 IGCC 공정에 비해 높은 공정 성능을 나타내지만, 천연가스 가격의 변동과 높은 비용으로 인하여 석탄 기반 발전 시스템에 비해 널리 사용되지 못하고 있다. 따라서 공정의 효율을 높이고자 천연가스의 소비를 제한하는 동시에 석탄의 가스화와 천연가스의 개질화를 통합한 공정이 제안되었다. 본 연구에서 두 가지 IGCC 기술을 기반으로 한 공정 모델을 개발하였고, CO₂ 포집 및 저장에 대하여 공정의 성능과 경제성 측면의 평가를 진행하였다. Case1 은 전통적인 IGCC 공정 모델이고, Case2 는 IGCC 기술과 메탄 개질 공정을 통합한 공정 모델이다. Case2 의 석탄 슬러리의 가스화 공정으로 생성된 높은 엔탈피의 스팀은 H₂ 발생을 위한 개질 공정에 사용된다. 메탄 개질 공정과 IGCC 의 통합은 흡열반응인 개질 공정에 필요한 열을 제공할 뿐만 아니라 생성된 합성가스(syngas)의 열량을 증가시킨다. 이 개념은 또한 공유하고 있는 수성 가스 전환 반응기와 CO₂ 포집 설비가 공정의 필요 조건을 만족하기 때문에 공정 개선의 기회를 제공한다. Case1 과 Case2 의 순 발전 용량과 효율은 각각

(375.08 MW_e , 472.92 MW_e) and (35.93%, 40.70%) 이다. 결과를 비교해보면, Case2의 설계가 CO₂ 포집을 결합한 Case1보다 약 4.7% 이상의 높은 효율을 나타냈다. 공정의 경제성 분석을 통해서 Case2의 경우에 Case1보다 공정 전체 수명을 기준으로 더 높은 CAPEX와 O&M이 요구되는 것을 알 수 있었다. 그러나 Case2의 경우는 높은 발전 용량으로 Case1에 비해 LCOE를 5.81% 절감할 수 있었다. 게다가 Case2의 경우는 Case1에 비해 적은 양의 CO₂ 포집이 이뤄지고, 원가를 절감할 수 있을 뿐만 아니라 더 짧은 시간 안에 투자비를 회수할 수 있었다. Case2는 높은 효율과 적은 양의 CO₂ specific emission(SE_{CO_2})으로 Case1에 비해 전력 생산의 경제적 비용 측면에서 더 실현 가능한 선택지로 고려된다. CO₂ 포집 및 저장 기술을 결합한 전력 생산 체계를 완성하기 위해서 CO₂ 주입 시스템에 대해서도 자세한 연구를 진행했다. CO₂의 지하 저장 장소가 해상에 위치하고, 해상 이송을 위한 파이프라인의 설치가 큰 비용을 수반할 경우에 선박을 이용한 경제적인 운반이 가능하다. 선박 운송은 포집된 CO₂가 가압된 열역학적 조건의 액체 상태로 존재해야 한다. 액상 CO₂의 지하 저장조로의 주입은 well-head의 안전한 운전 조건을 유지하기 위하여 가압과 가열과정을 거친다.

본 연구는 2 단계 NH₃ 랭킨 사이클을 운전하기 위해서 액체 CO₂로부터 이용 가능한 냉열을 회수하는 CO₂ 주입 공정의 발전된 설계 메커니즘을 제시한다. 결과적으로 2 단계 랭킨 사이클이 베이스 케이스 대비 약 56%의 적은 에너지를 소비한다는 것을 확인할 수 있었다. 게다가 경제성 분석을 통해서 개선된 설계의 경우에 CO₂ 주입의 specific cost 을 6.2%까지 감축할 수 있다는 것을 확인하였다. 마지막으로 공정 성능과 경제성의 몇 가지 주요 변수의 효과에 대한 민감도 분석 또한 실시하였다.

Keywords: IGCC, SMR, Process integration and intensification, Power generation, CCS, COE, Process economics, 2-stage rankine cycle, CO₂ transport & storage

Student Number: 2015-31025

